An Exploration of Secondary Fuel Injection as Actuation for Control of Combustion Instabilities in a Laminar Premixed Tube Combustor

by

John S. Richards

Thesis submitted to the Faculty of the Virginia Polytechnic Institute and State University in partial fulfillment of the requirements for the degree of

MASTERS OF SCIENCE IN MECHANICAL ENGINEERING

APPROVED:

William R. Saunders, Chair

Uri Vandsburger

Harry H. Robertshaw

May 27, 2000

Blacksburg, Virginia

Keywords: Active Combustion Control, Secondary Fuel Injection, Thermoacoustic Instability

An Exploration of Secondary Fuel Injection as Actuation for Control of Combustion Instabilities in a Laminar Premixed Tube Combustor

by

John S. Richards

William R. Saunders, Chairman

Mechanical Engineering

(ABSTRACT)

Active control of combustion instabilities through secondary fuel injection is a control method that has gained a lot of attention in the past decade. Previous control schemes with acoustic loudspeakers are not practical in full-scale gas turbines due to the extreme temperatures and acoustic power requirements. Much work has gone into controlling these thermoacoustic instabilities with secondary fuel control. Control of a laminar premixed tube combustor through secondary fuel actuation is the concentration of this work. It is the first known published attempt to control a laminar premixed tube combustor through secondary fuel actuation.

Due to the low flow rates within the tube combustor an innovative injection technique had to be constructed to perform the secondary fuel actuation. The gaseous fuel is injected only one millimeter above the location of the flame through one, two, or four injectors. These injectors were designed to overcome the serious problem of pulse diffusion. This technique enabled the tube combustor to be controlled through secondary fuel injection.

Accompanying the innovative fuel injection technique is a duty cycle modulation technique

that was a prime contributor to the success of the control system. This method enabled the system to be controlled at conditions that were uncontrollable with a fixed duty cycle. The overall result was a 35 dB suppression of the limit cycle amplitude with 20% secondary fuel injection.

ACKNOWLEDGEMENTS

I would like to thank my wife for her support during the last 22 months. She kept me working and motivated to finish this work.

I would like to thank my parents (Ron and Sherida). They paid for my undergraduate degree and made it possible for me to continue my education. I could never pay them back for all that they have given me.

What can I say about Will Saunders? Without his positive outlook and insight, this work would not have been. He was always there to hammer things out when I needed to.

I have to thank the entire VACCG (Virginia Active Combustion Control Group) crew. I received guidance, help, and friendship from its members. Our discussions made the difference between success and failure.

TABLE OF CONTENTS

NOMENCLATURE

R_I	Rayleigh index
p'	Acoustic pressure
Q'	Heat release
u'	Particle velocity
τ	Time delay
t	Time
K_P	Proportional gain
K_I	Integral gain
K_D	Derivative gain
B	Magnetic flux density
ϕ	Magnetic flux
A	Cross sectional area
H	Field intensity
μ	Permeability
μ_M	Permeability of magnetic core
μ_O	Permeability of air
mmf	Magnetic motive force
F_M	Magnetic motive force
L	Length
N	Number of turns of the coil
R	Reluctance
Rc	Core reluctance
Rg	Gap reluctance
R_T	Total reluctance
δ	Gap distance
V	Voltage
R	Resistance
L	Inductance
i	Current
F	Force
J	Rotational inertia
θ	Angle of rotation
k	Stiffness
c	Damping constant
M	Mass of pivot member
l	Length
x	Distance of travel
F_P	Pressure force
g	Acceleration due to gravity
D_X	Partial derivative with respect to x
D_V	Partial derivative with respect to y
$\bar{x}$	Mean of x
$\bar{v}$	Mean of v
$\bar{y}$	Mean of y

y'	Perturbation of y
x'	Perturbation of x
x_O	Static solution for x
i_O	Static solution for I
V_O	Static V
G_{XX}	Auto spectrum
G_{XY}	Cross spectrum
H_F	Frequency response function

LIST OF FIGURES

LIST OF TABLES

Chapter 1

Introduction

Heat-driven acoustic oscillations are phenomena that have been studied for more than a century [29,35]. They occur in the simplest of test rigs to the most complex full-scale combustors. In pressurized full-scale combustors these pressure oscillations can cause catastrophic failure. Since these oscillations are not well understood they must be dealt with in the development stage. A major effort has been put into actively controlling these oscillations through secondary fuel injection. Some of this thesis work concentrates on control of a laminar premixed tube combustor through secondary fuel actuation. No prior research has been published using secondary fuel actuation for control of a laminar premixed tube combustor thermoacoustic instabilities. The results of this work will be used as a foundation for secondary fuel control of larger combustors currently being constructed at Virginia Tech

1.1 Thermoacoustic Instabilities

To understand this work it is necessary to know how these thermoacoustic instabilities occur, and what they result in. Thermoacoustic instabilities are the result of an interaction between heat and sound [36]. The heat source adds to the pressure oscillations and the pressure oscillations modify the heat source. The result is a nonlinear self-excited system.

1.1.1 The Rayleigh Criteria

Lord Rayleigh [33] developed an accurate criterion for the growth of thermoacoustic oscillations. This criterion states that heat drives acoustic oscillations if it is added at the moment of greatest compression or removed at the moment of greatest rarefaction. The

Rayleigh index, a measure of the potential for heat driven oscillations to occur, is presented in Equation 1.1.1 and rewritten in Equation 1.1.3.

$$R_I = \int_t^{t+T} p'(t)Q'(t)dt \qquad \textbf{Eq. 1.1.1}$$

The heat release Q' is approximately equal to the velocity:

$$Q'(t) \sim \vec{u}'(t-\tau) \qquad \textbf{Eq. 1.1.2}$$

This puts the equation in the following form.

$$R_I \cong \int_t^{t+T} p'(t)\vec{u}'(t-\tau)dt \qquad \textbf{Eq. 1.1.3}$$

This equation says that when the pressure p' and velocity u' have the correct time delay τ then the Rayleigh index R_I will be at a maximum. Instabilities occur when the Rayleigh index is positive. The severity of an instability to occur increases with the index. This is illustrated in Figure 1.1.1. This figure shows the pressure and velocity ¾ wave modes with the Rayleigh index for a closed-open tube. Where the Rayleigh index is a positive value an instability can be driven by a heat source. This is the location where the heat release contributes negative damping to the system. Where the index is negative, heat addition will dampen the system and no instability will occur.

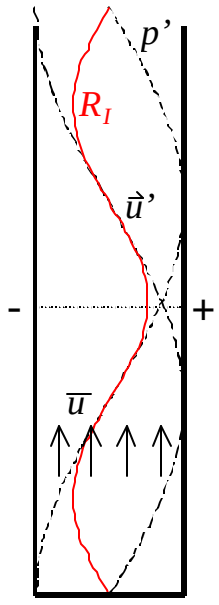

FIGURE 1.1.1 Closed-Open Tube Pressure and Velocity Mode Shapes and the Rayleigh Criteria

1.1.2 The Nonlinear System Characteristics

Two nonlinear system characteristics are important to this work. These characteristics are the limit cycle and the jump phenomenon. The limit cycle will be referred to in the remainder of this work to discuss the control system performance. The jump phenomenon will be examined in Chapter 5 to look into the effects of fuel pulsations on the tube combustor.

The first characteristic is a limit cycle. The nonlinear system oscillations will grow until a maximum amplitude is reached where it remains until the system is disturbed. This stable periodic oscillation is the limit cycle. Thus, the limit cycle amplitude and frequency are referred to when discussing the thermoacoustic instability.

The second important nonlinear system characteristic is the jump phenomenon. A good explanation of this phenomenon is found in Phillips and Harbor. In Chapter 5, the sub critical Hopf bifurcation point is evaluated using the fuel flow rate as the control parameter instead of frequency. The details will be discussed in Chapter 5.

1.2 Active Control of a Laminar Premixed Flame

A system with a heat source located where the Rayleigh index is positive is a “self-excited system”. A self-excited system is simply a system that drives itself and is mathematically described by autonomous differential equations with unstable roots. The heat release drives the pressure oscillations and the pressure drives the heat release oscillations. It is essentially a closed loop system in itself. A block diagram typically used to represent this system is shown in Figure 1.2.1.

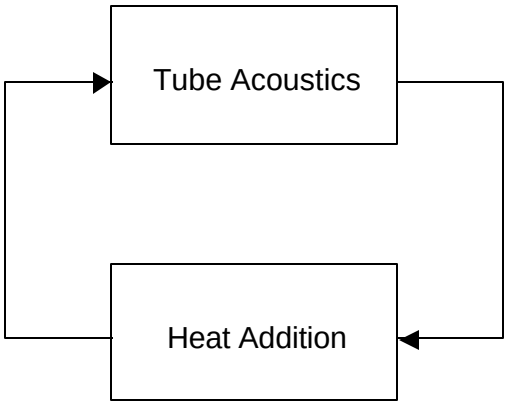

FIGURE 1.2.1 Block Diagram of the Self Excited System

These heat driven oscillations are a major concern in industry. They can grow as large as 10% of the mean pressure. Since operating pressures range from 2 to 40 Mpa, oscillations can be many times larger than atmospheric pressure. These large-scale pressure oscillations cause unwanted cyclic loading of the parts of these large-scale engines. In the worst case these pressure oscillations can cause a complete failure of the system. Not enough information is known about these oscillations to accurately model them, so they must be dealt with at the development stage. This means control through passive or active methods. The frequency of the instability is highly dependent on the operating condition making passive techniques such as resonators ineffective in damping the oscillations. Active techniques have been successful, but there are still many obstacles to overcome.

Thermoacoustic oscillations occur in much smaller systems as well. The simple closed-open boundary conditions for the 1-D acoustic system shown in Figure 1.1.1, can generate thermoacoustic instabilities. This is the type of system that has been studied during this research. The tube combustor, although much smaller in scale with reference to pressure oscillations and heat release, presents its own set of challenges in designing a control system. The system is simply a 60 inch closed-open tube with an outer diameter of approximately 3 inches. The flame is stabilized at the approximate center of the tube, which excites the ¾-wave mode of the tube. The ¾-wave mode occurs at approximately 162 Hz in absence of the flame. This frequency increases up to 178 Hz as the gases heat the tube. The fuel, methane, is premixed in a mixer with air and injected through four spokes at the bottom of

the tube. The premix charge convects up to the flame holder where it is ignited and stabilized on a ceramic matrix flame stabilizer. The flow rates of the system range from only 120 cc/sec to 150 cc/sec generating a typical Reynolds number of 250. The Reynolds number is a non dimensional number which is simply the fluid density multiplied by the velocity and diameter, and divided by the kinematic viscosity. A Reynolds number of 250 is well below the laminar limit of 2100. Equivalence ratio is the ratio of fuel to air in a combustion system. It is defined as:

$$\phi = \frac{\frac{m_{Air\ Actual}}{m_{Fuel\ Actual}}}{\frac{m_{Air\ Stoichiometric}}{m_{Fuel\ Stoichiometric}}} \qquad \textbf{Eq. 1.2.1}$$

The mixture is lean if the equivalence ratio is less than one. This means there is excess air. The mixture is rich if the equivalence ratio is greater than one. Typical equivalence ratios for the laminar tube combustor are 0.48 to 0.65. A photograph of this tube combustor is shown in Figure 1.2.2.

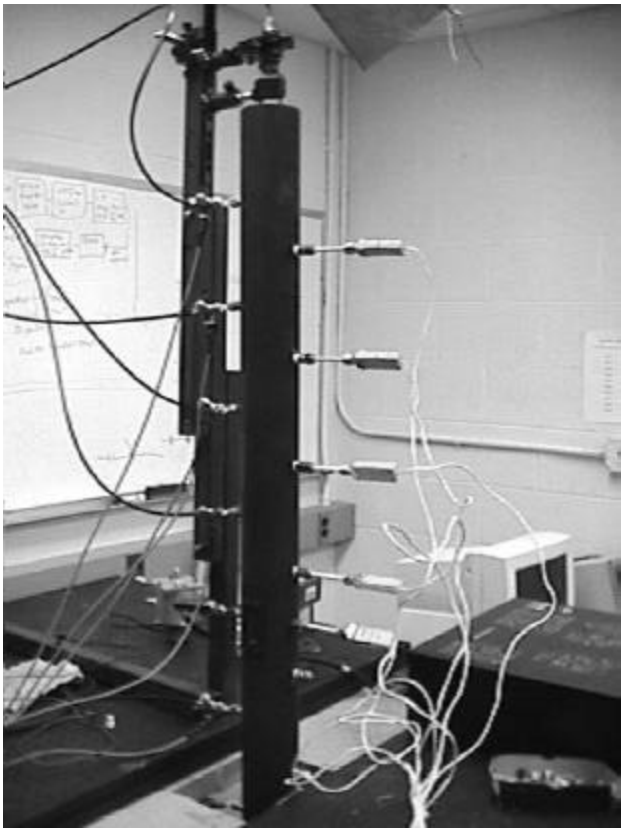

FIGURE 1.2.2 The Tube Combustor System

A diagram of the tube with all the necessary instrumentation is given in Figure 1.2.3. There is an array of pressure sensors and thermocouples to collect pressure and temperature data along the axis of the tube. Chemiluminescence measurements, a measure of the heat release rate, are taken through a monochrometer and a photo multiplier tube.

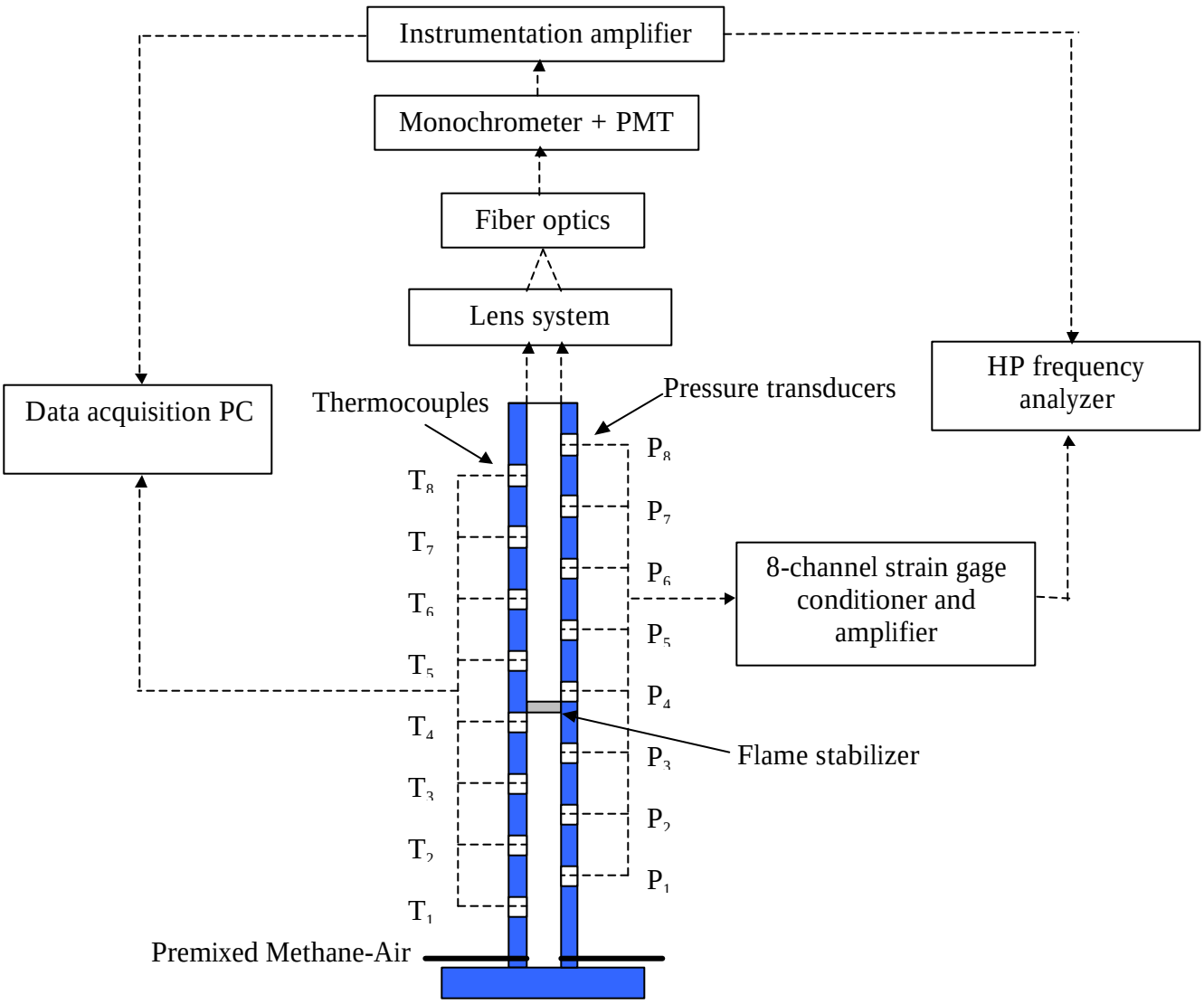

FIGURE 1.2.3 Diagram of the Tube Combustor with Instrumentation

A power spectrum of the pressure signal for 150 cc/sec total flow at four different equivalence ratios is given in Figure 1.2.4. The total flow is nominally 150 cc/sec. This figure shows that the level of the instability is dependent on the operating conditions. At the higher equivalence ratios the instability is more dominant than at the lower equivalence ratios and is inherently more difficult to control. This difficulty comes from the level of actuation authority required to achieve control of the linearly unstable system.

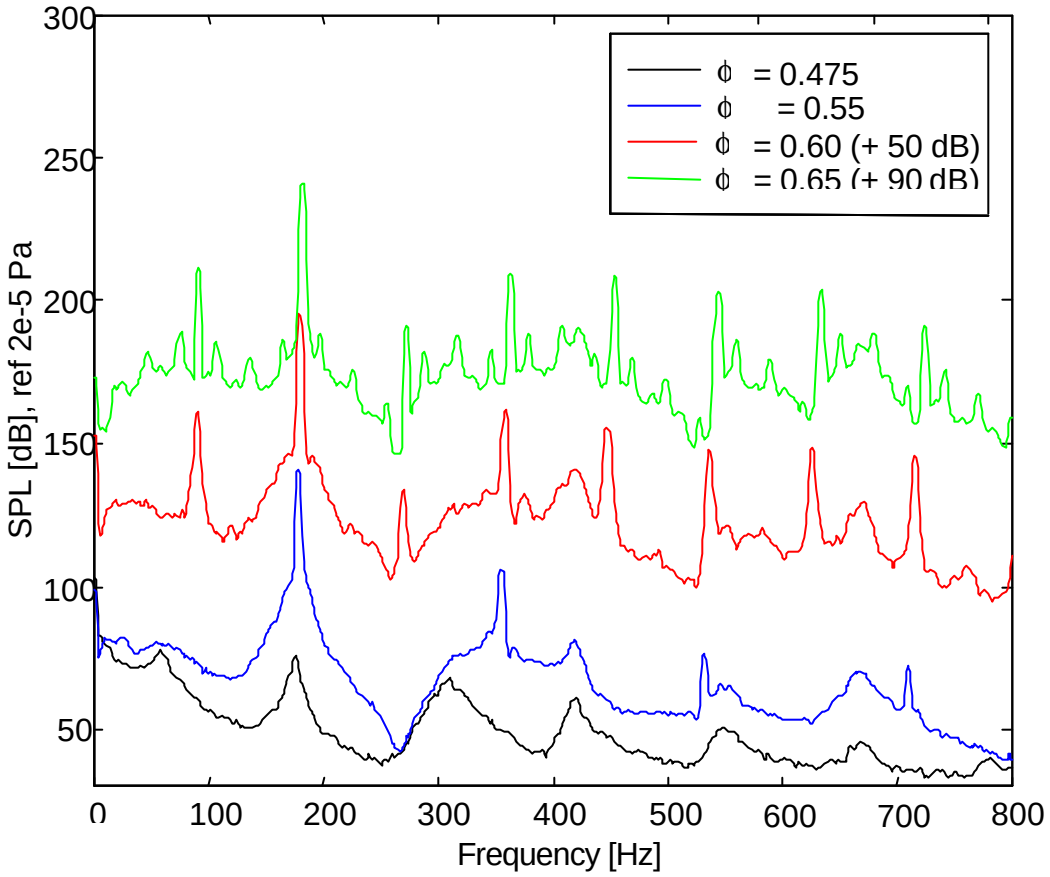

FIGURE 1.2.4 Pressure Power Spectrum for Various Equivalence Ratios

Parallel research, on the same plant, demonstrates control of the thermoacoustic instabilities has been achieved with an acoustic actuator and a digital phase shifter controller [41,42]. The acoustic actuator is a 3", 15 watt speaker mounted in a ported cabinet. A photograph is shown in Figure 1.2.5.

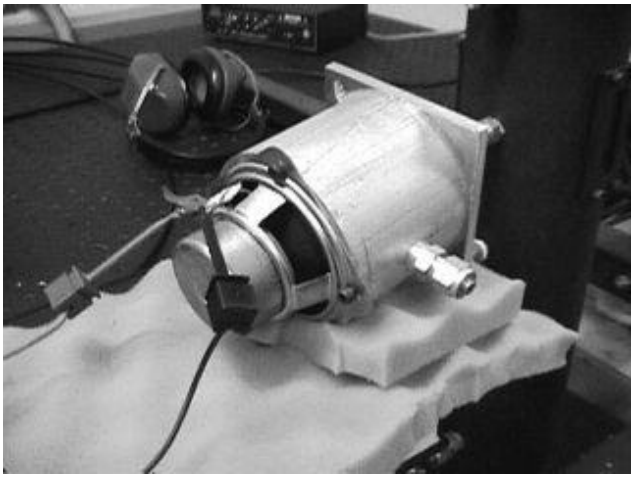

FIGURE 1.2.5 Acoustic Actuator

The ¼" diameter port of the actuator cabinet is connected to the tube just above the flame holder. A pressure signal, measured at the bottom of the tube, is fed through a narrow band-pass filter. This produces a sine wave that is fed to the controller. Control has been achieved through a phase shifter, neural network, and adaptive means. For the case of the phase shifter the input signal is delayed a specific number of samples then sent through a smoothing filter to the actuator. This process modifies the phasing between the heat release and the pressure and acts to move the system poles away from instability. This control process could also be done using the heat release signal from the PMT. The performance of the phase shift controller is shown in Figure 1.2.6. The system is completely stabilized, in this case, and the pressure spectrum is reduced to the reverberant levels associated with the hot acoustics of the tube. More details of the phase shifting control experiments can be found in the references [38,41,42].

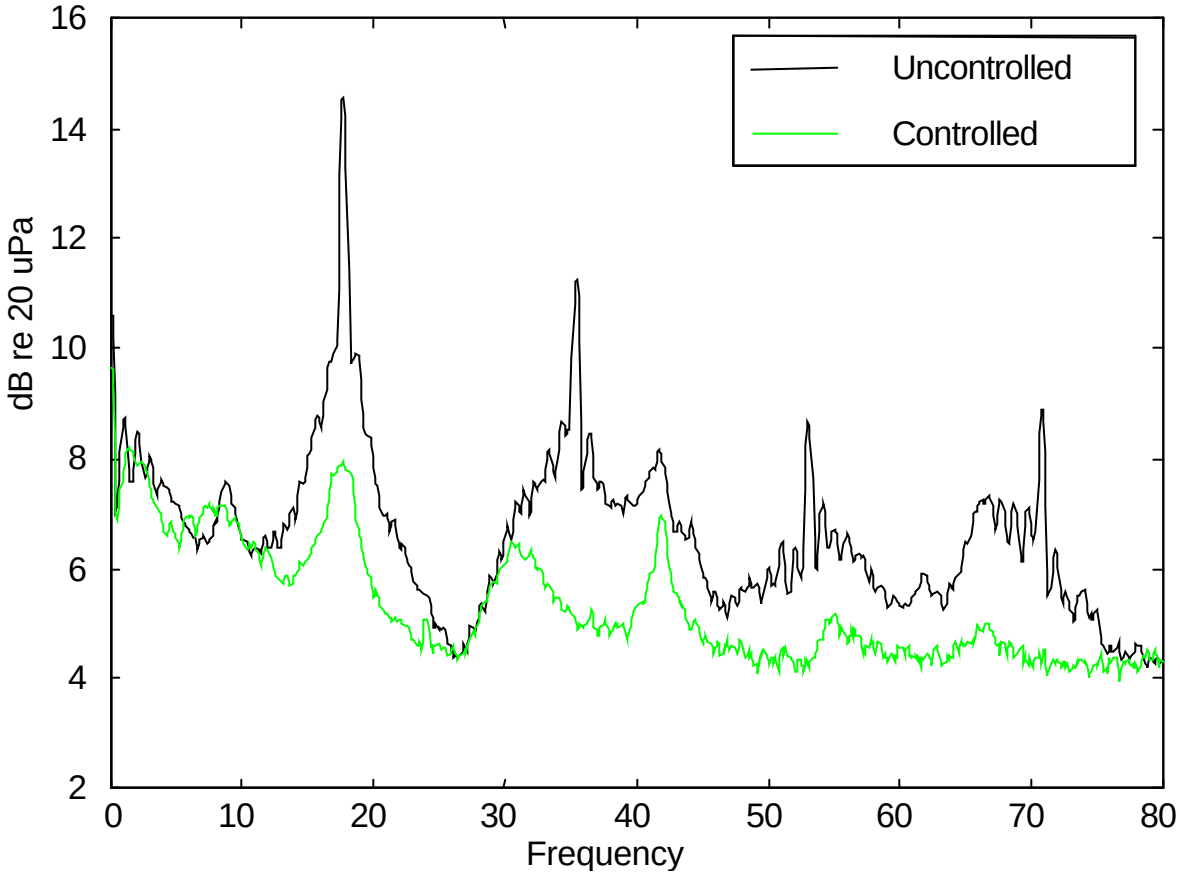

FIGURE 1.2.6 Plot of Pressure Spectrum for Controlled and an Uncontrolled Case in the Tube Combustor for $\phi = 0.50$ at 130 cc/sec

The acoustic actuator works well for atmospheric rigs like the laminar premixed tube combustor, but is not practical for many full-scale combustors. Temperatures and acoustic power requirements greatly exceeds the design features of most acoustic loudspeakers. This is the reason for the need of secondary fuel actuation, which works on modifying the heat release through injecting fuel with the proper timing instead of acting directly on the acoustic pressure field. Secondary fuel injection has been implemented by Langhorne, Hantschk, Hermann, Zinn, McManus, Yu, Seume, Cohen, Hibshman, and Richards [7,13,15,16,25,28,35,40,44,46]. The power outputs of the main plants range from Cohen's 4 MW single nozzle test rig to Sueme's 170 MW model V84.3A ring combustor gas turbine [7,40].

There are a number of challenges involved in implementing this secondary fuel actuation on the Virginia Active Combustion Control Group (VACCG) tube combustor. The maximum flow rate of 150 cc/sec is very low making the system very laminar. The convective and diffusion velocity are both approximately 5 cm/sec. This means that any fuel pulse injected into the system will diffuse quickly. If it is assumed the limit cycle is 180 Hz and the actuation is done at this frequency the period of oscillation is just 5.55 milliseconds. Since the fuel is gaseous, an on/off solenoid valve must be used to inject the secondary fuel. The solenoid valve requires a square wave. Assuming the duty cycle of the control signal is set to 50% the valve is kept open half of the period. This means there is only 2.78 milliseconds between fuel pulses. With a convective flow velocity of 5 cm/sec, a pulse of fuel injected into the system will have only moved 0.139 millimeters upwards before the next pulse of fuel enters the system. To add to the problem, the injector has to be smaller than 0.139 millimeters to be able to generate the fuel pulses at 180 Hz. In large-scale systems where the mean flow rate is much higher, this is not case. The pulses are separated sufficiently, by the flow, to maintain the rich/lean pockets and the relative wavelengths are orders of magnitudes larger.

The calculations presented above showed that an alternate secondary fuel injection scheme is needed. The solution is to inject the secondary fuel right at the location of the flame. This eliminates the concern of diffusion because the fuel is ignited right at the exit of the injector, but this form of fuel injection creates a new set of problems. If the flow coming out of the injector is too high the jet could blow out the flame. From the previous discussion, we want to make the injectors on the order of 0.139 millimeters to create the fuel pulses. The convective flow is 5 cm/sec and the flame speed is approximately 30 cm/sec higher than the convective flow. This gives a flow rate of 35 cm/sec right at the injection point. This is the desired exit velocity of the injection system. In order to come up with an injector exit diameter, the amount of flow required must be determined. Based on a typical operation condition of 150 cc/sec total flow, the fuel is about 10% of 150 or 15 cc/sec. Relying on experiments done by other researchers in this field, a base value of 10% fuel modulation was chosen. This gives 1.5 cc/sec as the total volumetric flow for the secondary fuel injection. Injecting this amount of fuel through an injector with a diameter of 1 millimeter would

produce an exit velocity of 1.67 m/sec. This flow rate could potentially blow out the delicate laminar flame. The solution is to divide the flow through four injectors. This injection method divides the exit velocity by four. Stainless steel tubing with an inner diameter of 1 millimeter is used. This gives 41.9 cm/sec of flow for each of the four injectors based on the 10% fuel modulation. This velocity is slightly higher than the 35 cm/sec that was targeted, but it is low enough not to blow out the flame. There are other considerations for this injection technique that were discovered in use of the system and will be discussed in Chapter 5.

The injector system is designed, but the valve must be able to perform at the frequency of the limit cycle. Frequencies above 200 Hz are high for solenoid valves. A solenoid valve operates on electromagnetics. Some act very much like a speaker where the core moves within the magnetic field of the coils. Others act as an electromagnetic switch to open and close the exit of the valve. A typical frequency range for a solenoid is around 200 Hz. This frequency range doesn't tell the user what the frequency response looks like at 200 Hz. The valve used for this project is a specialty valve made by Matrix Inc. out of Italy. This valve operates in a unique way to give a much higher frequency response. The claimed bandwidth, for this particular valve, is 500 Hz. The details of how the valve operates and how it performs are covered in Chapter 3.

1.3 Actuator Requirements

There are four main requirements of the actuator for secondary fuel control. The first is bandwidth. As already discussed, the valve must be able to actuate at the frequency of the instability. Since the instability frequency is dependent on the geometry of the combustor, this frequency can be in excess of 500 Hz or even 1000 Hz. The second requirement is power consumption. If the actuator were to take too much energy to control the instability the actuator would be useless. The third requirement is to be able to perform in the environment of the system. In the case of the laminar premixed tube the valve is not subjected to any extreme conditions such as elevated temperatures and pressures. In larger combustors these are serious issues. Lastly, the actuator needs to be able to operate for a large number of cycles before failure. With the relatively high operation frequency required

for control, the valve must be able to operate for millions of cycles before replacement. It is not cost-efficient to shut down a land-based gas turbine to replace the actuator. Depending on the rig there may be even further requirements, but these are the main ones. It is easy to see that finding an actuator for active combustion control is a difficult part of the problem. Much research has gone into developing new types of actuators with new types of materials with higher frequency responses. MOOG has invested a significant amount of money developing a high response solenoid valve that has been successfully used on a large-scale gas turbine by Sueme of Siemens and a test rig by Hantschk of the Technical University of Munich [44,13]. In the academic research area, Zinn et al. have put significant efforts into their high response magnetostrictive valve for secondary liquid fuel injection [46]. These actuators are discussed in more detail in Chapter 2. The actuator used for this work is a solenoid valve produced by Matrix. It is a high response solenoid valve that operates as an electromagnetic switch. When energized the valve generates an electromagnetic force which raises a pivot member and opens the valve. A photograph of the valve is shown in Figure 1.3.1.

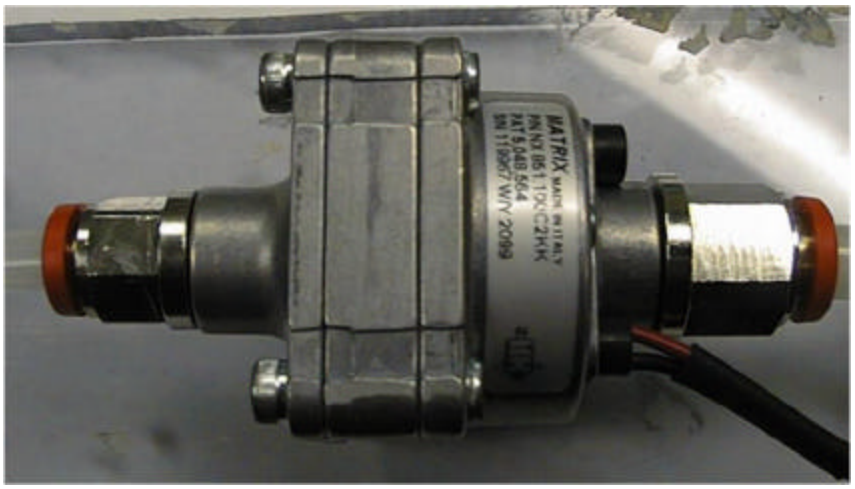

FIGURE 1.3.1 Matrix Solenoid Valve

1.4 Methods of Control

There are numerous control schemes that have been used for suppression of thermoacoustic instabilities. They vary from simple phase shifters to very complex adaptive algorithms and neural networks. Although the system does not require a complex control algorithm to obtain control of the instability, there are some benefits from more sophisticated algorithms. With a phase shifter an operator must change the phase to obtain and maintain control. This means that as conditions change, the controller will not. Different algorithms, such as extremum-seeking, use a mathematical scheme that determines the direction to search for the best control of the system. This type of controller will maintain control and adapt as conditions change [1,4,21,22]. It is left to the reader to explore the details of these control schemes. A simple phase shift controller will be used for this work.

1.5 Organization of the Thesis

This thesis will cover the secondary fuel actuation literature review, the valve modeling, the experimental setup, results from the flame dynamics rig, the testing setup and results for the laminar premixed tube combustor, the active combustion control results, and future work. The literature review, covered in Chapter 2, will describe the test setup for each researcher and the results of their secondary fuel actuation efforts. The valve modeling, covered in Chapter 3, will discuss the modeling background and derivation of the solenoid valve model. The magnitude response of the model and the actual valve are compared as well. The flame dynamics rig setup and test results will be discussed in Chapter 4. This test was simply to verify the injection system would work and to observe how the flame reacts to the injected fuel. The setup and active combustion control test results for the laminar premixed tube combustor are discussed in Chapter 5. This will cover the description of the control system, the results of a number of tests, and the final results. A summary of the closed-loop active combustion control results and future work is discussed in Chapter 6.

Chapter 2

Literature Review

Much research has gone into combustion instabilities, but research into active combustion control is fairly new. Only since about 1988 have papers been published describing the use of active control to attack the instability issue. The primary focus of this literature review was to find work published using secondary and primary fuel actuation. This includes two types of actuators. The first type of actuator is the on/off type, such as a solenoid valve. The second type of actuator varies the inlet area in a proportional way. Much work has been done using acoustic actuators such as speakers, but those will not be included in the literature review.

2.1 [Bloxsidge et al. 1988]

Bloxsidge worked on a 0.25 megawatt tube combustor, running ethylene for fuel, at Cambridge University. A diagram of this rig is shown below in Figure 2.1.1.

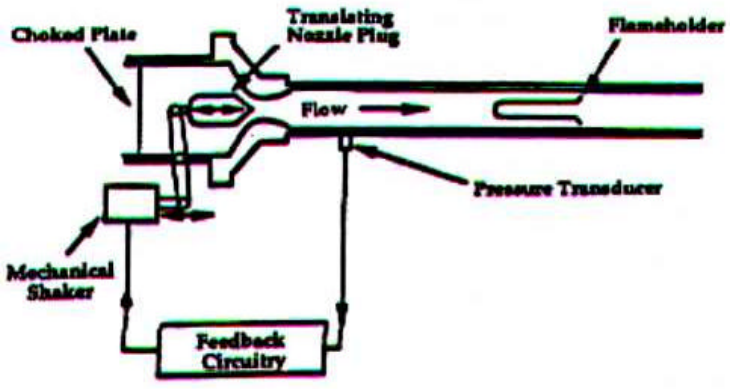

FIGURE 2.1.1 Schematic of Experimental Setup Used by Bloxsidge et al[5]

A mixture of fuel and air entered the inlet nozzle through the variable area nozzle where a mechanical shaker moved a nozzle plug to achieve an area variation. This area variation created a flow variation and provided a means for control. This is not secondary fuel modulation. It is primary fuel-air mix flow modulation. This is one of the first cases of modulating the flow of gases by some other means than a speaker. The pressure signal was measured with a transducer and sent through a filter that eliminated unwanted frequency components. The result was a sine wave of the frequency of the instability. This signal was then fed to the controller, which was a simple phase shifter. For a typical equivalence ratio of 0.66 and a mass flow of 0.135 kg/sec the instability at 88 Hz had a sound pressure level of 162 dB. With the controller on, the sound pressure level was reduced by 26 dB at the frequency of the instability. The power spectrum for the controlled and uncontrolled case is given in Figure 2.1.2.

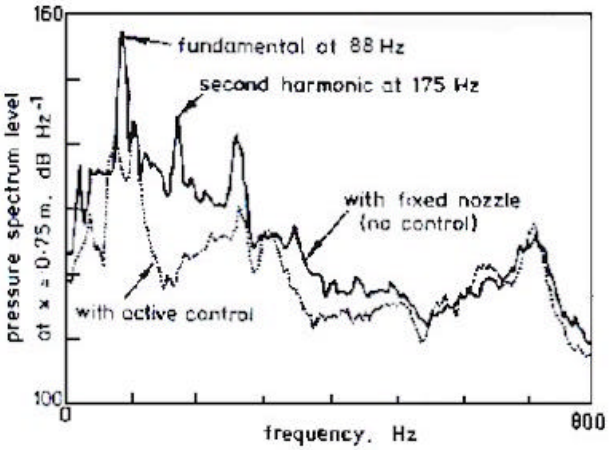

FIGURE 2.1.2 Power Spectrum for the Controlled and Uncontrolled Cases[5]

2.2 [Langhorne et al. 1988]

Langhorne worked on the same test rig as Bloxsidge at Cambridge University. The difference in the setup was the actuator. Instead of using a nozzle plug to vary the flow of fuel and air, Langhorne used solenoid valves to pulsate secondary fuel injected just upstream of the flame holder. This setup is shown in Figure 2.2.1

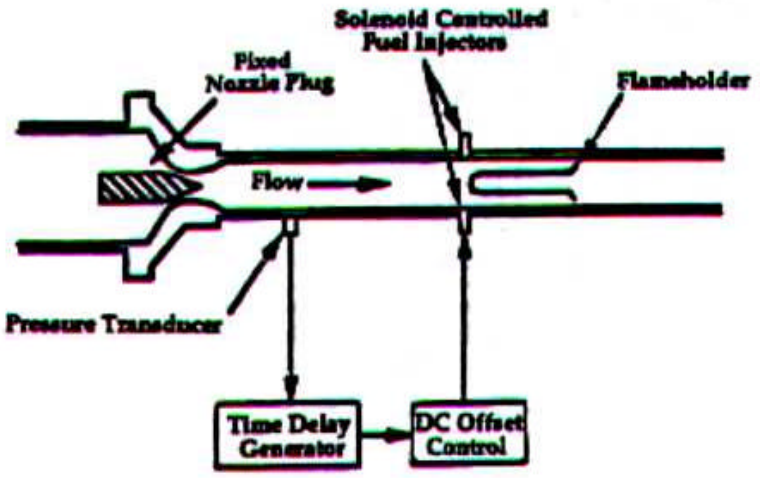

FIGURE 2.2.1 Schematic of Experimental Setup Used by Langhorne et al[25]

The actuator arrangement consisted of a series of four Bosch automotive fuel injectors arranged to inject fuel into a ring where it was mixed with air. The fuel air mixture then departs through a series of 24 holes into the rig. Automotive fuel injectors were used because they were cheap and had a response time of typically less than 1 millisecond. The fuel again was liquid ethanol with a typical total equivalence ratio between 0.63 and 0.73 and a steady mass flow of 0.135 kg/sec. The controller was the same phase shifter, but the output was different from before. Bloxsidge could feed a filtered sine wave to the shaker to control the tube. Langhorne could not feed the filtered sine wave to the valves. The dc component of the signal had to be removed and a square wave had to be generated from the ac part of the signal. As long as the signal was positive the valves were kept open. Once the value of the signal went negative the valves were closed. This scheme is illustrated in Figure 2.2.2.

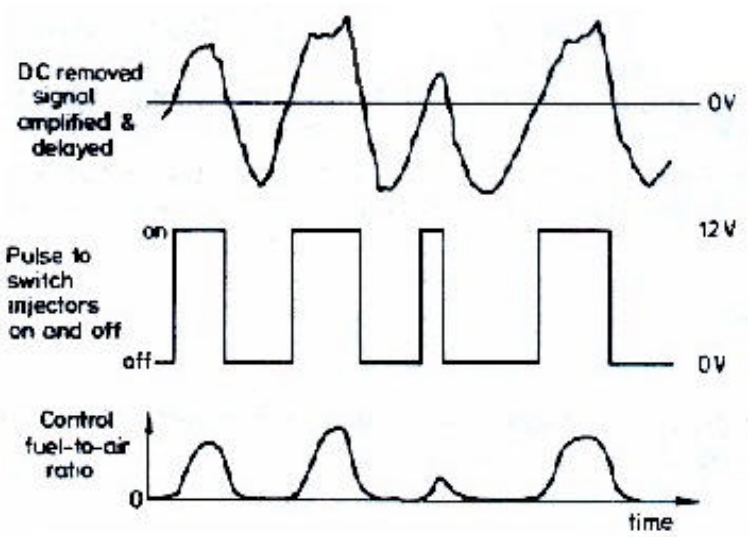

FIGURE 2.2.2 Control Scheme Used by Langhorne et al[25]

The sound pressure level of the instability at 75 Hz was 164 dB. With the control on, the sound pressure level of the instability was reduced by at least 12 dB. The power spectrum for the controlled and uncontrolled case is shown in Figure 2.2.3.

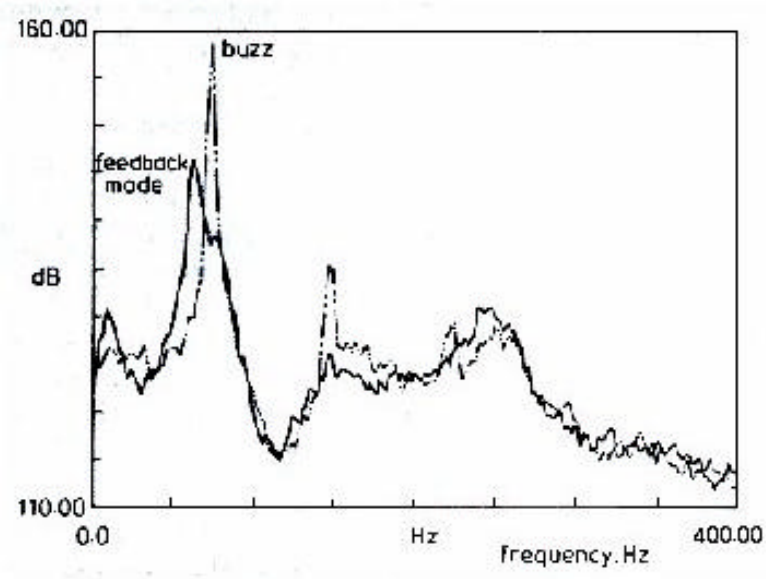

FIGURE 2.2.3 Power Spectrum for the Controlled and Uncontrolled Cases[25]

2.3 [Hantschk et al. 1997]

Hantschk worked on an experimental rig at the Technical University of Munich. The rig was a 4 megawatt single nozzle spray combustor running on liquid fuel. The actuator for control was a high response solenoid valve produced by MOOG. This valve has a flat frequency response up to 500 Hz. The rig with control system is shown in Figure 2.3.1.

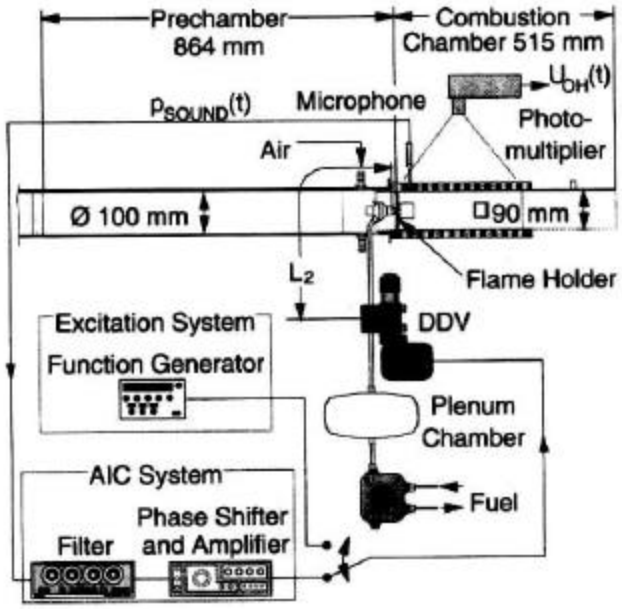

FIGURE 2.3.1 Schematic of Experimental Setup Used by Hantschk et al.[13]

As shown above, the pressure is measured with a microphone and fed through a filter to the phase shifter. The phase-shifted signal was then used to create a square wave that was fed to the DDV (Direct Drive Valve). The fuel line (L_2 in the above figure) was tuned acoustically to the frequency of the instability. The acoustic tuning of the fuel line takes advantage of the physical resonance of the fuel line to increase the overall effectiveness of the control. The equivalence ratio was kept between 0.95 and 1.2 and the volumetric flow rate was 0.001 m^3/min. The 275 Hz instability was reduced from 155 dB to 125 dB. This is shown in the power spectrums of Figure 2.3.2.

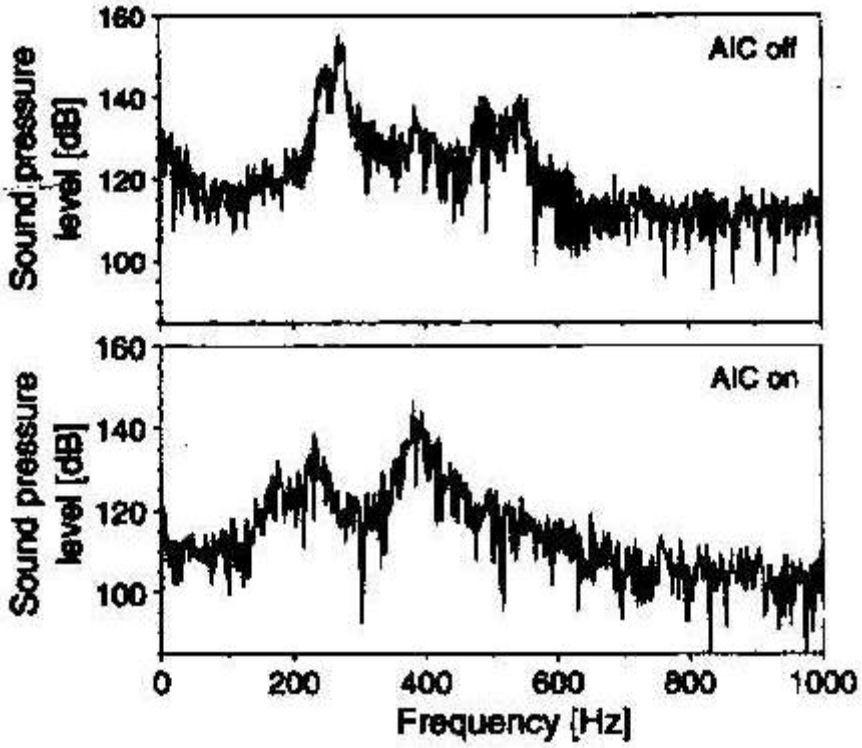

FIGURE 2.3.2 Power Spectrums for the Controlled and Uncontrolled Cases[13]

2.4 [Hermann et al. 1996)

Hermann worked with Hantschk at the Technical University of Munich. His test rig was a 36 kW turbulent burner with No. 2 diesel fuel. The equivalence ratio was generally around 0.95 with a fuel flow rate of 3.1 kg/hr. The proportional actuator used piezo stacks to vary the area of the fuel supply line and thus modulate the fuel flow. Due to the high response of piezoelectric stacks, a bandwidth of up to 1000 Hz was claimed. The rig is shown in Figure 2.4.1.

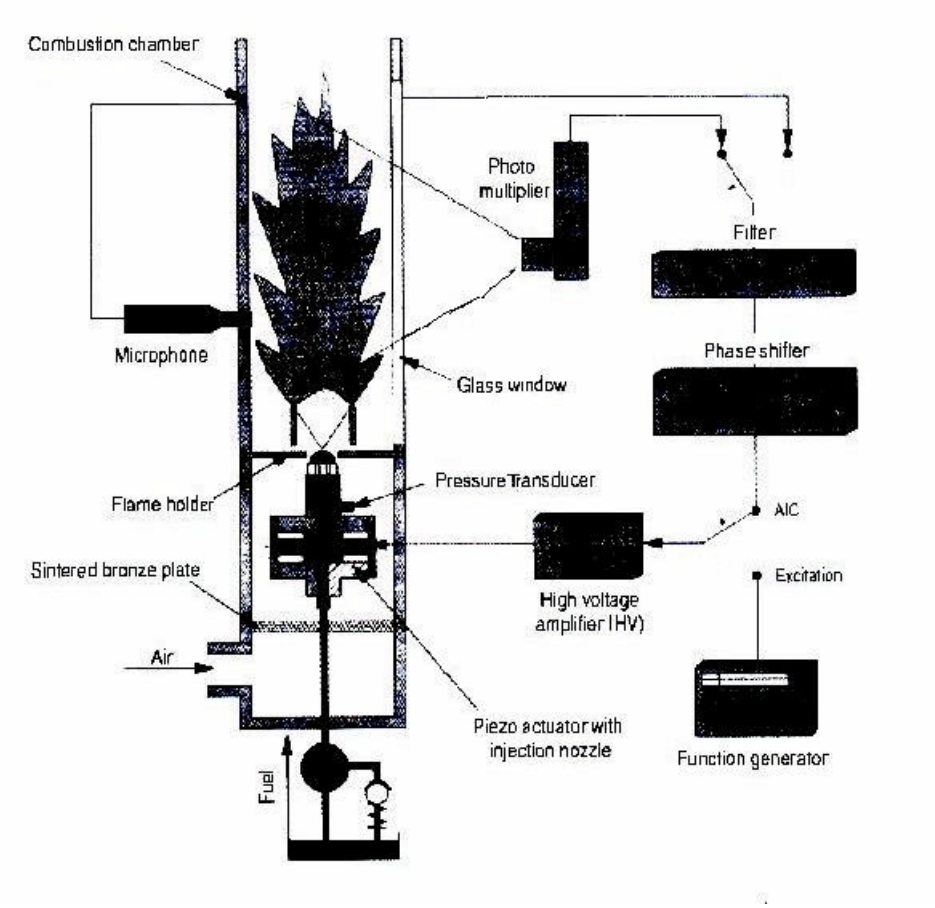

FIGURE 2.4.1 Schematic of Experimental Setup Used by Hermann et al[15]

The control setup was very similar to Hantschk. Where Hantschk only used the pressure measurement to control the actuator, Hermann looked at the pressure and the chemiluminescence taken by the PMT (Photo-Multiplier Tube). The PMT measures the OH radical emissions from the flame. This measurement is directly related to the heat release of the flame. Once again, the phase shifted signal was used with a function generator to produce the control signal. Since piezoelectric materials require relatively high voltages, a high voltage amplifier was used to increase the level of the control signal. The fuel line was acoustically tuned to the frequency of the instability as done by Hantschk. The 350 Hz limit cycle was reduced from 145 dB to 105 dB when control was applied. This is shown in Figure 2.4.2.

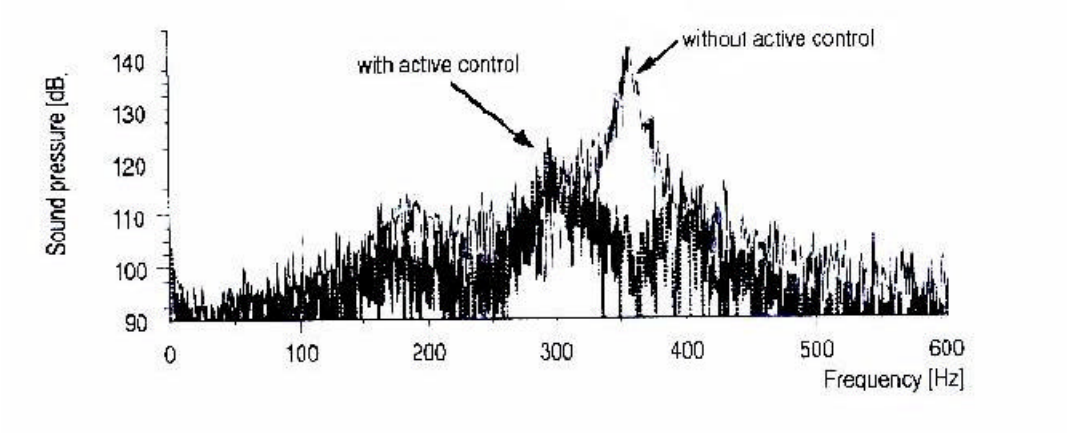

FIGURE 2.4.2 Power Spectrum for the Controlled and Uncontrolled Cases[4]

2.5 [Zinn et al. 1997]

Zinn worked on a variable length gas rocket, running methane for fuel, at Georgia Tech. The variable length was used to change the frequency of the instability. The actuator was custom built from magnetostrictive material. A magnetostrictive material changes length with a change in magnetic field. This material is much like the piezoelectric, but is more efficient in terms of input power. This material enabled the actuator to have a 400 Hz bandwidth. The experimental setup is shown in Figure 2.5.1

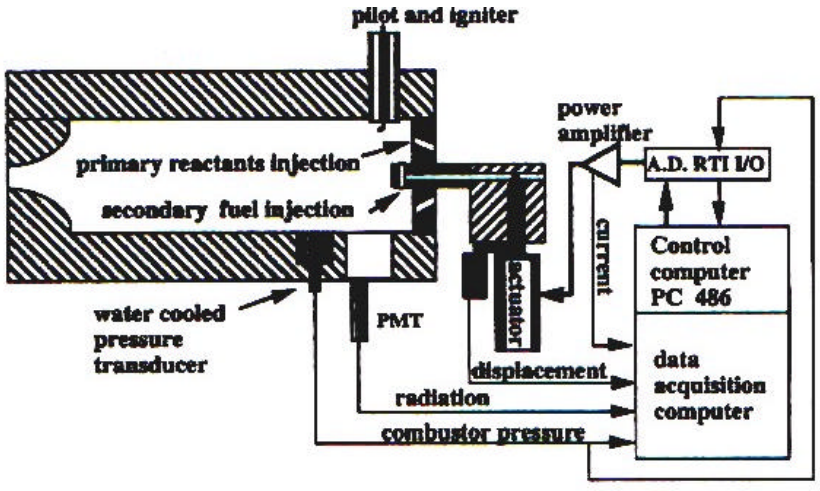

FIGURE 2.5.1 Schematic of Experimental Setup Used by Zinn et al[46]

The control setup was much different than any of the ones described earlier. Zinn fed the pressure signal into an observer. This observer was used to output out all the modes of the system from the measured signal. Once all the modes were found, each mode was given a gain and phase shifted. The modes were combined into one control signal, which was then sent to the actuator. The observer looked for a predetermined frequency. Once it was detected the actuator was turned on at that frequency. If the frequency changed during control the actuator would turn off and the observer would once again look for the unstable frequency. For the 370 Hz limit cycle the amplitude was reduced by 26 dB when control was applied. This is shown in Figure 2.5.2.

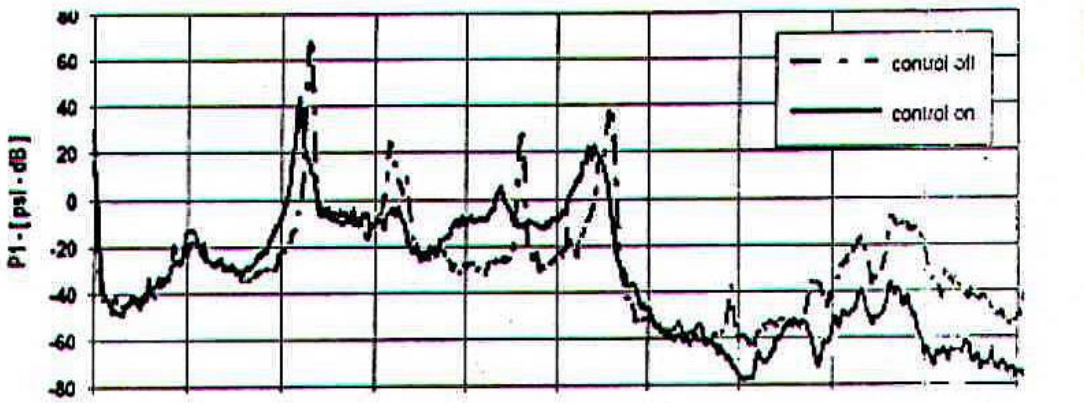

FIGURE 2.5.2 Power Spectrum for the Controlled and Uncontrolled Cases[46]

2.6 [McManus et al. 1997]

McManus did testing on a 15 kW combustor, fueled by liquid heptane, at Physical Sciences Incorporated. The actuator was a high response solenoid valve with bandwidth in excess of 300 Hz. Liquid fuel was initially used for control but required too large of a percentage of the main flow to achieve control. The percentage was in excess of 30% with liquid fuel and below 5% for gaseous fuel. Air flow was kept around 12 m/sec and the primary fuel flow rate was kept at 0.4 gal/hr. The experimental setup is shown in Figure 2.6.1.

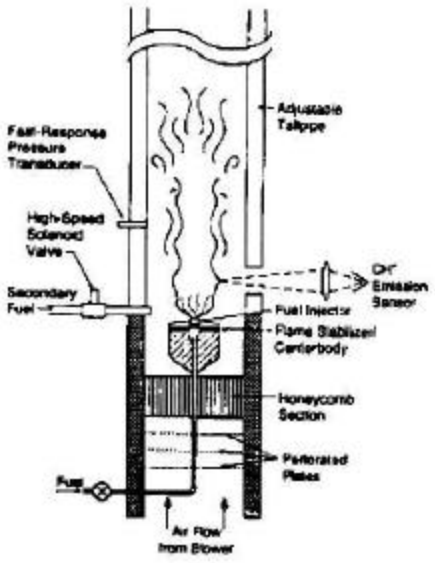

FIGURE 2.6.1 Schematic of Experimental Setup Used by McManus et al[28]

The control scheme was PWM (Pulse Width Modulation) based on the level of the limit cycle. As the limit cycled increased in level the duty cycle of the control signal was increased. This meant that as the limit cycle increases in level, the actuator stayed open longer to let more fuel pass through. The added fuel reduced the limit cycle amplitude. The control scheme is illustrated in Figure 2.6.2.

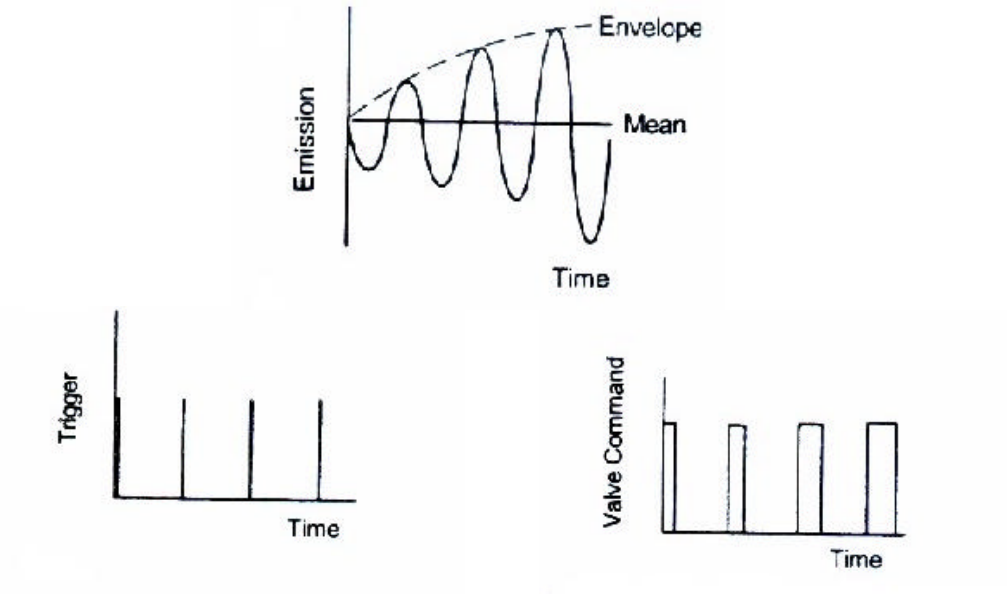

FIGURE 2.6.2 Pulse Width Modulation Based on Level of the Limit Cycle[28]

As a result of this control scheme the 80 Hz limit cycle amplitude was reduced by 25%. This is shown in Figure 2.6.3.

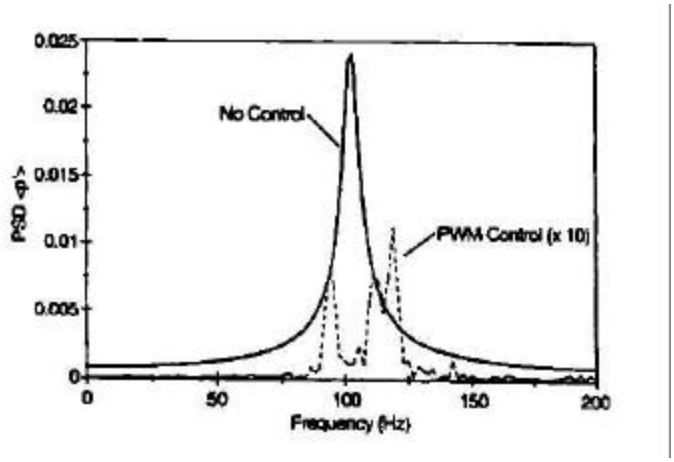

FIGURE 2.6.3 Power Spectrum for Controlled and Uncontrolled Cases[28]

2.7 [Yu et al. 1997]

Yu worked on a 110 kW axis symmetric dump combustor, run on gaseous ethylene, at the Navel Air Warfare Center in the research and technology group. Actuation was performed with a series of four high response solenoid valves. The control fuel was ethanol, or heptane mixed with ethylene. With use of all four solenoid valves, each with a bandwidth of 250 Hz, a total bandwidth of 1000 Hz was achieved. The modulated fuel flow was kept between 0.27 g/sec and 1.6 g/sec, while the steady mass flow was kept between 0.66 g/sec and 1.6 g/sec. The equivalence ratio was kept between 0.4 and 0.8 for all of their experiments. The experimental setup is shown in Figure 2.7.1.

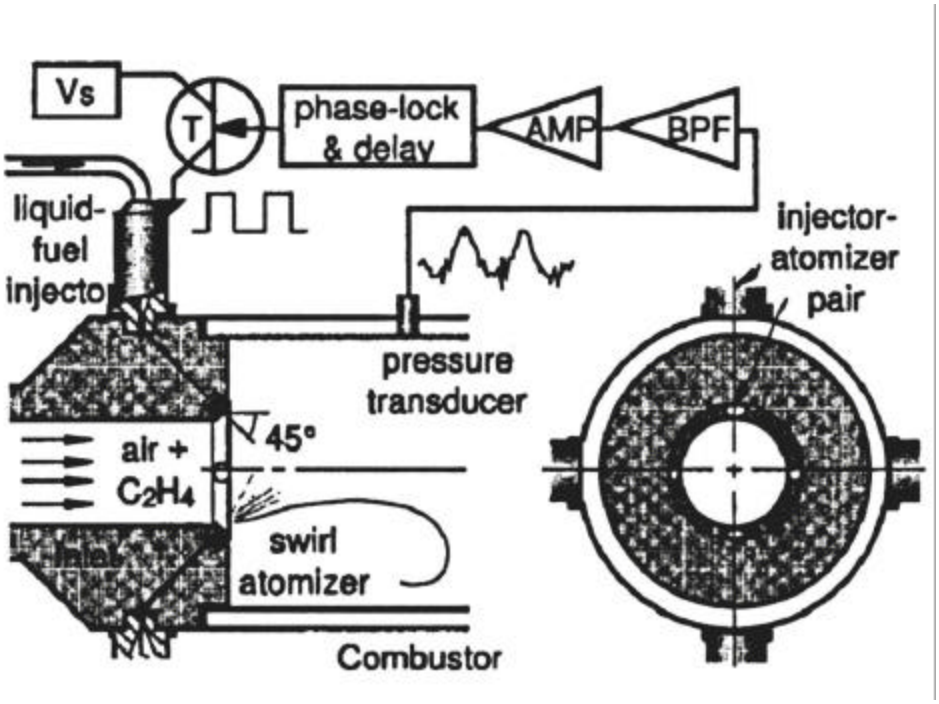

FIGURE 2.7.1 Schematic of Experimental Setup Used by Yu et al[44]

The control scheme was a simple phase locking control. The pressure signal was fed through a filter into the phase locking circuit, which created a trigger for the signal wave generator. A time trace of the control signal and the combustor pressure is shown in Figure 2.7.2.

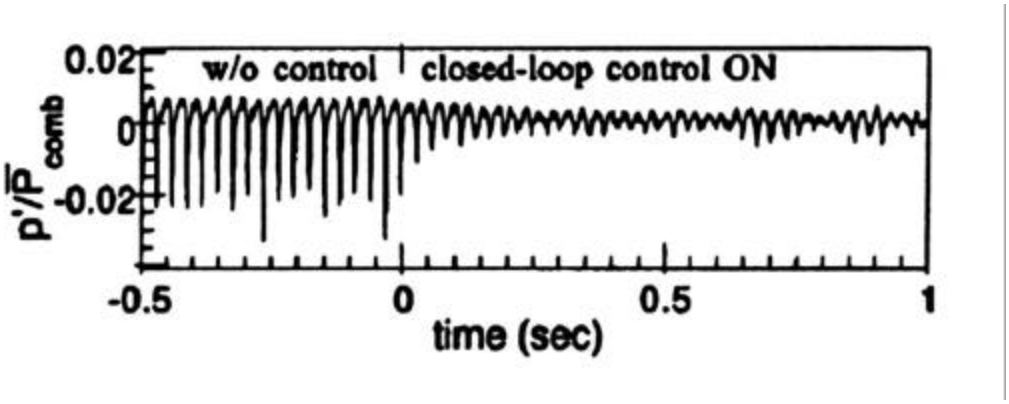

FIGURE 2.7.2 Combustor Pressure Traces Before and After Control[44]

Much time was spent exploring the effects of duty cycle on the frequency response of the system. The pulsating injection was found to have the highest frequency response when the duty cycle was set to 50%. The result of this work was a reduction in the total sound power

level by 12 to 15 dB for a frequency range of 0 to 400 Hz. This result is shown in Figure 2.7.3.

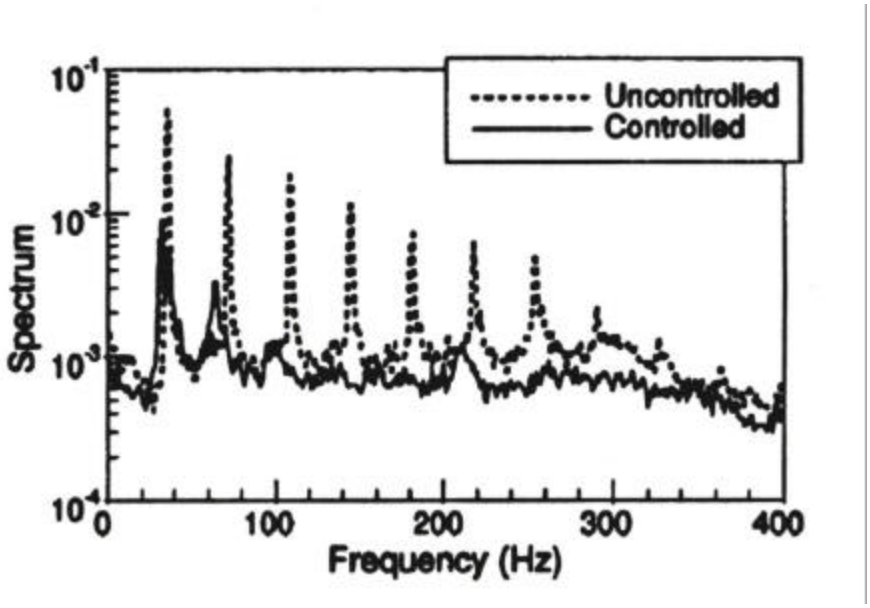

FIGURE 2.7.3 Power Spectrum for Controlled and Uncontrolled Cases[44]

Yu has done more recent work at a higher output condition of 270 kW [40]. The primary fuel for the combustor was changed to ethanol, and heptane was used for the control fuel. The result of this study was that control could not be maintained. Control was intermittently lost at this high output condition. This loss of control was attributed to the limitation of the phase shifter to adapt as the instability frequency changes during control. The time trace and frequency spectrums for the controlled and uncontrolled case are shown in Figures 2.7.4 and 2.7.5.

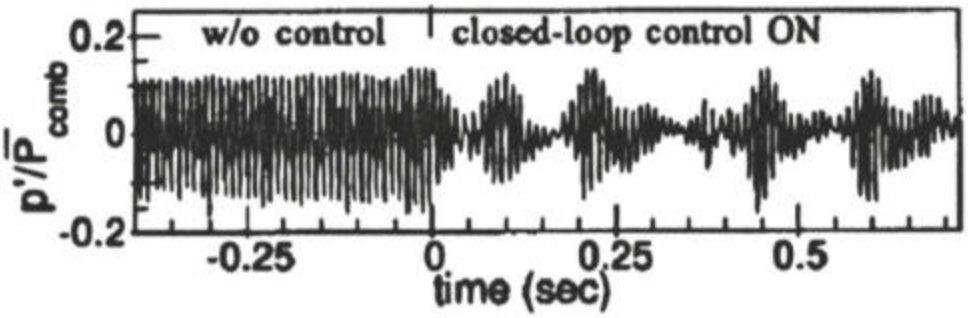

FIGURE 2.7.4 Time Trace for Higher Output Condition[44]

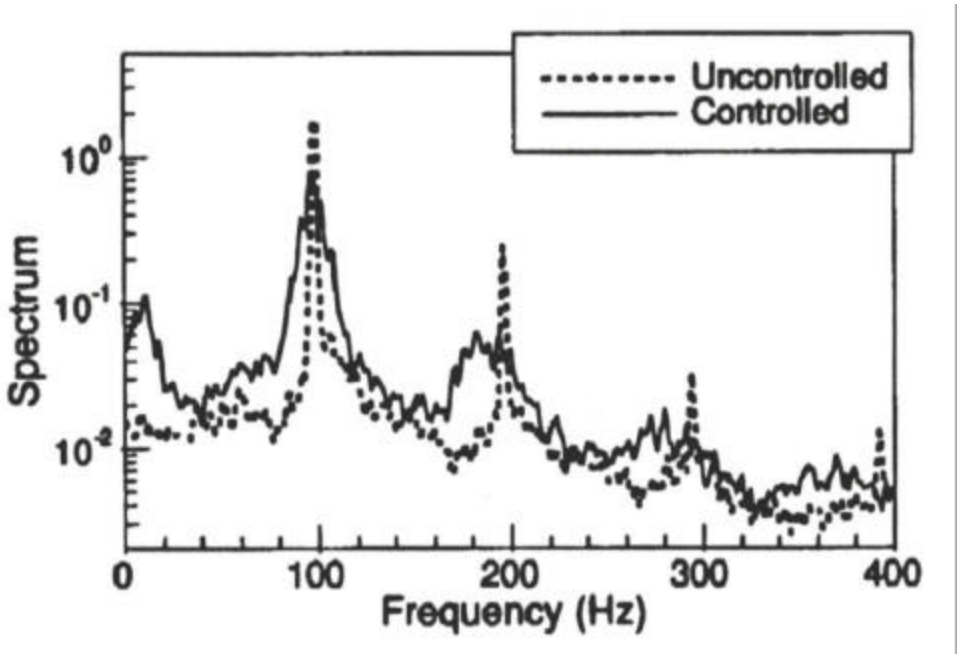

FIGURE 2.7.5 Power Spectrum for Controlled and Uncontrolled Cases for the Higher Output Condition[44]

2.8 [Seume et al. 1997]

Seume worked on a 170 megawatt Siemens model V84.3A ring combustor gas turbine. The mass flow of fuel was 9 kg/sec. Actuation was performed using four MOOG high performance solenoid valves. These were the same valves used by Hantschk. A diagram of the control setup is shown in Figure 2.8.1.

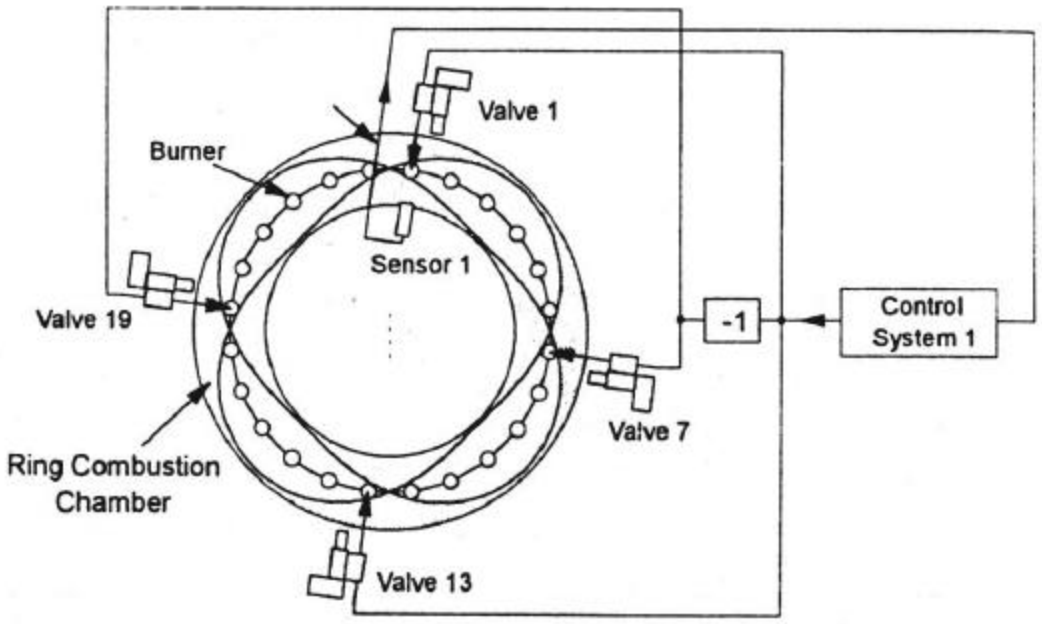

FIGURE 2.8.1 Schematic of Control System used by Seume et al.[40]

No details of the MIMO (multi-input milti-output) control system were given, but it was stated that the pressure signal was fed to the control system that drove the valves. Seume was able to reduce the 433 Hz limit cycle by 17 dB from the uncontrolled case. A pressure spectrum was not published, but time traces of the control system gain and average pressure level were given for the controlled and uncontrolled cases. These time traces are shown in Figure 2.8.2.

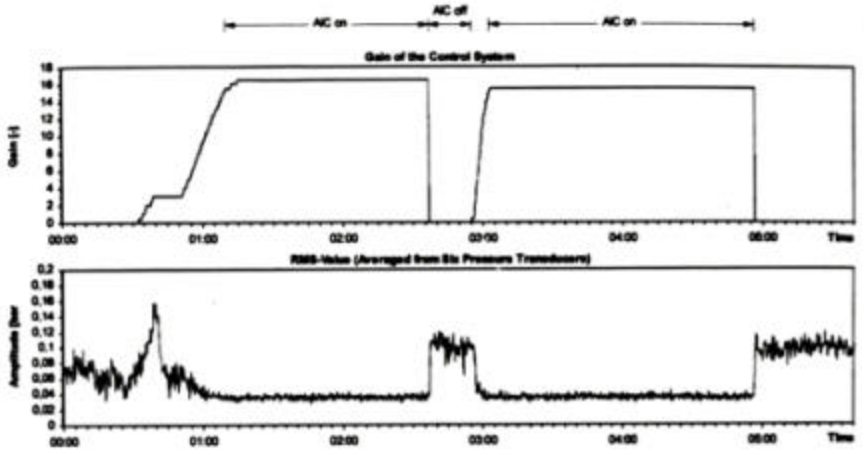

FIGURE 2.8.2 Control System and Pressure Level Time Traces[40]

2.9 [Lacy et al. 1998]

Lacy worked on a ducted flame at the University of Michigan. The rig simply consisted of sections of piping with a "T" section positioned such that the flame could be observed. The rig was fueled by propane and the flame was stabilized on a 1.625" diameter grid on top of a Meeker Burner. The control system was an Armarkov adaptive controller. The actuation done on by a servo valve produced by HR Textron. It is a high response valve rated up to 200 Hz. The actuator pulsed the air supply instead of the fuel or secondary fuel supply. Since it is the modulation in the heat release that stabilizes the system air can be used the same as fuel. Lacy was able to achieve up to 18 dB of suppression of the 265 Hz limit cycle. This is shown in the pressure spectrum of Figure 2.9.1.

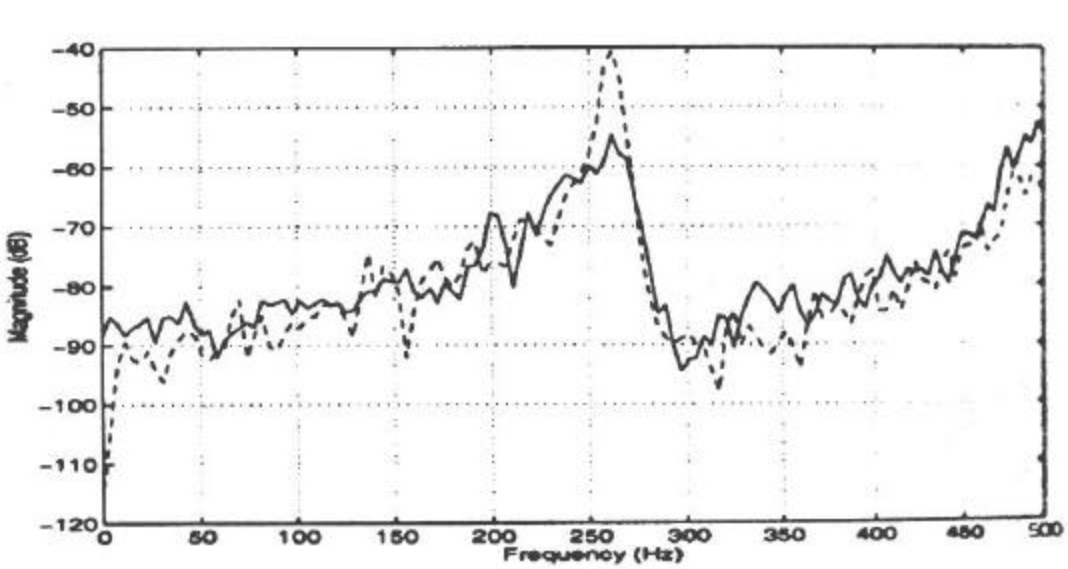

FIGURE 2.9.1 Pressure Spectrum for Controlled and Uncontrolled Cases[24]

2.10 [Cohen et al. 1998]

Cohen worked on a 4 megawatt test rig, running No. 2 diesel fuel, at UTRC (United Technologies Research Center). The rig was designed to have a limit cycle at 200 Hz under the same pressure, 1.4 Mpa, and equivalence ratios, 0.47 to 0.56, as run in the full-size

combustor. Actuation was performed with a high response solenoid valve with a bandwidth of 250 Hz. The test rig is shown in Figure 2.10.1.

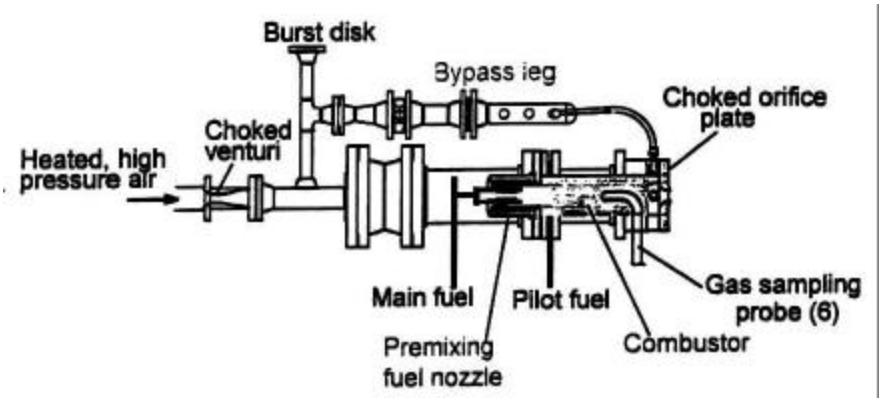

FIGURE 2.10.1 Schematic of Experimental Setup Used by Cohen et al[7]

The control system was a simple phase shifter as described in earlier works. The chemiluminescence signal was filtered, phase shifted, and used to trigger the control signal, which had a fixed duty cycle of 50%. The valve was actuated through the spokes of the premixing fuel nozzle shown in the previous figure. The 200 Hz limit cycle was reduced by 15 dB through active control. This is shown in Figure 2.10.2, where the dashed line is the uncontrolled case.

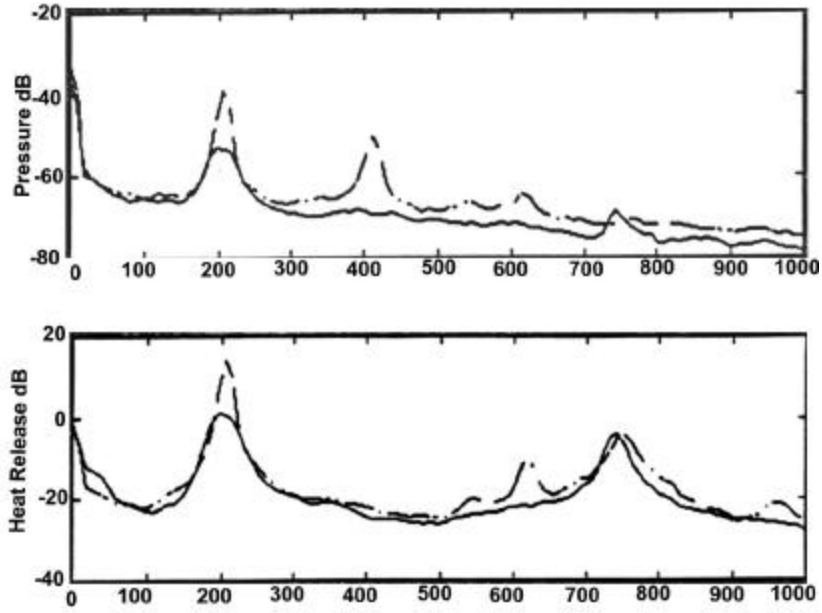

FIGURE 2.10.2 Power Spectrums for Heat Release and Pressure for the Controlled and Uncontrolled Cases[7]

2.11 [Hibshman et al. 1999]

Hibshman worked with Cohen at United Technologies Research Center. His work involved a sector rig composed of 67.5° sector cut with three nozzles instead of the single nozzle test rig used by Cohen. This rig was again designed to have a 200 Hz limit cycle with No. 2 diesel fuel. The inlet pressure was 1.1 Mpa and the equivalence ratio was kept between 0.41 and 0.45. Actuation was done with the same high response solenoid valves used by Cohen on one of the two spokes of each of the three nozzles. This rig is shown in Figure 2.11.1

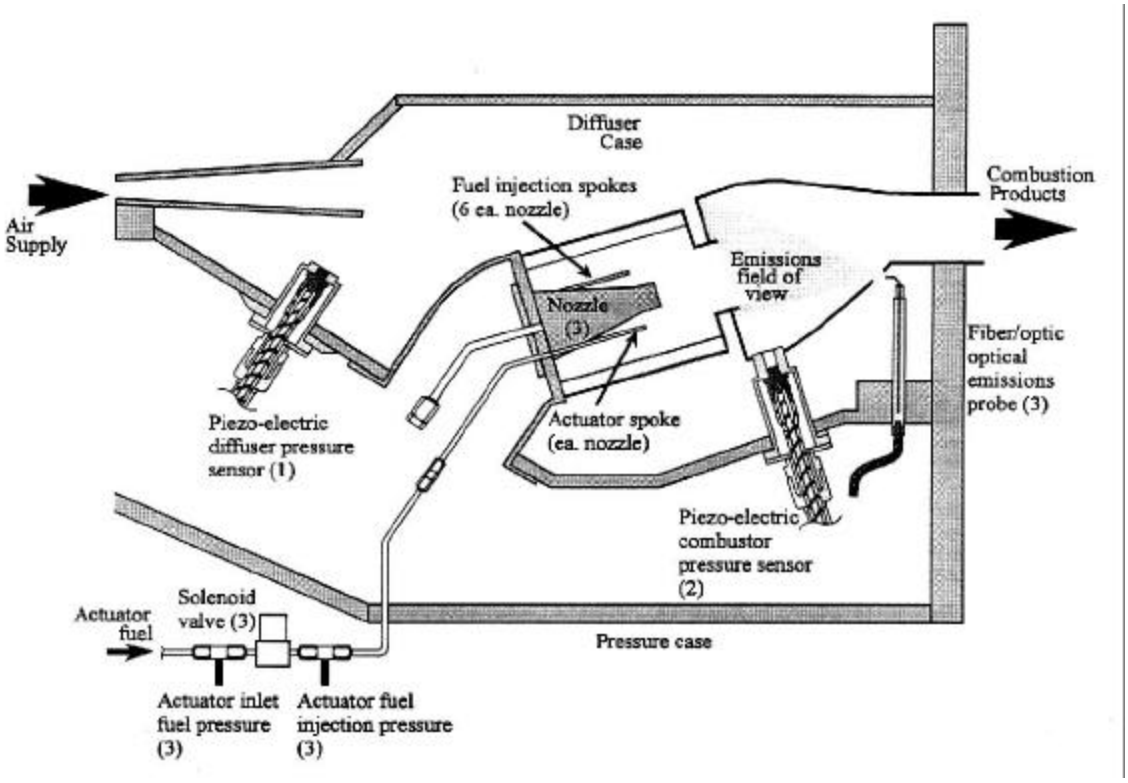

FIGURE 2.11.1 Schematic of Experimental Setup Used by Hibshman et al[16]

The control scheme was a software observer, which identified the frequency and magnitude of the limit instability. The signal from the observer was phase shifted and used to create a control signals for each of the actuators. The duty cycle was again fixed at 50%. The phase shift was adjusted independently for each of the three nozzles. This test produced a maximum of 6.5 dB reduction in the level of the limit cycle. This is shown below.

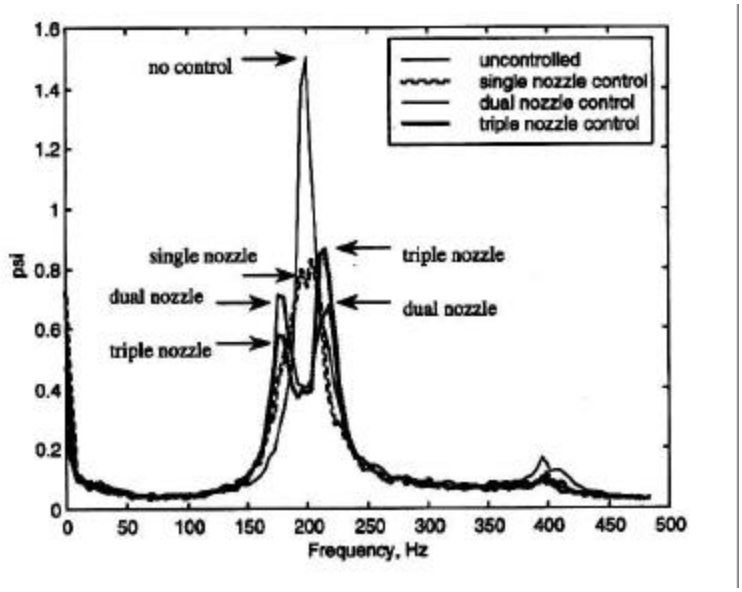

FIGURE 2.11.2 Pressure Spectrum with Multi-nozzle Acutuation[16]

2.12 [Richards et al. 1999]

Richards worked on a 30 kW premixed swirl-stabilized combustor with the U.S. Department of Energy (DOE). The actuator for this rig was a single solenoid valve that actuated the secondary fuel supply that was added to the main fuel supply. This mixture was then fed to the pre mixer. The fuel for this rig was natural gas. The equivalence ratio was kept between 0.65 and 1.0 with an actuated mass flow of 9.4 to 20.8 grams/sec. The rig is shown if Figure 2.12.1.

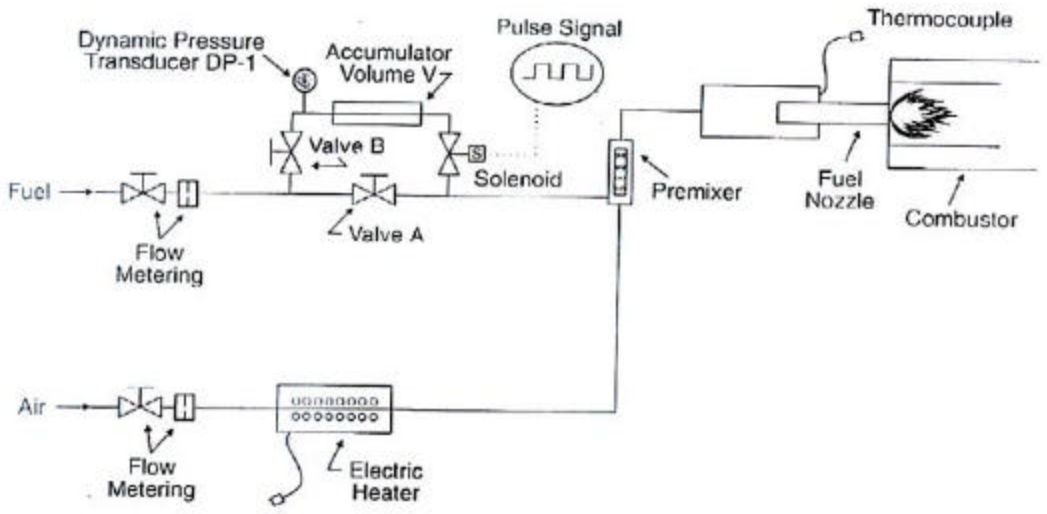

FIGURE 2.12.1 Schematic of Experimental Setup Used by Richards et al[35]

The control scheme for this system was not a typical one. The limit cycle was at 300 Hz and the fuel was modulated at below 20 Hz. The idea was that the pockets of fuel could change the equivalence ratio enough to stabilize the system. The principle is that the combustion system moves back and forth from the instability region to the region of stability. The operating condition was chosen such that this scheme could work. The end result was that they were able to reduce the limit cycle amplitude by 10.5 dB. This is an interesting case because of the low frequency of control. All other control schemes require actuating at the frequency of the instability and since these valves have a limited life span this control scheme could greatly reduce the down time for maintenance of the actuation system.

2.13 Literature Review Summary

This is all the papers containing research in the area of secondary fuel actuation for combustion control. Each of these cases had their unique conditions on their unique rigs. Fuel types also varied throughout each of these works. In all but the last case the actuator was run at the frequency of the instability with some control scheme. The limit in performance of these systems did not come primarily from the control algorithm. It mainly came for the limitations of the actuator. Table 2.12.1 is a summary of these works.

TABLE 2.12.1 Summary of Literature Findings

Researcher	Actuator Type	Bandwidth (Hz)	Fuel Type	Combustor Power	Limit Cycle Frequency (Hz)	Controller Performance
Bloxsidge	Shaker	NA	Ethylene	.25 MW	162	20 dB reduction
Langhorne	Solenoid	142	Ethanol	.25 MW	74	12 dB reduction
Hantschk	Moog	450	Liquid	4 MW	275	30 dB reduction
Hermann	Piezoelectric	1000	Diesel	36kW	360	40 dB reduction
Zinn	Magnetostrictive	400	Methane	NA	370	26 dB reduction
McManus	Solenoid	300	Gaseous	15 kW	80	25% reduction
Yu	Solenoid	4x250	Ethylene / Ethanol / Heptane	110 kW / 270kW	48	15 dB reduction
Seume	Moog	450	Gaseous	170 MW	433	17 dB reduction
Lacy	HR Textron Servo valve	200	Propane	NA	265	18 dB reduction
Cohen	Solenoid	250	No. 2 Diesel	4 MW	200	15 dB reduction
Hibshman	Solenoid	250	No. 2 Diesel	Sector Combustor	200	6.5 dB reduction
Richards	Solenoid	250	Natural Gas	30 kW	300	10.5 dB reduction

Chapter 3

Actuator Model Development

The valve is the heart of any control system used to control these thermoacoustic instabilities. To understand the operation of the valve is an important step in the control system design. It can reveal the limitations in the valve and how these limitations may be avoided in future designs to improve such things as bandwidth and control authority. A diagram of the Matrix 850 valve with the important components identified is shown in Figure 3.0.1

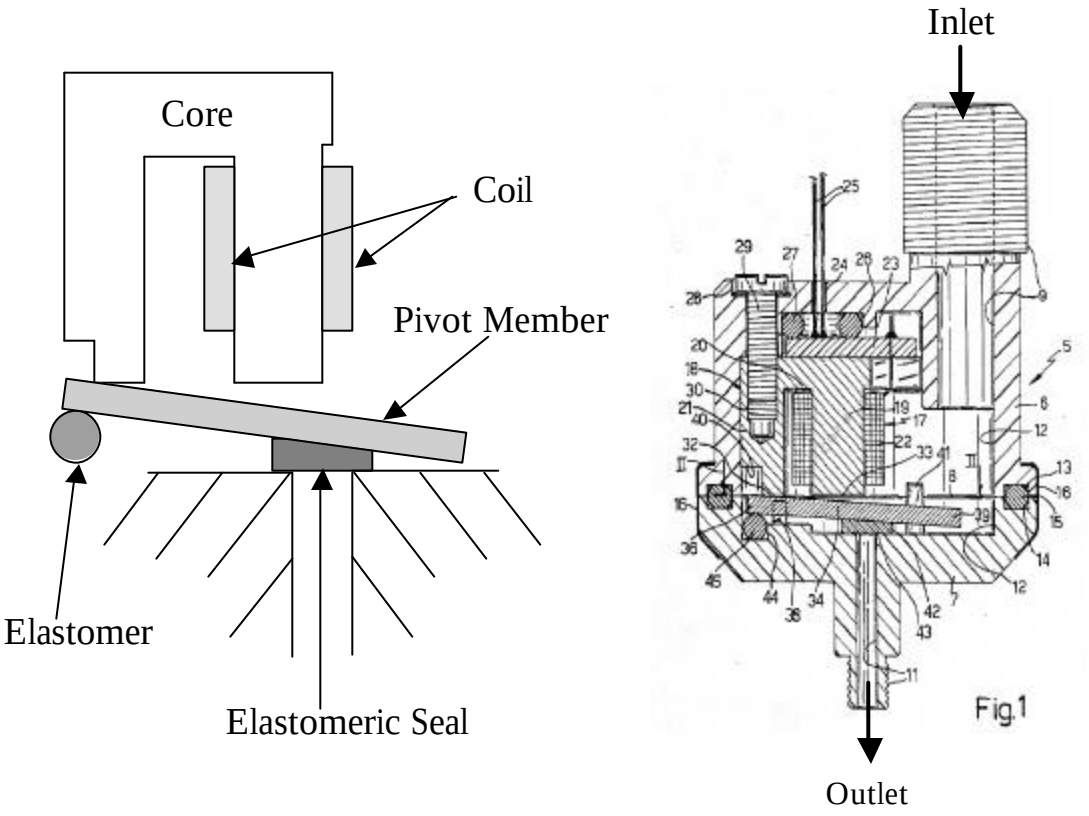

FIGURE 3.0.1 Diagram of the Valve and Its Important Components

Due the complexity of solenoid valves such as this one, a background in the fields of electromagnetics, electrical circuit theory, and mechanics is necessary to establish the required vocabulary. This background will yield the tools required to accurately model this highly nonlinear actuator and many others. The valve model is required for the actuation block of the closed-loop control simulation that will be used to accurately predict the closed-loop active combustion control experimental results.

3.1 Electromagnetics Background

The magnetic equivalent circuit technique is used for analyzing electromagnetic devices such as the one shown in Figure 3.1.1.

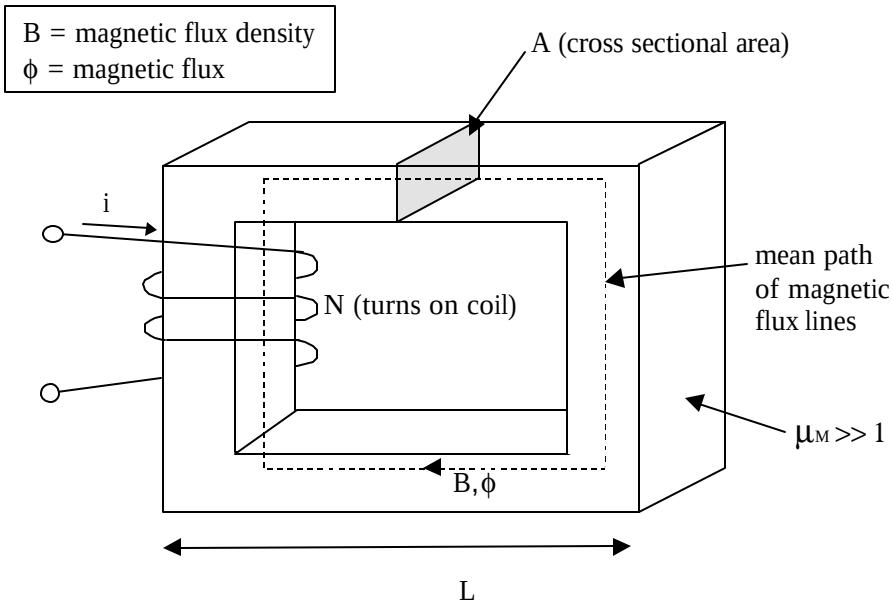

FIGURE 3.1.1 Electromagnetic Circuit

The first step is to assume a mean path for the magnetic flux. The magnetic flux density is assumed approximately constant across the entire perpendicular cross-sectional area A. This gives us the expression for flux density shown in Equation 3.1.1.

$$B = \frac{\phi}{A} \qquad \textbf{Eq. 3.1.1}$$

Using our knowledge of the flux density we can come up with the expression for the field intensity H:

$$H = \frac{B}{\mu} \qquad \textbf{Eq. 3.1.2}$$

The mmf (magnetic motive force) F_M is then found to be:

$$F_M = HL = Ni \qquad \textbf{Eq. 3.1.3}$$

Using the previous two equations the mmf is equal to the magnetic flux times the length over the permeability μ and the cross-sectional area:

$$F_M = \phi \frac{L}{\mu A} \qquad \textbf{Eq. 3.1.4}$$

In much the same way voltage is equal to current times resistance, the mmf is equal to the flux times the term $L/\mu A$. This term is referred to as the reluctance.

$$F_M = \phi R \qquad \textbf{Eq. 3.1.5}$$

Thus, reluctance is equivalent to electrical resistance, flux is equivalent to current, and mmf is equivalent to electrical voltage. Utilizing this electrical equivalence method a variety of electromechanical systems can be analyzed including the system with a gap.

The evaluation of a circuit with a gap is the same as the evaluation of a circuit without a gap. You simply find the reluctance for each individual part of the circuit and then proceed in the same manner. Figure 3.1.2 is an illustration of a system with a gap.

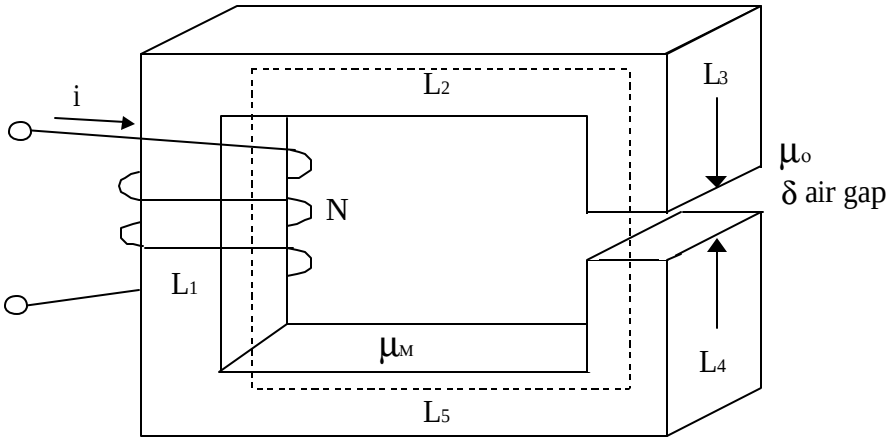

FIGURE 3.1.2 Electromechanical Circuit With a Gap

The reluctance of the core material is the total length of the mean path within the core material over the permeability and cross sectional area. This is shown in Equation 3.1.6 while the reluctance for the gap is given in Equation 3.1.7.

$$Rc = \frac{(L_1 + L_2 + L_3 + L_4 + L_5)}{\mu_M A} \qquad \textbf{Eq. 3.1.6}$$

$$Rg = \frac{\delta}{\mu_O A} \qquad \textbf{Eq. 3.1.7}$$

The total reluctance is simply the sum of Rg and Rc. The mmf in then found using Equation 3.1.5.

$$F_M = \phi \cdot (Rg + Rc) \qquad \textbf{Eq. 3.1.8}$$

Notice that the mmf is now a function of the gap size. This will prove to be an important relation in the modeling of the valve. Now that necessary electromagnetics have been presented, the necessary electrical background can be covered.

3.2 Electrical Background

A basic understanding of a resistive-inductive circuit is needed to evaluate the electrical part of the valve modeling. A basic schematic of an RL circuit is given in Figure 3.2.1.

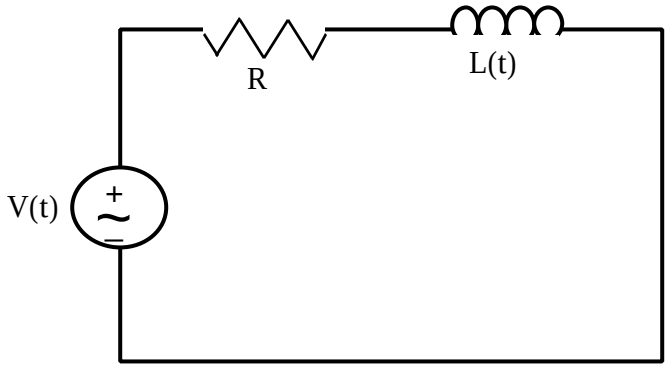

FIGURE 3.2.1 Diagram of an RL Circuit

Performing Kirchhoff's voltage law (KVL) around the circuit yields equation 3.2.1.

$$V(t) = Ri(t) + L\frac{di}{dt} \qquad \textbf{Eq. 3.2.1}$$

The inductance is the link between the electrical inductance and the reluctance of the magnetic circuit. This is shown below:

$$L = \frac{N^2}{R_T} \qquad \textbf{Eq. 3.2.2}$$

The total reluctance is equal to the reluctance of the gap plus the reluctance of the core material. Remembering that the reluctance is inversely proportional to the permeability of the material, an approximation can be made. The permeability of the material is much larger than the permeability of air making the reluctance of the air much larger than that of the core material. This leads to Equation 3.2.3.

$$L = \frac{N^2}{R_T} = \frac{N^2}{(Rg + Rc)}$$

$$Rg >> Rc$$

$$L \approx \frac{N^2}{Rg}$$

$$L \approx \frac{\mu_O A N^2}{d} \qquad \textbf{Eq. 3.2.3}$$

3.3 Mechanical Background

A basic understanding of a spring mass damper system is required to understand the mechanical part of the valve modeling effort. An example spring mass damper system is shown in Figure 3.3.1 where M is the mass of the pivot member, k is the spring constant, c is the damping constant, and θ is the angle of rotation.

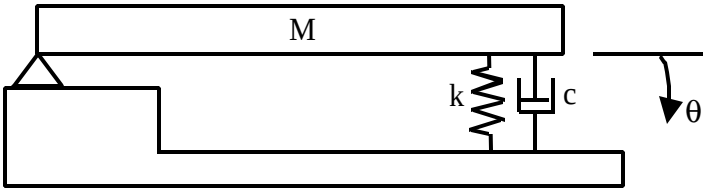

FIGURE 3.3.1 Diagram of Spring Mass Damper System

The equation of motion is then written as the sum of moments equal to the inertial moment. This equation is as follows:

$$\sum F = J\ddot{\theta} \qquad \textbf{Eq. 3.3.1}$$

The equation of motion for the system, where k and c are rectilinear stiffness and damping, shown in Figure 3.3.1 is:

$$J\ddot{\theta} = kl^2\theta + cl^2\dot{\theta} \qquad \textbf{Eq. 3.3.2}$$

The inertia J of the system is given in Equation 3.3.3 where l is the length of the pivot member.

$$J = \frac{Ml^2}{3} \qquad \textbf{Eq. 3.3.3}$$

Relating the angle θ to a displacement x the equation of motion is written in following manner:

$$x = l\theta; \dot{x} = l\dot{\theta}; \ddot{x} = l\ddot{\theta}$$

$$M\ddot{x} + 3c\dot{x} + 3kx = 0 \qquad \textbf{Eq. 3.3.4}$$

This is the basic equation of motion for the system shown in Figure 3.3.1. There are other more complex forms of damping such as hysteretic and columbic damping. These have not been applied to the simple mechanical system, but are known to exist in the actual valve.

3.4 The Full Nonlinear Model

The model begins, as with any mechanical system, with the free body diagram of the system. This free body diagram is shown in Figure 3.4.1. The elastomeric components of the valve shown in Figure 3.0.1 have been combined into an equivalent stiffness and damping term for simplicity.

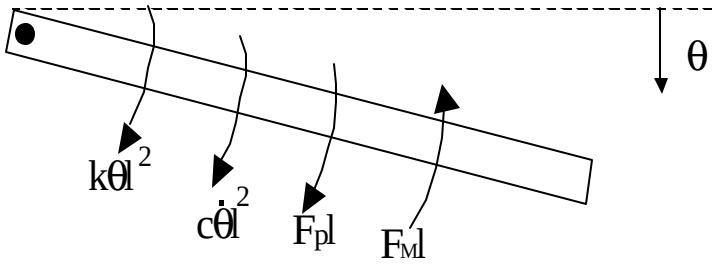

FIGURE 3.4.1 Free Body Diagram of Valve Pivot Member

The equation of motion can be written for the system, where Fp is the pressure force on the pivot member and F_M is the restoring force due to the magnetic flux or the mmf.

$$J\ddot{\theta} = -k\theta l^2 - c\dot{\theta} l^2 - F_p l + F_M l \qquad \textbf{Eq. 3.4.1}$$

This equation can be rewritten as Equation 3.4.2 using $x=l\theta$ and $ml^2/2$ for J.

$$M\ddot{x}(t) = \frac{3F_M(t)}{l} - \frac{3F_p}{l} - 3kx(t) - 3c\dot{x}(t) \qquad \textbf{Eq. 3.4.2}$$

From the background on electromagnetics earlier we saw that the magnetic motive force F_M is equal to the magnetic flux ϕ times the reluctance R. From Equation 3.2.3 we saw that the total reluctance can be approximated by the reluctance of the air gap. Using this approximation and Equation 3.1.1 the magnetic force is:

$$F_M(t) = \frac{N^2 i(t)^2 \mu_O A}{2x(t)^2} \qquad \textbf{Eq. 3.4.3}$$

Combining Equations 3.4.2 and 3.4.3 and rearranging we get the following nonlinear differential equation**.**

$$M\ddot{x}(t) + 3c\dot{x}(t) + 3kx(t) = \frac{3N^2 i(t)^2 \mu_O A}{2x(t)^2 l} - \frac{3F_p}{l} \qquad \textbf{Eq. 3.4.4}$$

Notice the damping term is just viscous damping. In the actual valve we have columbic damping due to the sliding friction of the guides for the pivot member and hysteretic damping due to the complex stiffness of the elastomer. These both have been combined into the lumped viscous damping term for simplicity.

The electrical part of the valve model is fairly straightforward. Since the valve appears as a resistor and inductor we do a simple KVL around the circuit. This is the same approach shown in the electrical background section that is shown in Equation 3.2.1. Through combining Equation 3.2.1 and 3.2.3 and placing an x in for δ we get the second differential equation that completes the electromagnetic valve model.

$$V(t) = Ri(t) + \frac{\mu_O A N^2}{x(t)} \frac{di}{dt} \qquad \textbf{Eq. 3.4.5}$$

Equations 3.4.4 and 3.4.5 make up the full nonlinear model of the valve. Due to the complexity of dealing with nonlinear equations such as these it is desirable to have a linearized version of the model that can be perturbated to see the linear range of the model.

3.5 The Linearized Model

A simple Taylor series expansion is all that is needed to linearize this model. Assume you are given that x is equal to a function of x and v. Then you can define the derivative of y in the following manner:

$$\dot{y} = F(\bar{x}, \bar{v}) + D_x(\bar{x}, \bar{v})y' + D_v(\bar{x}, \bar{v})x' \qquad \textbf{Eq. 3.5.1}$$

$$x = \bar{x} + x'$$

$$y = \bar{y} + y'$$

This is for $\bar{x}$ and $\bar{y}$ defined as the mean of x and y and x' and y' is the perturbation of x and y. The result of this Taylor series expansion is the state space model of the valve. This is shown in Equation 3.5.2. The values x_O and I_O are found by solving the statics of Equations 3.4.4 and 3.4.5 for a given V_O. For the analysis the voltage was set to 12 volts and the perturbations were centered on this point.

$$\begin{bmatrix} \frac{di}{dt} \\ \frac{dx}{dt} \\ \frac{d\dot{x}}{dt} \end{bmatrix} = \begin{bmatrix} \frac{-Rx_O}{\mu_O N^2 A} & \frac{V_O - Ri_O}{\mu_O N^2 A} & 0 \\ 0 & 0 & 1 \\ \frac{3\mu_O N^2 A i_O}{M x_O{}^2 l} & \frac{-3\mu_O N^2 A i_O{}^2}{M x_O{}^3 l} - 3\frac{k}{M} & -3\frac{c}{M} \end{bmatrix} \begin{bmatrix} i \\ x \\ \dot{x} \end{bmatrix} + \begin{bmatrix} \frac{x_O}{\mu_O N^2 A} \\ 0 \\ 0 \end{bmatrix} V(t) \qquad \textbf{Eq. 3.5.2}$$

3.6 Nonlinear/Linear Model Results

The linear model and the nonlinear model had to be simulated using two different methods. The linear model was simulated through a Maltab script file using Equation 3.5.2 and the LSIM command. This script file is available in Appendix A. The full nonlinear model required a nonlinear differential equation solver to simulate the results. Saturations needed to be used as well, to simulate the pivot member of the valve reaching the stops within the valve. For these reasons, the Simulink tool in Matlab was used. The full nonlinear simulink valve model is shown here in Figure 3.5.1.

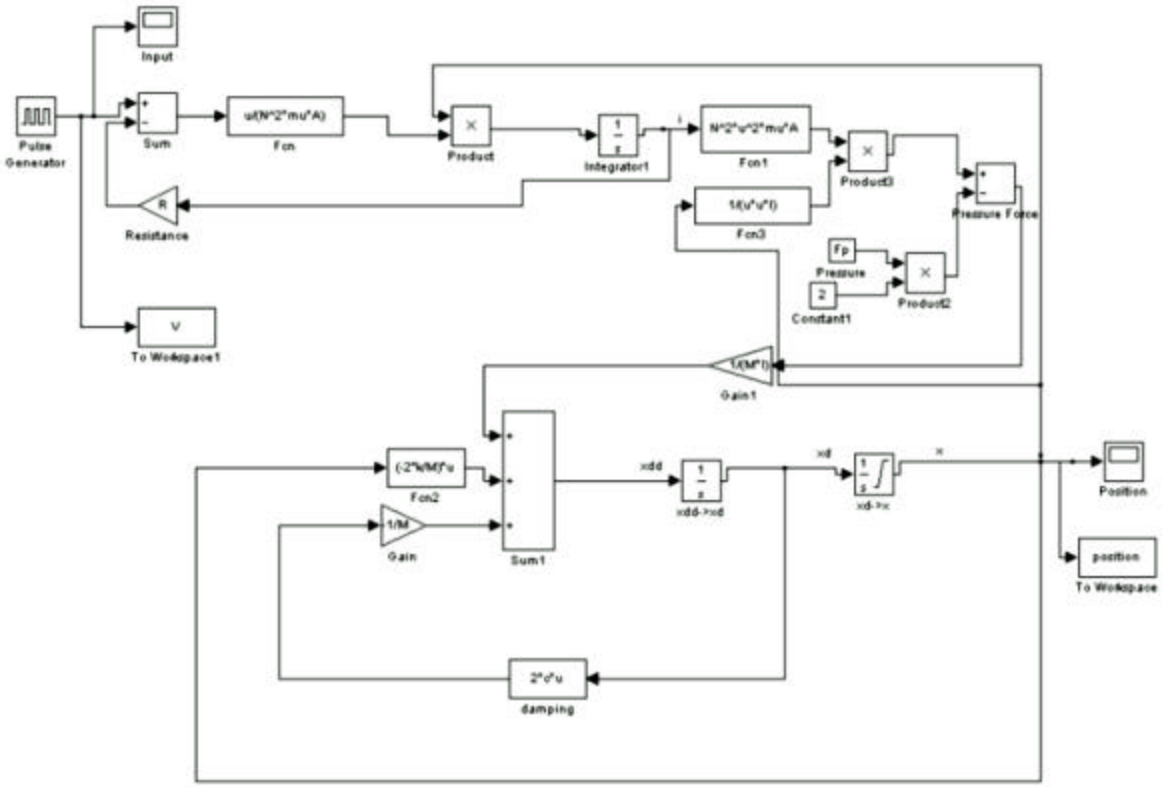

FIGURE 3.6.1 Nonlinear Model Simulink Diagram

The valve operates as an on/off valve requiring a square wave input. For the analysis of the linear range of the nonlinear model, the perturbations in the control voltage were centered on the mean voltage of 12 volts. Through plotting the linear and nonlinear results for increasing perturbations, the linear range can be identified by the agreement between the two

models. The results for four different perturbation levels are given in Figure 3.6.2. Notice the agreement between the linear and nonlinear model is beginning to degrade when a 1 volt perturbation is reached.

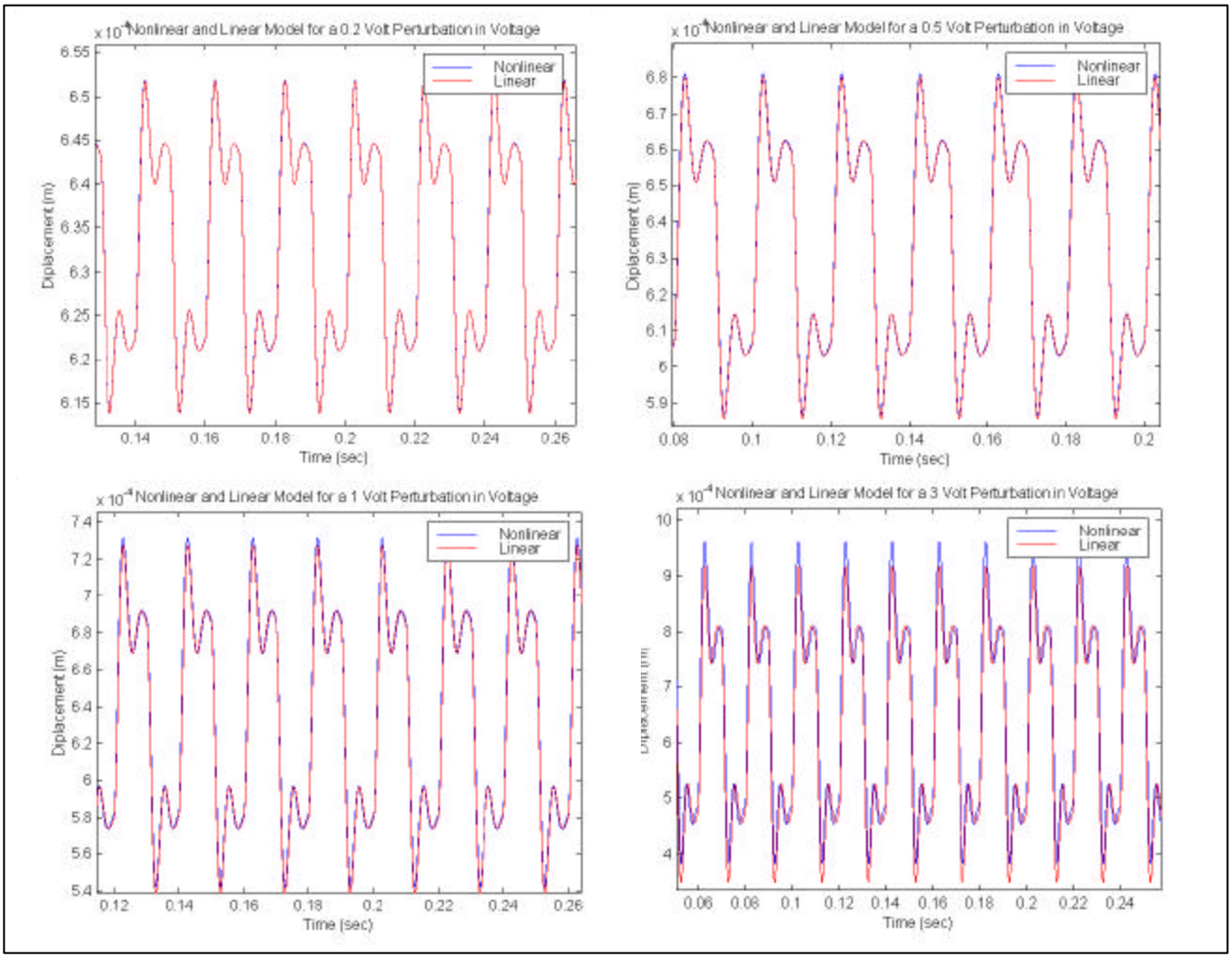

FIGURE 3.6.2 Linear and Nonlinear Model Results for Various Levels of Perturbation

These comparisons proved that our nonlinear model was functioning properly, but the voltage perturbations are not realistic. The actual valve operates on a 0-24 volt square wave. Using the full scale input, the model performance characteristics can be seen and compared to the actual valve. The full-scale model response to three different input frequencies is shown in Figure 3.5.3.

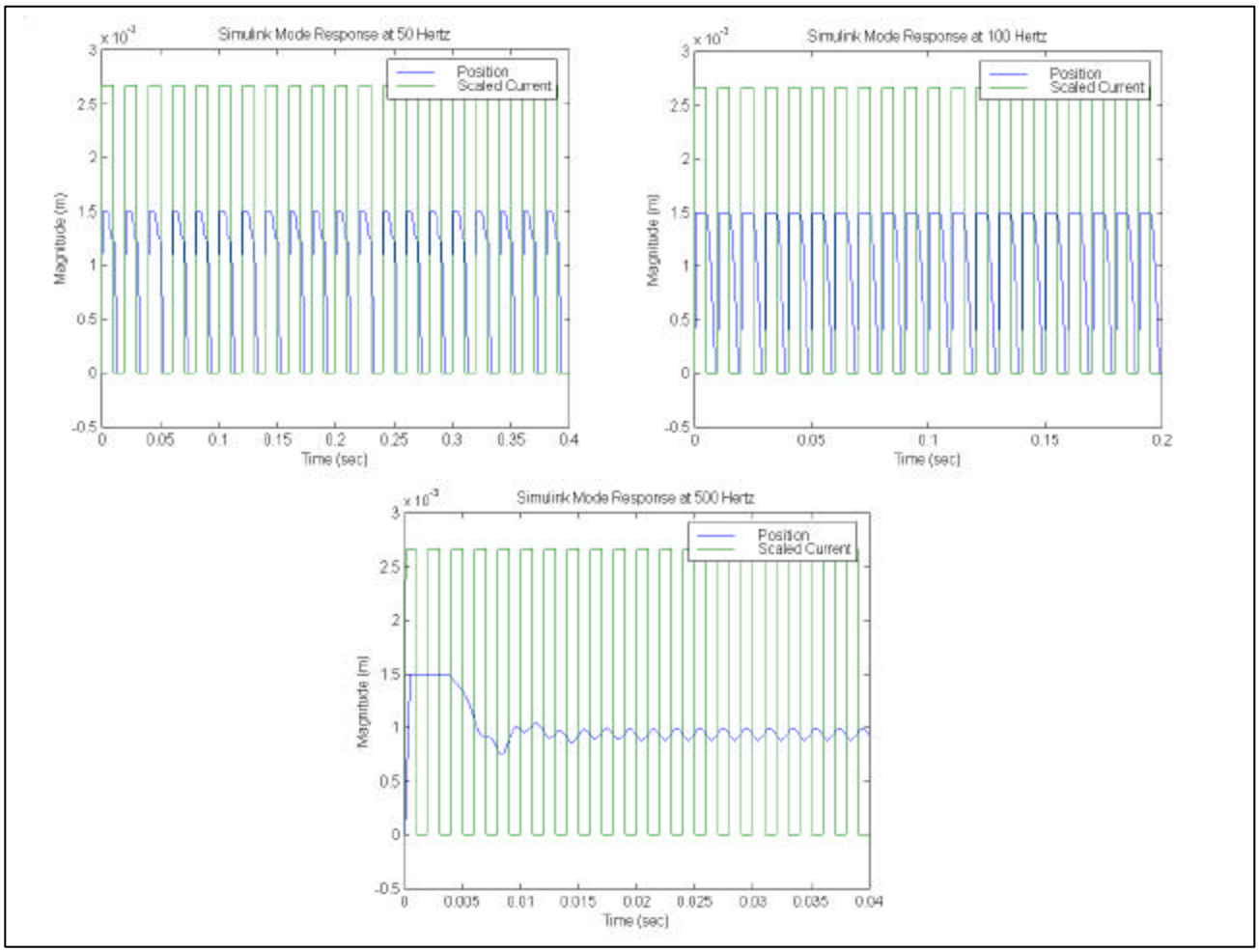

FIGURE 3.6.3 Full Scale Nonlinear Model Results for 50,100 and 500 Hz

Notice how the response of the model degrades at 500 Hz. This is the maximum frequency the actual valve can respond, according to the manufacturer. This output is a time trace. In order to generate the FRF of the model response to compare with the actual valve these time traces must be converted to the frequency domain. Once converted to the frequency domain, an FRF can be generated for the model and compared to the actual valve.

3.7 Model/Valve Comparison

The velocity of the fluid exiting the valve is the important parameter. It can be used to gage how well the fluid is being pulsed. This measurement is also necessary to compare the model to the valve. The velocity of the actual valve was measured with a hotwire. A hotwire is a very thin piece of wire that responds to fluctuations in the fluid flowing over it. It measures mean flow and the amount of flow perturbated. The hotwire signal and control signal were connected to a frequency analyzer, and the frequency response function (FRF) was recorded. The driving frequency was varied from 10Hz to 500Hz to evaluate the performance of the valve.

The FRF of the model can be found the same way. The input and output signals are used to compute the FRF. The expression for the FRF is shown below in Equation 3.7.3. G_{XX} is the product of the FFT of the input signal and its complex conjugate. G_{XY} is the product of the FFT of the input signal and the complex conjugate of the FFT of the output signal.

$$G_{XX}(f) = X(f) \cdot X(f)^* \qquad \textbf{Eq. 3.7.1}$$

$$G_{XY}(f) = X(f) \cdot Y(f)^* \qquad \textbf{Eq. 3.7.2}$$

$$H_F(f) = \frac{G_{XY}(f)}{G_{XX}(f)} \qquad \textbf{Eq. 3.7.3}$$

The response of the model and valve are shown in Figure 3.7.1. The magnitude has been normalized by the maximum value to put the two plots on the same scale. The model response compares well with that of the actual valve. The phase of the model could not be presented because the model is nonlinear. The primary assumption in performing the FFT is that the system is linear. The magnitude can be presented without error, but the phase cannot. Efforts will continue on developing a method to determine the phase without error.

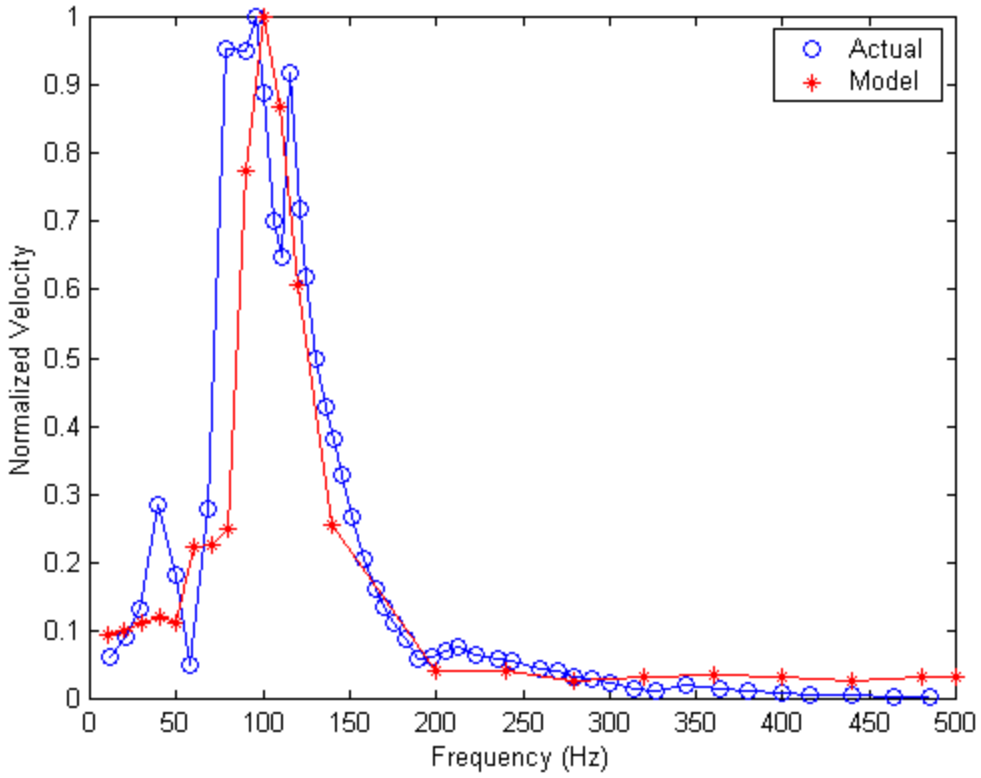

FIGURE 3.7.1 Plot of Magnitude for the Model and Valve

Chapter 4
Testing the Effects of Secondary Fuel Injection

The performance of the Matrix 850 solenoid valve was previously discussed in section 7 of Chapter 3. This test was done without an injection system and without combustion. The effect of the injection technique, discussed in Chapter 1 and to be described in more detail, on the laminar flame needed to be explored. This meant measurements of the pulse authority had to be measured, and observations needed to be made of how the injection fuel affected the existing laminar premixed flame. Making observations on the actual tube combustor was somewhat difficult due to the lack of visibility of the flame. Pressure sensors could tell how much of an effect a pulse of fuel has on the system, but observing how the flame reacted to the same pulse of fuel was not so simple. That is reason for experimenting on the laminar flame dynamics rig. Pressure sensors existed to give a measure of the amount of pulsation that the fuel had exiting the injectors. The flame's reaction to the injected fuel could be fully observed by the user due to the construction of the flame dynamics rig. This visual data revealed how the injection fuel interacted with the existing flame. Once this data was collected testing could begin on the actual tube combustor.

4.1 The Laminar Flame Dynamics Rig

The laminar flame dynamics rig was designed to be a test bed for laminar flame experiments. Due to its design, the secondary fuel injection system could be added without much intrusion. Sensors existed to measure the acoustic pressure and the flame could easily be observed making this an excellent rig for testing the injection system. The flame dynamics rig operated in a premixed fashion very similar to the actual tube combustor system. Operating conditions, with respect to equivalence ratios and flow rates, were the same. This system lended itself very well to initial testing of the injection system. A photograph of the system is shown in Figure 4.1.1. The premix was injected through the copper tube as shown in the picture. The premix traveled upwards from the injection point through the reducing

section to the final cross sectional diameter. This diameter was the same as that of the tube combustor. The mixture then traveled through the ceramic flame holder where it was ignited. The flame holder is shown in Figure 4.1.2. There were two microphones inside the rig for measuring the acoustic pressure and particle velocity and two thermocouples for measuring the flame holder temperature on the top and the bottom.

FIGURE 4.1.1 Laminar Flame Dynamics Rig

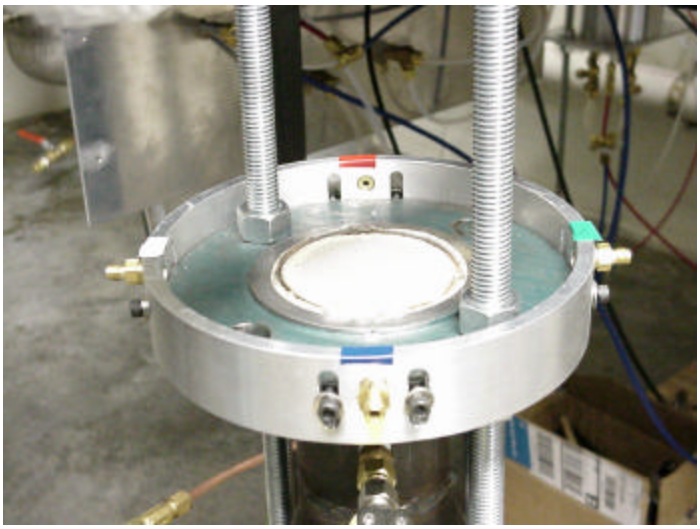

FIGURE 4.1.2 Flame Holder and Injector Ring

4.2 The Injection System

To implement the secondary fuel injection system to the flame dynamics rig, an Aluminum ring was constructed with ports for four injectors. This ring was set at a height to where the injectors were situated 1 millimeter above the flame holder. This can be seen in the previous picture. The injectors were made up of a length of ¼" tubing that breaks the fuel into four branches. Each of the four ¼" branches are reduced to 1/8" tubing that has an inner diameter of 1/16". A flow scheme for this system is shown below in Figure 4.2.2. Injection can be performed using one, two, or all four injectors.

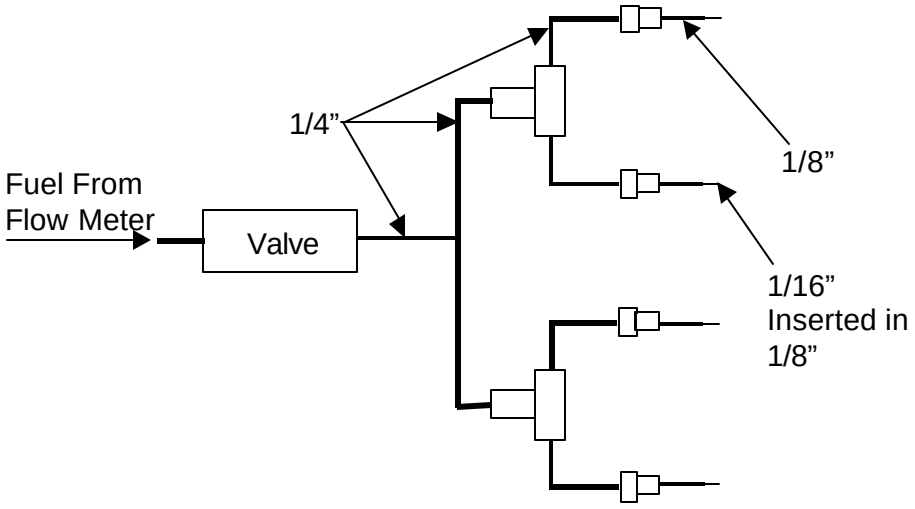

FIGURE 4.2.2 Diagram of Secondary Injection System

Into this tubing was inserted the 1/16" tubing with the inner diameter to give the desired flow rate out desired as discussed in Chapter 1. As stated earlier, the total flow rate of the tube is 150 cc/sec of which approximately 10% is fuel. That is:

$$\dot{V}_{Fuel} = 0.1 \cdot 150 \frac{cc}{sec} = 15 \frac{cc}{sec}$$

Based on this amount of fuel we wanted the modulated fuel to be 10%. That gave a total of 1.5 cc/sec of modulated fuel. With a convective flow rate of 5 cc/sec and a flame speed of 30 cm/sec the flow coming out of each of the injectors had to be approximately 35 cm/sec. That gave an exit area for each of the four injectors of:

$$A = \frac{\dot{V}_{Mod.}}{V_{Flame}} = \frac{1.5 \frac{cm^3}{sec}}{4 \cdot 35 \frac{cm}{sec}} = 0.01071 cm^2$$

This gives an inner diameter of:

$$d_{inner} = \sqrt{\frac{4 \cdot A}{\pi}} = 1.167 mm$$

The actual inner diameter of the tubing used was 1.06mm that gives a theoretical flow out of 41.9 cc/sec.

Another major concern with the injection system was phasing. With four branches to the system, and such low velocities, matching the phase of each branch was very difficult. Given a goal of 10% error in phase between the branches and a frequency of 180Hz the maximum permissible difference in length is as follows:

$$T = \frac{1}{180Hz} = 0.00555 sec$$

$$A_{1/4"} = \frac{\pi(.21in)^2}{4} = 0.0346 in^2 = .223 cm^2$$

$$V = \frac{1}{4} \cdot \frac{1.5 \frac{cm^3}{sec}}{.223 cm^2} = 1.68 \frac{cm}{sec}$$

$$\Delta L_{Max} = 1.68 \frac{cm}{sec} \cdot 0.1(0.00555 sec) = 0.000933 2cm$$

This gives less than 0.4 thousands of an inch difference in length to have at most 10% difference in phase. This is a very tight tolerance to meet. As the volumetric flow rate increases this tolerance becomes more relaxed, but is still very small.

4.3 Cold and Hot Comparison

In order to best see the effects of the fuel injection on the system, tests were performed with and without the flame. Cold flow refers to the system without combustion and air injected through the rig and pulsed through the valve. Hot flow refers to the system with combustion going on and fuel injected and pulsed through the valve. To start out simple, and to avoid any effects of phase discrepancies, only one injector was first tested. The valve was operated between 170 Hz and 180 Hz in 2 Hz intervals. This forcing of the valve was done with a wave generator at a constant duty cycle of 15%. The frequency range was chosen to examine the authority of the valve at frequencies close to the limit cycle in the tube combustor. The total flow through the rig was fixed at 180 cc/sec. The secondary injection flow rate was set to 3 cc/sec. This would be equivalent to 20% fuel modulation in the actual tube combustor. For the hot flow condition the equivalence ratio was set to 0.6 with a total flow of 180 cc/sec and the secondary injection of methane was set to 3 cc/sec. The entire process was done for two injectors as well. They were constructed to be as close to identical in length as humanly possible. The power spectrum results, taken from the top microphone inside the rig, are tabulated in Table 4.3.1 for cold flow and Table 4.3.2 for hot flow. An example of the power spectrum and coherence plot for the two injector hot and cold flow testing is given in Figure 4.3.1.

TABLE 4.3.1 Open Loop Cold Flow Test Results

Frequency (Hz)	1 Injector Power Spectrum ($dBVrms^2$)	2 Injectors Power Spectrum ($dBVrms^2$)
170	-109.7	-103.5
172	-109.5	-103.6
174	-110.5	-103.0
176	-109.6	-103.6
178	-109.9	-103.1
180	-107.0	-102.7

TABLE 4.3.2 Open Loop Hot Flow Test Results

Frequency (Hz)	1 Injector Power Spectrum ($dBVrms^2$)	2 Injectors Power Spectrum ($dBVrms^2$)
170	-104.8	-99.6
172	-104.8	-99.7
174	-104.4	-100.5
176	-104.5	-100.8
178	-105.1	-102.3
180	-105.1	-102.2

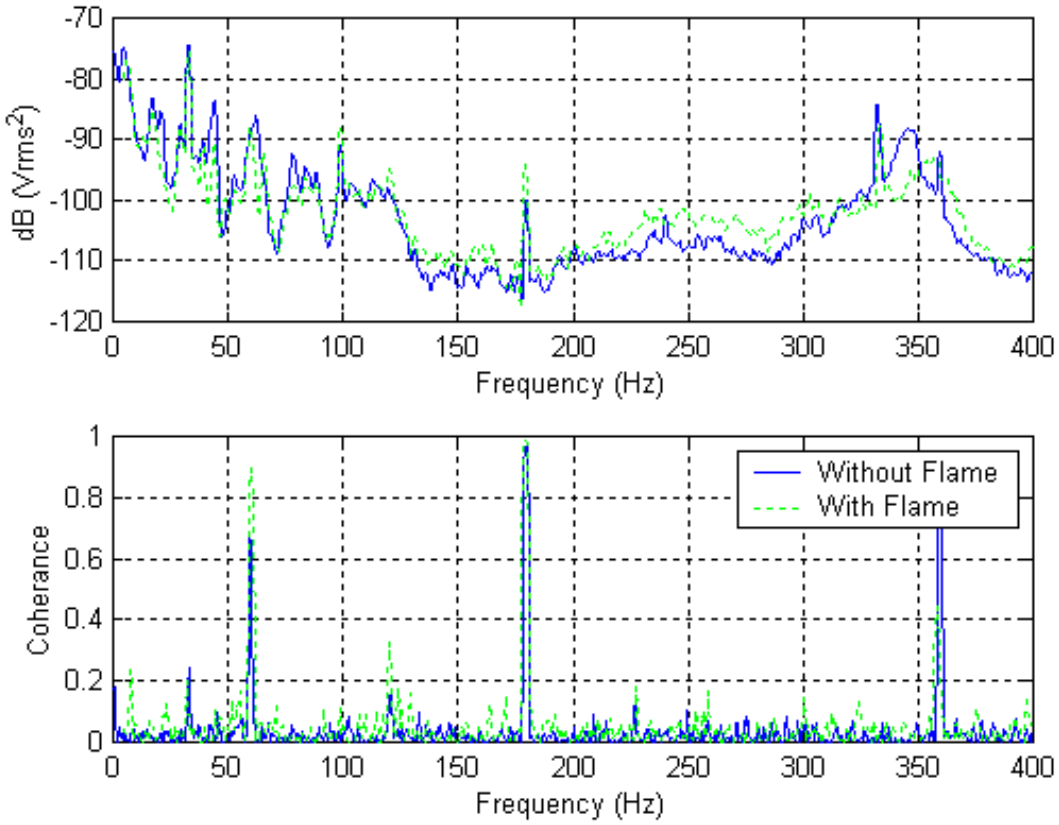

FIGURE 4.3.1 Power Spectrum and Coherence Plot for one Condition for Hot and Cold Flow

The data shows that this injection technique does have enough authority to produce a highly coherent signal at the frequency driven. Whether this is enough authority to gain control of the tube remains to be seen. The data also indicates that two injectors give a better response than one injector. Keep in mind that there may still be substantial amounts of phase difference between the two branches of injection. This variable in the experiment will never be removed. There is no way to manufacture the injectors to be sure that they are phase matched exactly.

The purpose of this experiment was for visual data as well. The manner in which the flame would respond to these jets was unknown. Two diffusion flames formed at the exit of each of the injectors that had little effect on the primary flame at an equivalence ratio of 0.6. A large portion, up to 80%, of a diffusion flame's heat release is radiated by the soot. This means that only approximately 20% of the flames heat release couples to the gases. If control authority is defined as heat release coupled to the gases, theses flames have little authority. It was also observed that at lower equivalence ratios, below an equivalence ratio of 0.55, the injected fuel would pull the primary flame up off the flame holder. At higher equivalence ratios, an equivalence ratio of 0.65 or higher, the primary flame has too much gain to be effected by the secondary injection fuel. This means that the injection fuel can have more affect on the primary flame at low equivalence ratios due to the lower gain. This jet-flame interaction was verified by a thermocouple that was imbedded in the flame holder. The flame holder temperature dropped in excess of 300K when the injectors were turned on. This data gives evidence that injection fuel authority, where authority is defined as heat release coupled to the gases, at low equivalence ratios is enough to disturb the primary system.

The purpose of this test was met. It was verified that some authority can be obtained from this injection technique. A more useful measurement variable would have been the heat release, but this measurement was not available at the time of test. Useful observations were made with respect to the interaction of the primary flame with the secondary jets. The visual and thermocouple data suggested that the pending control system will have more authority at lower equivalence ratio conditions where the injection fuel can interact with the primary flame.

Chapter 5
Attempting to Control the Actual System

With the injection system testing complete, the next part of this research focuses on closed-loop control of the actual tube combustor. Only when control is attempted on the actual system will all the requirements for secondary fuel control be discovered. Controlling this laminar premixed tube combustor is not a simple task. In fact, this is the first published attempt to control the laminar premixed tube combustor with secondary fuel actuation. In this system diffusion is a very important consideration. The gaseous methane is low in energy density, relative to liquid and even other gaseous fuels, effectively lowering the control gain. On the other hand, the flame is very thin that promotes a high energy density. The required control must be high to over come the self-exited system. In the works presented in Chapter 2 the premixed swirled flames were spread out over an area and lower in energy density while the control fuels were higher in energy density. Also, diffusion was not a problem in those cases due to the high flow rates relative to the diffusion velocity. The tube combustor system may be low in energy output, but still presents many challenges that are similar to those found in more realistic combustors. These challenges were overcome, and the primary goal to control the system thermoacoustic instability was reached.

5.1 The Laminar Premixed Tube Combustor

The tube combustor was described in Chapter 1. It is a 60-inch, closed-open tube with a flame holder normally located at 30 inches. Due to the injection technique it was necessary to move the flame holder up 1 inch. This change in flame holder location did not affect the unstable characteristics of the tube combustor. It simply allowed the use of two ¼" NPT threaded holes, already in the tube, for the secondary fuel injection. The details of implementation of the injection system will be explained further in the section to follow. The fuel is premixed with air and then injected into the tube at its bottom. The mixture convects

up through the flame holder where it is ignited. The tube is typically operated at 120 cc/sec to 150 cc/sec total flow, with equivalence ratios of 0.5 to 0.8.

5.2 The Fuel Injection System

The injection system is the same system that was used on the flame dynamics rig. It consists of four injectors constructed of 1/8" tubing with 1/16" tubing cemented inside. All the lengths of tubing have been cut to be the same length as closely as possible. Looking back at the calculations done in Chapter 4, the lengths must be within 0.004" to insure the phasing of the branches are correct. An example of an injector, used for control, is shown in Figure 5.2.1.

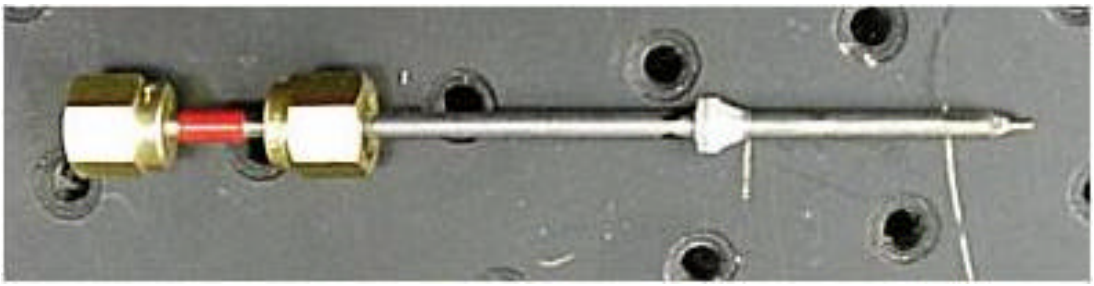

FIGURE 5.2.1 Fuel Injector

The injectors were attached to the tube combustor using two means. As already stated, the flame holder was moved up 1 inch so two existing ¼" NPT threaded holes could be used for injection. The rod, connected to the flame holder, was pushed up from the tube's bottom until the flame holder was in the proper location for the experiment. The proper location, for the flame holder, was chosen so that the injectors, already attached to the tube through the preexisting holes, were 1 mm above the flame holder. Two 1/8" Swagelok to ¼" NPT conversion fittings were drilled and threaded onto the tube. The fittings were drilled so the 1/8" tubing could slide through the fitting freely. Once in place 1/8" Swagelok nuts, using nylon front and back ferrules, were tightened. This is illustrated in Figure 5.2.2. In order to perform four point injection, two slotted plates were constructed to replace the windows of the tube combustor with two injection points. The tube with the windows in place can be seen in Figure 5.2.3. . The plates were slotted so that the injectors

could be placed 1 mm above the flame holder through moving the injection plates. The plates used the existing holes for the machine screws that held the windows in place. The injectors were inserted through a 1/8" normal pipe threaded hole, in the injector plates, with 1/8" Swagelok to 1/8" NPT conversion fittings. These fittings were cut off flush with the plates on the sides facing the tube prevent the fitting from interfering with the flame holder. These fittings were also drilled through so the 1/8" tubing could slide freely through the entire fitting. Once the injectors were in place, they were fasted in the same manner as before. In connecting the plates to the tube, the window frames were used as spacers to allow the plates to slide freely without infringement from the tube. A flameproof fabric was cut to form gaskets that went between the tube and window frame, and then between the window frame and injector plate. The final result was four injectors situated 1 millimeter above the flame holder. This is also illustrated in Figure 5.2.2. The tube, with the injectors attached, is shown in Figure 5.2.4. The injectors were fed by the valve through a series of equal length ¼" plastic tubing. This tubing scheme was presented in Figure 4.2.2.

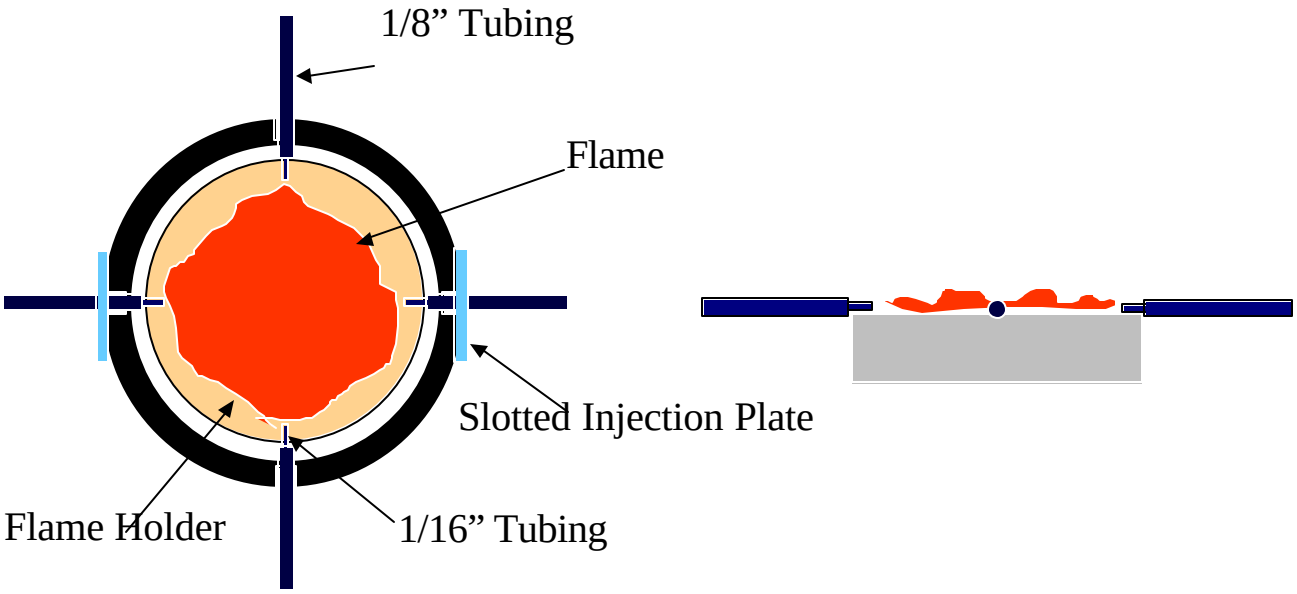

FIGURE 5.2.2 Schematic of Injectors Implementation

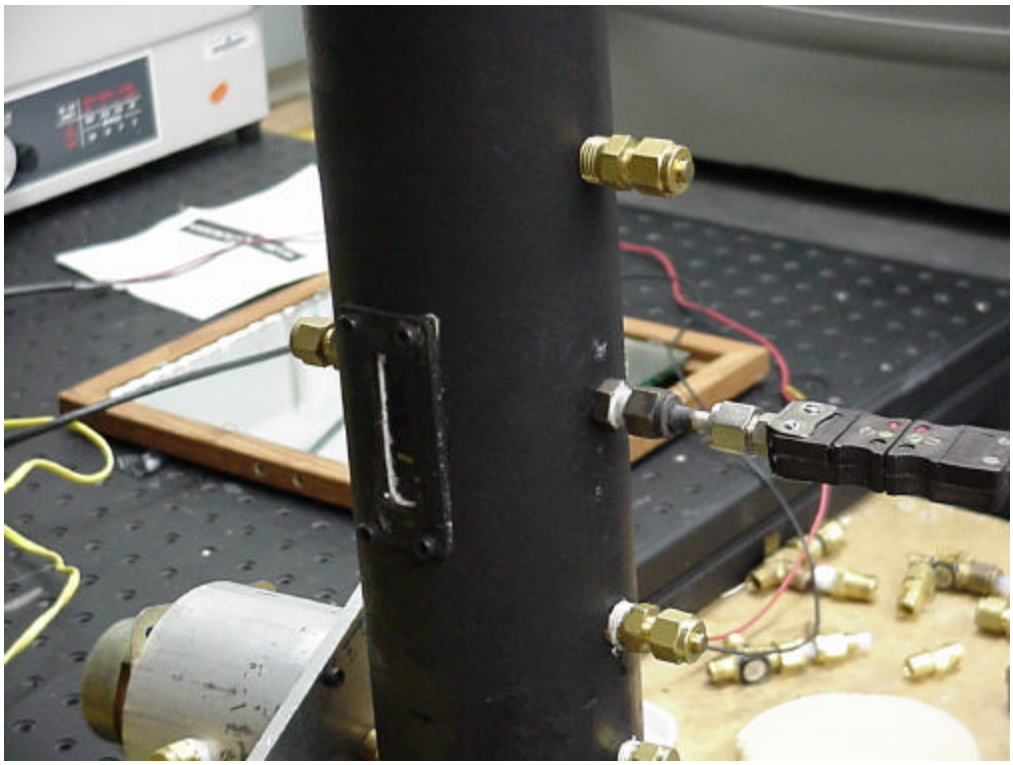

FIGURE 5.2.3 The Tube Combustor Without the Injection System

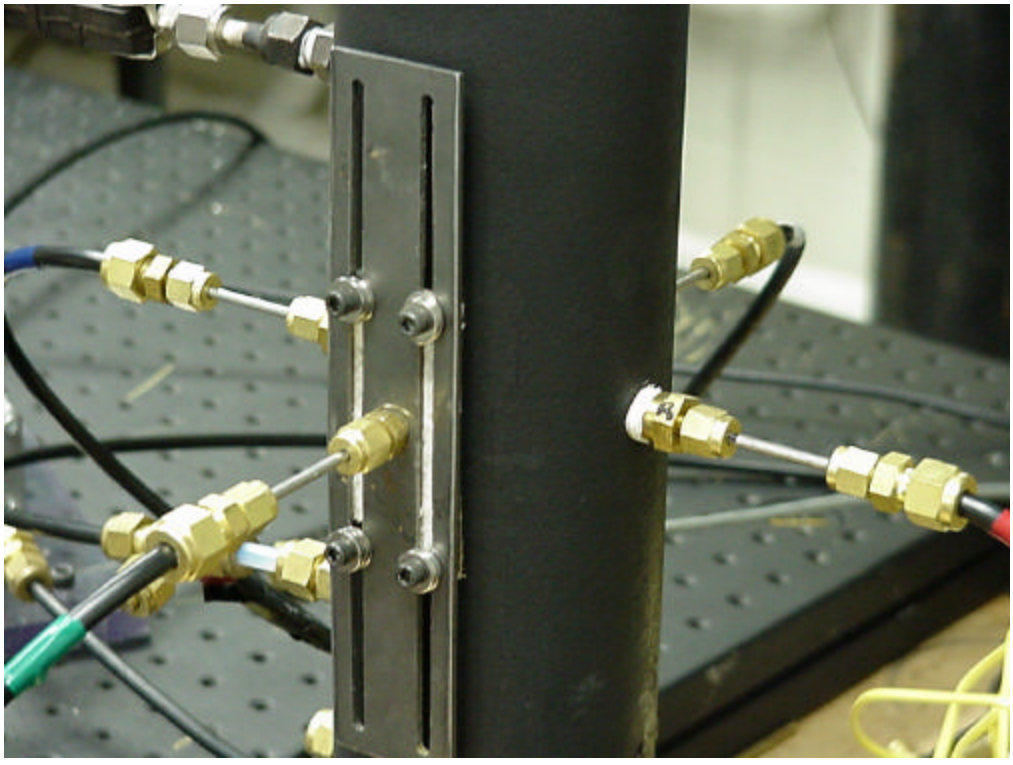

FIGURE 5.2.4 The Tube Combustor with the Injection System

5.3 The Control System

The control system is a simple phase shifter. The implementation of this phase shifter is a little more complex than normal due to the on/off operation and power requirements of the Matrix Corp. Model 850 valve. The input signal to the phase shifter comes from the pressure transducer in the bottom of the tube. First the pressure signal is amplified and filtered. The resulting signal is a sine wave of nominally 5 volts peak-to-peak amplitude to utilize the full dynamic range of the A/D converter of the DSP board. The phase shift is done using the DSP board and C-code, developed for previous research, that simply delays the input signal a specified number of samples. The output from the DSP board is run through a smoothing filter to a trigger circuit. This trigger circuit generates a 270 μsec pulse, at positive sloped zero-crossings, that is sent to a microcontroller. A diagram of the trigger circuit is presented in Figure 5.3.1.

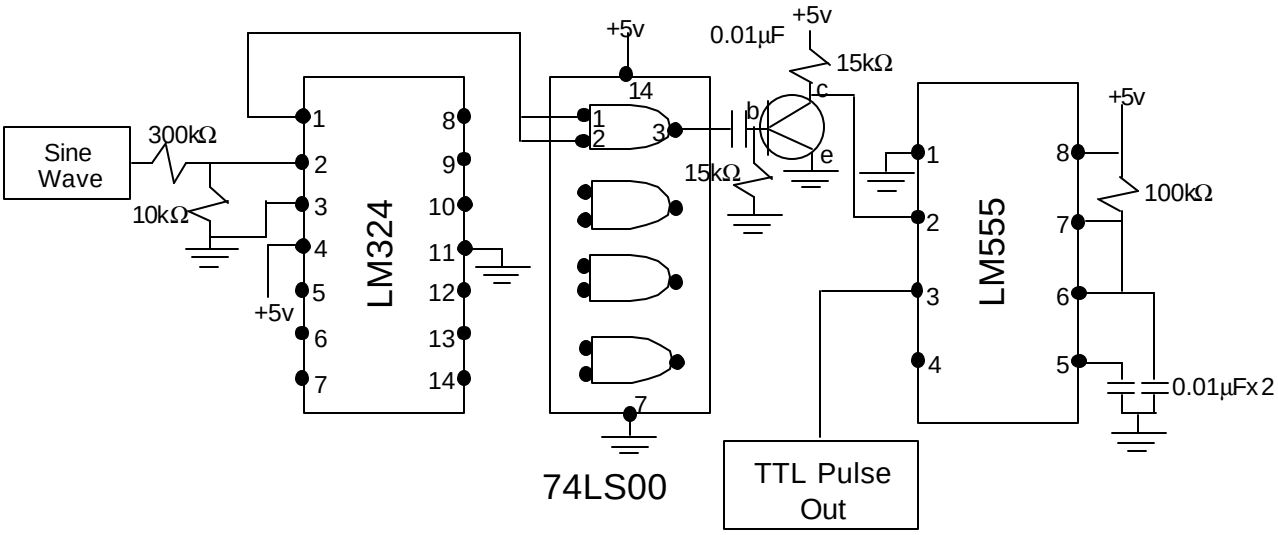

FIGURE 5.3.1 Circuit Diagram of the Trigger Circuit

The microcontroller is the VT84 board, built by students in the Mechatronics course at Virginia Tech. It consists of a PIC16F84 controller, 8 bit DAC, serial communication chip,

and buffer chip. This controller board is shown in Figure 5.3.2. The phase shift could not be performed using the VT84 microcontroller due to the computation time. Every operation of the PIC16F84 microcontroller takes 1 microsecond. The time required to compute the necessary components was on the order of 400 microseconds depending on operations required. Also, there is not the necessary hardware on the PIC 16F84 microcontroller to calculate the period of the input waveform in real time. The result was the output signal could not be generated at the exact frequency of the input, and thus a successful phase shift could not be achieved. Thus, the dSPACE system was used to perform the phase shift and the VT84 controller with some analog circuitry was used to create the square wave input to the valve electronics.

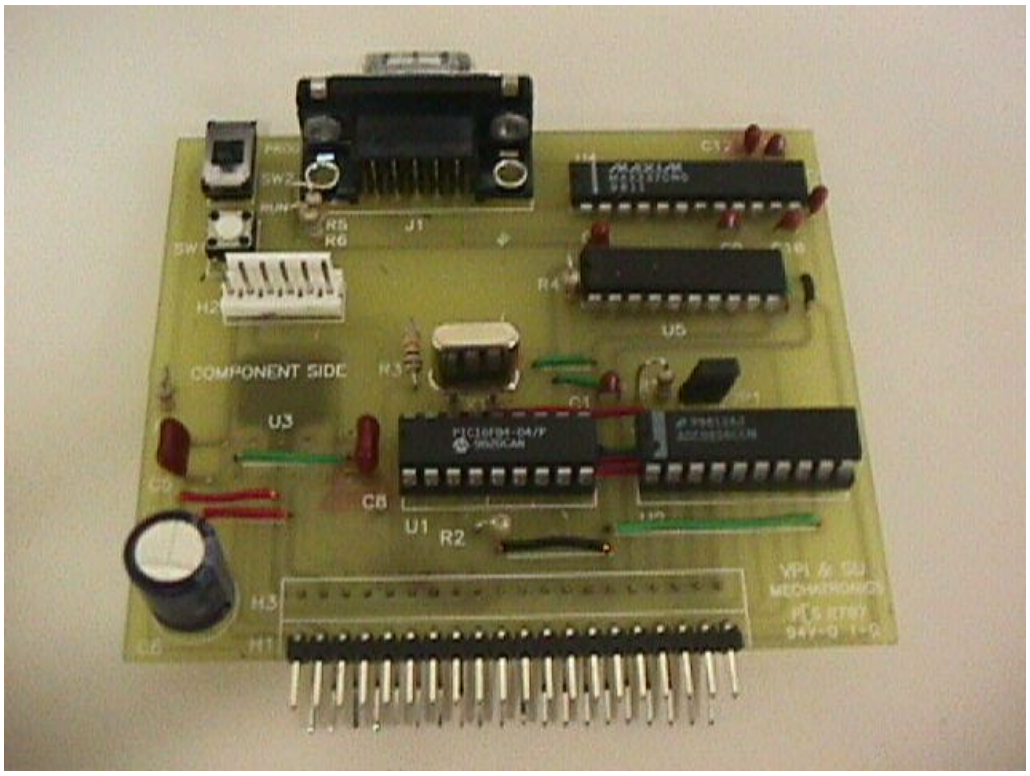

FIGURE 5.3.2 The VT84 Board

This VT84 controller was programmed at the machine language level, using Microchip's MPLAB software, to produce a 0-5 volt square wave with a variable duty cycle at the exact frequency of the input signal. This control code works through the chip's interrupt function.

The controller waits for an interrupt to occur on the RB0 port. The interrupt is the leading edge of the TTL pulse from the trigger circuit. Once interrupted, the code sets the output, Port A, high for a designated duty cycle, does the D/A conversion of the next duty cycle, and exits the interrupt. The controller waits until the next interrupt and continues the process. The user controls the duty cycle through a potentiometer that is connected to channel 0 of the A/D converter. The microcontroller reads in the voltage from the potentiometer through the A/D converter and stores it, as a hex number, for the next interrupt cycle. This means there is a one period delay in the duty cycle from when it is read by the microcontroller. A flowchart, for the code, is given in Figure 5.3.3.

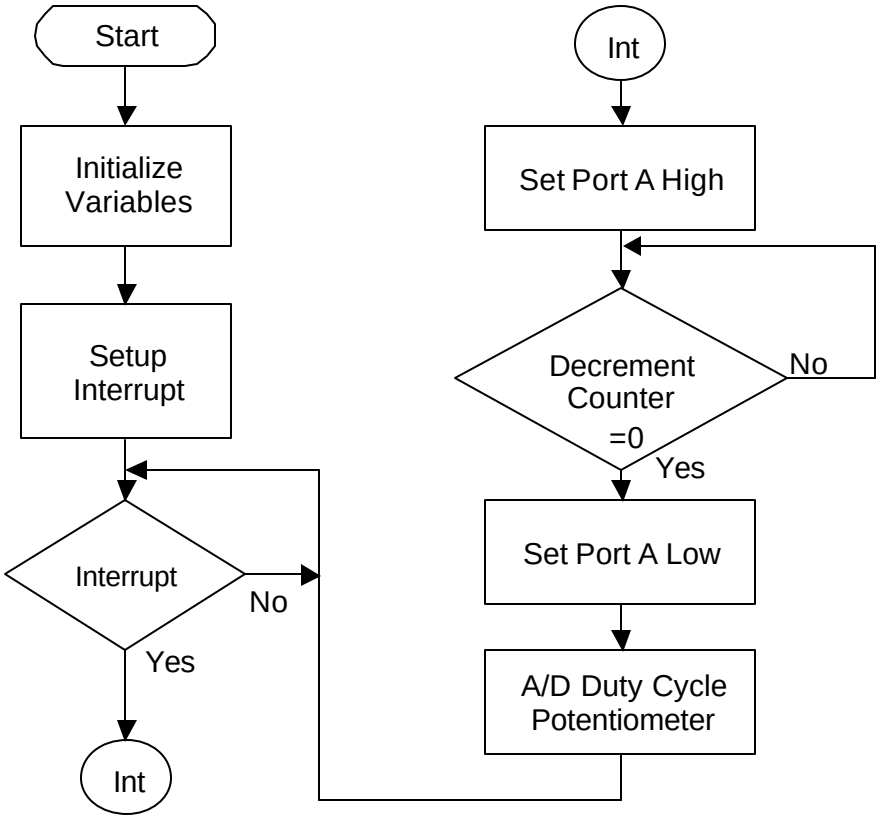

FIGURE 5.3.3 Flowchart of Square Wave Generation Code

This square wave signal, generated by the microcontroller, is then sent to the power circuit that increases the voltage to 24 volts at 500 milliamps. This power circuit consists of a digital logic level transistor that acts as a gate, opening and closing the circuit from the 24 volt power supply, creating the 0-24 volt square wave. A circuit diagram for the power

circuit is shown in Figure 5.3.4. This signal drives the valve. A block diagram of the entire system is shown in Figure 5.3.5.

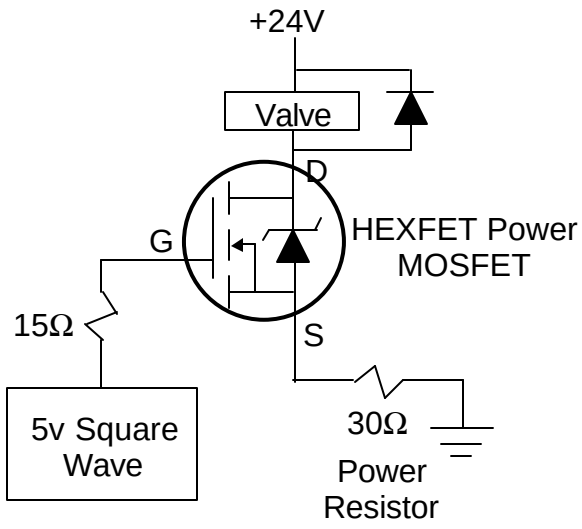

FIGURE 5.3.4 Circuit Diagram for Power Circuit

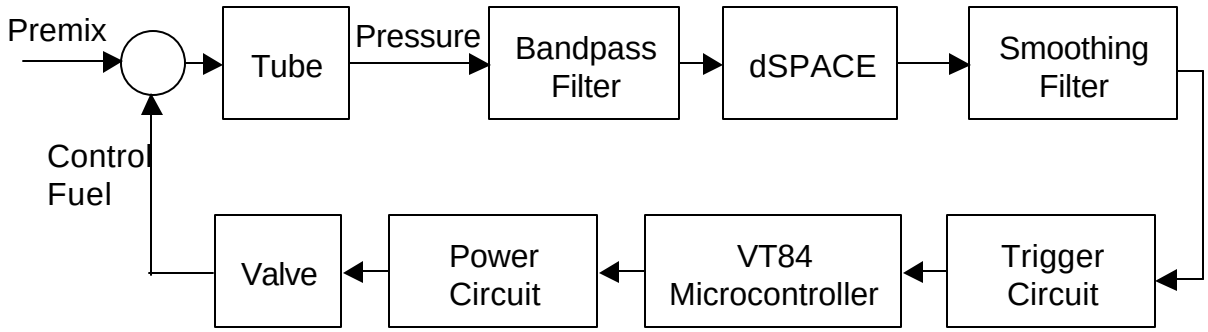

FIGURE 5.3.5 Block Diagram of Complete Control System

A picture of part of the control system with some of the required electronics is shown in Figure 5.3.6. A close-up photograph of the enclosed controller, power circuit, and trigger circuit is shown in Figure 5.3.7.

FIGURE 5.3.6 The Control System

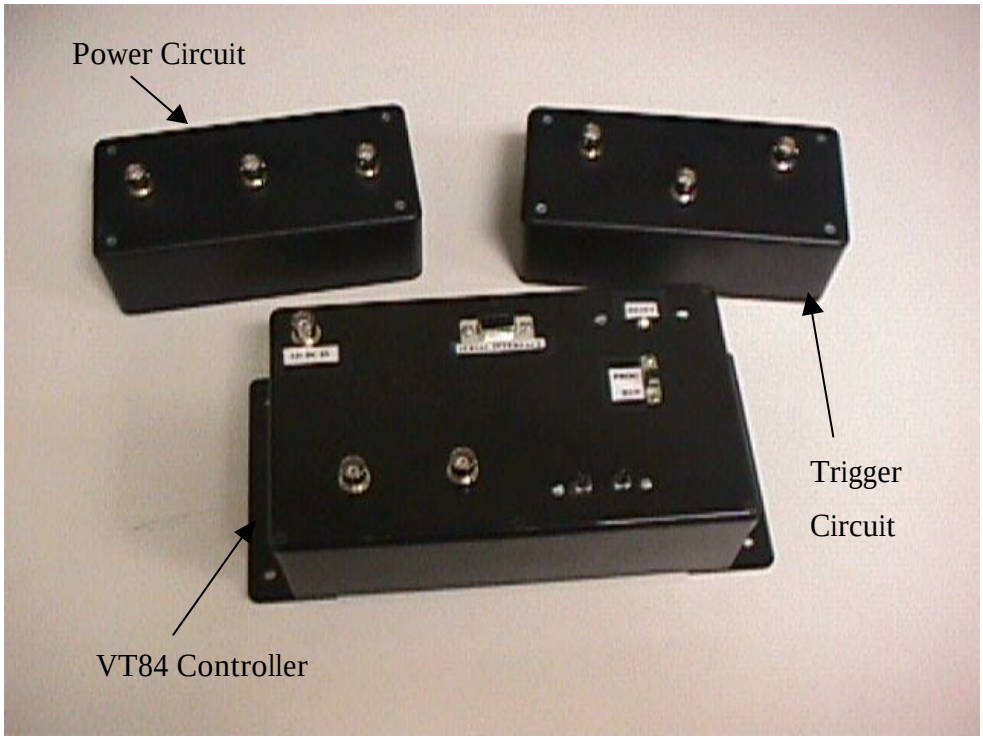

FIGURE 5.3.7 VT84 Controller, Trigger Circuit, and Power Circuit

5.4 The Closed Loop Test Results

The overall primary objective was to gain control of the tube combustor thermoacoustic instability. To meet this objective a number of steps were taken. The first step was to attempt control of the system instability driven by fuel from the injectors only. This means no primary fuel flow. The purpose of this test was to explore how well the heat release from injection diffusion flames coupled into the gases. The next step was to explore the effects of modulation on the system through a bifurcation analysis. Next, the effects of the duty cycle on control authority were explored. Once these steps were completed, control was attempted with main flow fuel and a primary flame. From the findings of these tests, a second set of injectors was built and the process was repeated.

5.4.1 Test Results Without Main Fuel Flow

Closed-loop control was attempted using one, two, and four injectors without the main flow combustion process. Photographs of the flames for one, two, and four injectors are shown in Figure 5.4.1.1. The fuel flow rate was fixed at 7 cc/sec, keeping the system at an equivalence ratio of 0.6 for a total flow of 120 cc/sec. The controller phase was set to enhance the system's instability. At this condition, the injector flames created an instability of the same frequency and amplitude as system with primary fuel combustion.

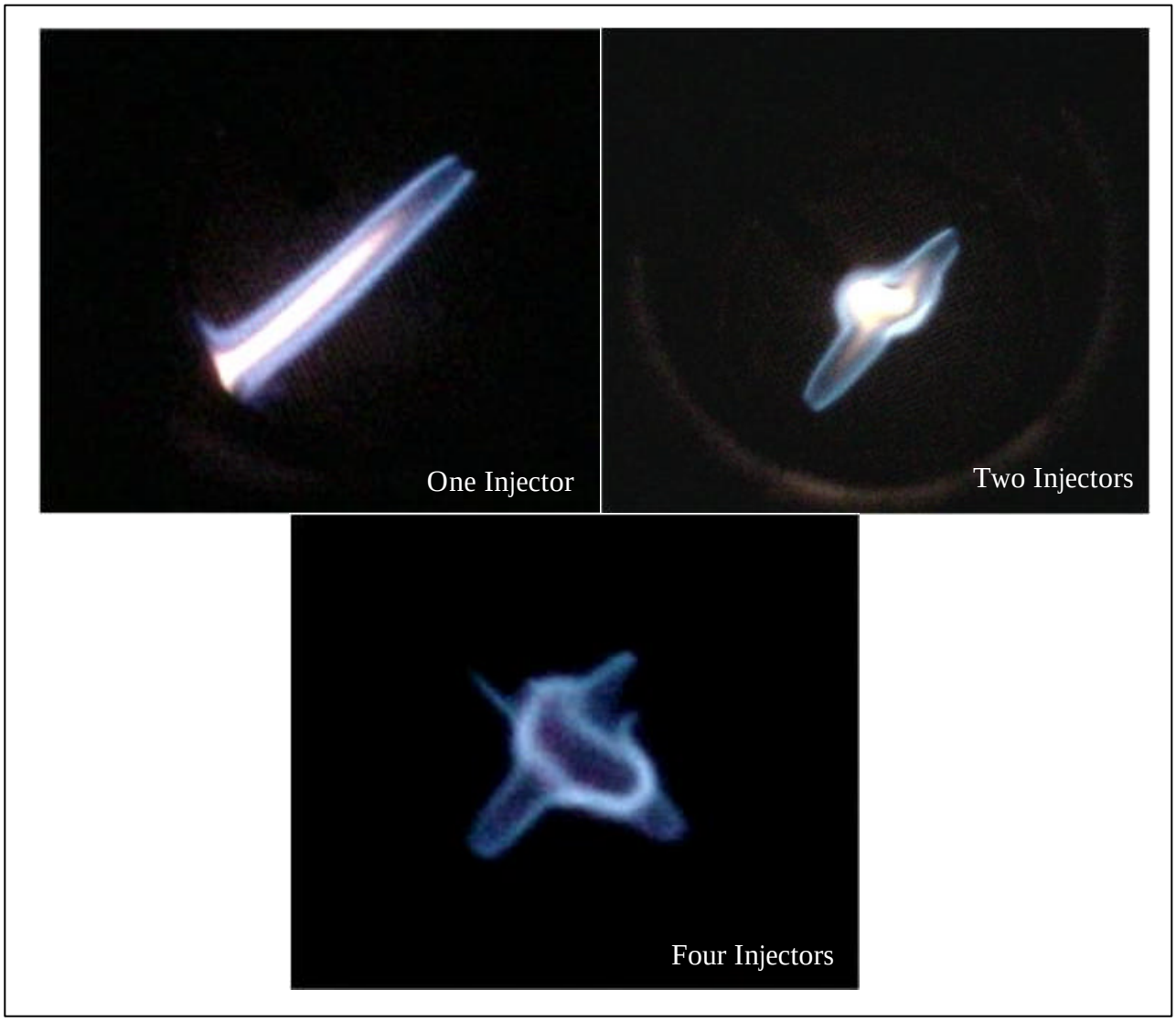

FIGURE 5.4.1.1 Photographs of the Flame for One, Two, and Four Injectors

The primary result of this closed-loop test was that control could be achieved using one and two injectors, but not with four injectors. All efforts to find a phase that would stabilize the system with four injectors failed. To verify that the phasing of the injection branches was not the reason for the inability to control the system with four injectors, the two opposite pairs were tested individually. The phase to control the system for each pair of branches was the same. This verified that the branches were matched in phase, and this was not the reason for the loss of control with four injectors. A possible explanation for the loss of control with four injectors could be seen in the flame photographs. For the one and two injector cases the flames were very yellow in color. This color is the result of the soot

formed by the diffusion flame. A diffusion flame is one where the oxidizer, air, meets the fuel at the flame front. A candle is a good example of a diffusion flame. This type of flame has very little coupling between the heat release and the gases. Only about 20% of the heat release from a diffusion flame goes into the gases. The other 80% is lost in the form of radiation to the walls of the tube. In the four-injector case the flame is not diffuse in nature. The flame is relatively more mixed from the additional jet interactions and lower exit velocity. The exit velocity is half that of the two-injector case. Therefore one would expect the heat release from this type of flame to be more coupled to the gases. Thus, from the perspective of coupled heat release, the four-injector case would seem to be the best for controlling the instability. From the perspective of exit velocity, this is not the case. Due to the lower exit velocity, in the four-injector case, the fuel pulses are closer together, and tends to lower the amount of modulation in the control fuel. The one-injector case is the best for control from the view point of pulse separation due to the highest exit velocity for the different injectors.

A new set of injectors was built to verify that the lower exit velocity results in less control authority. The 0.03" inner diameter injectors have slightly less than half the exit area of the 0.042" injectors used in the previous tests. This reduction of area increased the exit velocity of the four-injector by a factor of two. Close-loop control was attempted with one, two, and four of the new 0.03" inner diameter injectors. The flow rate and equivalence ratio were kept at 120 cc/sec and 0.60 as before. Control was achieved using one and two injectors, as before, but now control was also achieved using all four injectors. A plot of the controlled and uncontrolled pressure spectrum for two 0.03" injectors is shown in Figure 5.4.1.2.

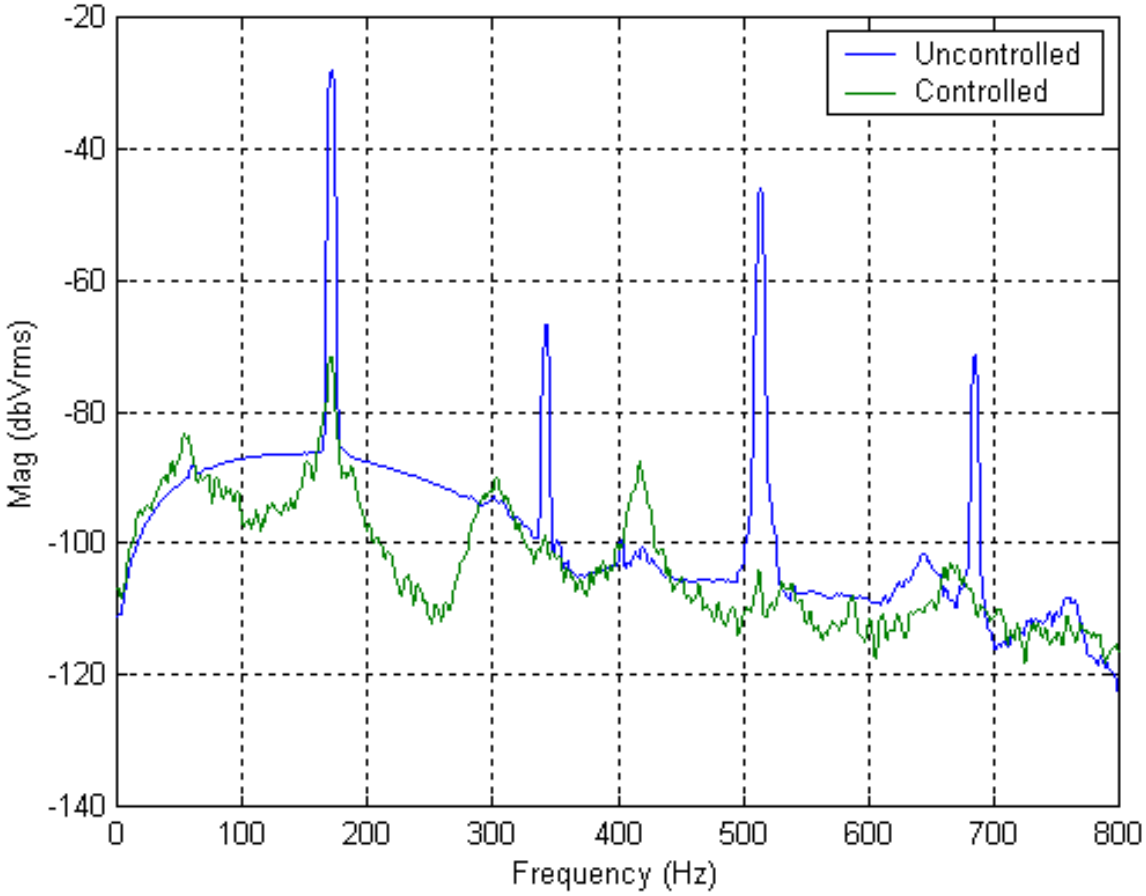

FIGURE 5.4.1.2 Power Spectrum for the Controlled and Uncontrolled Cases with Two 0.03" Inner Diameter Injectors and No Main Flow Fuel

(ϕ=0.6 and 120 cc/sec total flow)

The level of the limit cycle was reduced by 35 dB when closed-loop control was applied. The results, above, were typical for each of the one, two, and four injector test cases without primary fuel.

Since the system is nonlinear the sub critical Hopf bifurcation point can be evaluated, where the fuel flow rate is the main control parameter, to explore the effects of fuel modulation on the system. A sub critical Hopf bifurcation point is the point where a system jumps from a stable condition to an unstable condition, due to a change in the control parameter. For this test the point is found by simply increasing the fuel flow rate until the system transitions from a stable condition to unstable condition. The opposite can be performed to find the

supercritical bifurcation point. In order to perform this test, the injectors were open-loop forced at 176 Hz with a function generator. The duty cycle was kept constant at 10%. This was done with two and four 0.03" inner diameter injectors. As a basis for comparison, a bifurcation analysis of the tube supplied with main flow fuel and four injectors with no modulations was also performed. The total flow was, once again, kept at 120 cc/sec with 7 cc/sec of fuel flow giving an equivalence ratio of 0.6. The results of these bifurcation tests are shown in Figure 5.4.1.3.

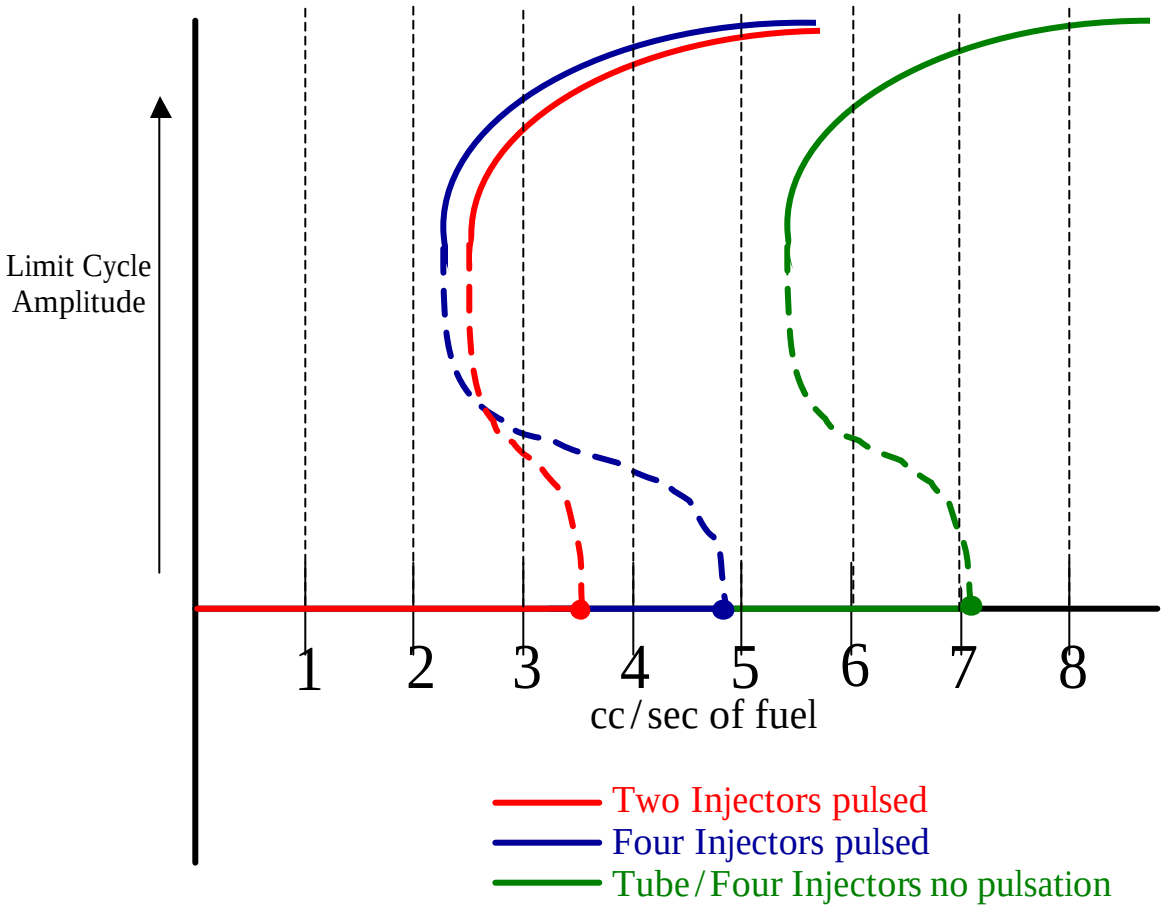

FIGURE 5.4.1.3 Bifurcation Diagram for the Tube, Two Injectors, and Four Injectors

The sub critical Hopf bifurcation points for the pulsed injectors occur at much lower fuel flow rates than that of the tube fed by main fuel flow and the four injectors without modulation. The system went unstable at 3.6 cc/sec and 4.8 cc/sec of fuel for the pulsed

injectors, and 7.1 cc/sec of fuel for the tube and four injectors with no pulsations. The results with the tube, fed by the main fuel supply, and four injectors with no modulation were the same. This demonstrates that it is the modulation that changes the inception point of the instability and the pulsations of the fuel are coupled into the system.

The sub critical Hopf bifurcation point was lower for the two-injectors case than for the four-injectors case. This is due to the lower exit velocity for the four-injector system. As discussed earlier, the exit velocity from the four injectors is half that of two injectors. The fuel pulses are more tightly spaced together at the lower velocity and have less momentum. This lower exit velocity means there is less modulation in the fuel flow by the time it is burned, lowering the overall effectiveness of the four-injector case. Just as the pulsed injectors were used to drive the system unstable at much lower fuel flow rates, the pulsed injectors can be used to stabilize the system with closed-loop control and the correct phase. These results say that the two-injectors case is coupled to the system more than the four-injectors case due to the larger amount of fuel modulation caused by the higher exit velocity.

All the previous tests were performed with a fixed duty cycle, but the duty cycle is an important parameter of control. It was observed that the time required to gain control of the system increased as the tube combustor was operated. This change in control time was dramatic. In an attempt to gain control of the system in less time, the duty cycle was modulated. The result was a decrease in time to gain control. To explore the effect of the duty cycle modulation on control authority, a timed test was performed with two 0.03" inner diameter injectors. Once again the total flow was fixed at 120 cc/sec and 7 cc/sec of fuel was fed through the valve. There was still no main fuel flow supplied by the tube combustor's premixer. The tube was run continuously and control was applied at chosen points in time. In one case the duty cycle was kept constant at 10%. In the other case the operator modulated the duty cycle from 25% to 2% to attempt increase control authority. The user performed this modulation at a maximum rate of 5 Hz. The result of this test is shown in Figure 5.4.1.4. At 55 minutes into the test the difference in time to control between the two cases was over 420 seconds.

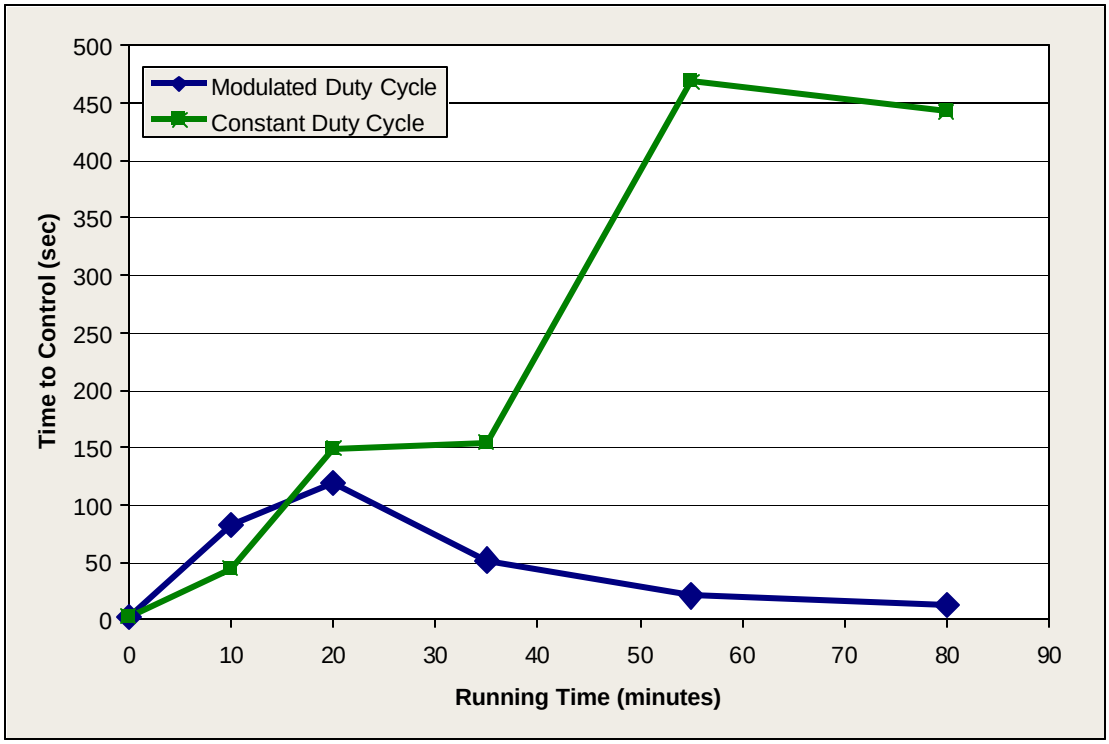

FIGURE 5.4.1.4 Time to Control With and Without Duty Cycle Modulation

The mechanism behind this increased control authority is still being explored, but a hypothesis has been formed. The hypothesis is that the pulse of fuel at 25% duty cycle adds enough fuel to make the flame more of a diffusion flame. This diffusion flame is more decoupled from the acoustics thereby lowering the gain of the self-excited loop. While the system is momentarily disturbed the 2% duty cycle pulse is injected, which has a large level of control authority due to the extremely low duty cycle. This amount of control authority is enough to move the system away from of its lower level limit cycle, and thus gain control. In other words the system is moved away from its limit cycle by a disturbance, and allows the control input to stabilize the system. The duty cycle could be fixed at 2% instead of 10% and the timed result would be the same. The control authority of the 2% duty cycle pulse is not enough, in itself, to stabilize the system. It is only when the modulation of the duty cycle occurs that the system is stabilized as shown in the previous figure. This is evidence that the hypothesis may be true, but it is very difficult to prove that this is the mechanism.

5.4.2 Test Results With Main Fuel Flow

All the previous tests have dealt with no fuel flowing through the tube. A test was devised to find the limits of control on the tube with main flow. From observations made during the experiment, the tube cannot be controlled when the total amount of fuel is above 8 cc/sec. This was suggested by the flame observations discussed in Chapter 4. The total flow was kept constant at 120 cc/sec. The tube was tested for a variety of conditions between 6 cc/sec and 8 cc/sec of total fuel flow with the two 0.03" inner diameter injectors giving equivalence ratios from 0.50 to 0.67. The sub critical Hopf bifurcation point experiment and injector tests, without main fuel flow, suggested that two 0.03" injectors were the most effective in controlling the system. The results are tabulated in Table 5.4.2.1. Control was obtained up to 5 cc/sec of tube fuel flow, with as little as 1 cc/sec, or 20% secondary fuel injection. This amount of control fuel is similar to results presented in the literature review of Chapter 2. It is important to stress that these main fuel flow experiments were only successful at equivalence ratios that would not support a flame without the fuel from the injectors. The implication of this is that the control was still primary injector fuel control only. It was not a true form of secondary fuel control. Only if the equivalence ratio from the primary fuel was high enough to support a flame that promoted an instability would it be true secondary fuel control.

TABLE 5.4.2.1 Range of Control Mapping

Primary Equivalence Ratio

Valve Fuel Flow (cc/sec) \	0	0.042	0.083	0.13	0.17	0.21	0.25	0.29	0.33	0.38	0.42	0.46	0.50	0.54	0.58
1											C	LE	NO	NO	NO
1.5										C	C	LE	NO	NO	
2									C	C	C	LE	NO		
2.5								C	C	C	LE	LE			
3							C	C	C	C	LE				
3.5						C	C	C	C	LE					
4					C	C	C	C	MSC						
4.5				C	C	C	C	MSC							
5			C	C	C	C	MSC								
5.5		C	C	C	C	MSC									
6	C	C	C	C	MSC										
6.5	C	C	C	C											
7	C	C	C												

C – Controlled
MSC – Marginally Stable Control
LE – Little Effect
NO – No Effect

5.4.3 Summary of Closed-Loop Control Experiments

A qualitative summary of the closed loop test results is presented in Table 5.4.3.2. These control limit results are slightly lower than that obtained by the acoustic actuator. Control could be achieved up to a total flow of 130 cc/sec at an equivalence ratio of 0.6 with the acoustic actuator giving a total fuel flow rate of 8 cc/sec. Control, through secondary fuel actuation, was achieved up to 8 cc/sec of total fuel, but 7 cc/sec of fuel flow was through the injector. The best control condition, for secondary fuel actuation, was with 5 cc/sec of fuel through the tube and 1 cc/sec of fuel injected through the actuator. This corresponds to an equivalence ratio modulated from 0.42 to 0.50.

TABLE 5.4.3.1 Summary of Closed Loop Test Results

	One Injector	**Two Injectors**	**Four Injectors**
0.042" Inner Diameter	Control without main flow only	Control without main flow only	No control
0.03" Inner Diameter	Control without main flow only	Control with main flow up to 5cc/sec	Control without main flow only

It is surprising that control for the one injector case could only be maintained without main flow. From the perspective of pulse diffusion this case should have the least amount of diffusion. The hypothesis is that, in this case, the jet interactions with two and four injectors promote some mixing producing flames that are slightly less diffusive in nature. With a diffusion flame radiation is high and very little heat release couples into the gases, making the single injector case have less control authority than the two or four injector cases. This hypothesis is yet to be proven. Future work will be done to prove or disprove this hypothesis and the other hypothesis mentioned throughout the chapter.

Chapter 6

Results and Future Work

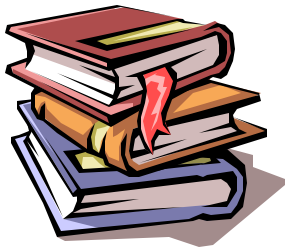

6.1 Summary of Results

The primary goal of this research was to demonstrate control of combustion instabilities in a laminar premixed tube combustor using secondary fuel actuation. In order to achieve this goal the problem of pulse diffusion had to be overcome. This problem was overcome through a novel injection technique and the goal was met. Control of the laminar premixed tube combustor was obtained for primary fuel flow rates up to 5 cc/sec to tube main fuel flow using 20% secondary control fuel through two 0.03" inner diameter injectors. This result somewhat exceeded the expectation that it would take the same amount of fuel to control the system as that being burned from the primary fuel injection. This is the first published attempt of controlling a laminar premixed tube combustor through secondary fuel actuation.

Valuable observations have been made about the reaction of the laminar flame to this method of secondary fuel injection. It was observed, in the flame dynamics rig, that at lower equivalence ratios the primary flame is affected by the secondary injection flames, but not at higher equivalence ratios. The flame photographs of the injection flames, through its blue color, showed that four of the 0.042" inner diameter injectors would not work due the low exit velocity. This led to the development of the 0.03" injectors that ultimately gained control of the system with main flow fuel.

Hypotheses have been formed on the mechanism behind the increased control authority to the duty cycle modulation, and why one injector has less authority than two injectors. These will be investigated further.

6.2 Future Work

There is much work to be done to further examine this "purely academic" study. Questions still remain about the mechanism behind the increased control authority due to the duty cycle modulation. The reason why one injector has less authority than two is still not completely understood. Quantification of the amount of control fuel required to control the thermoacoustic instability has not yet been attempted. The feasibility of developing a high response actuator custom to the requirements of the system needs to be looked into. There is much to explore. A researcher could invest a significant amount of time in exploring the many facets of this simple laminar premixed tube combustor.

In order to disprove or prove the hypotheses stated earlier a number of measurements need to be taken. Heat release data is the most notable piece of data yet to be collected. It can be collected with the PMT or a heat flux gage. This data needs to be taken with the valve continuously pulsed, using a constant duty cycle and varied duty cycle. This data in the form of time traces or frequency spectrums will give some information about how the flame reacts to the control fuel injection. The heat flux can be used to examine the different heat release mechanisms such as radiation, convection, and conduction. The radiation would a particularly good measurement for testing the theory of the higher percentage duty cycle making the flame more diffuse in nature. This would be shown as an increase in the amount of radiation given off due to the increase in soot formation. Radiation is also a key measurement for understanding why one injector has less authority than two injectors. A higher level of radiation would also be proof of the hypothesis that the single injector produces more of a diffusion flame than two injectors.

Phase locked photo images of the flame with a ccd camera would also be a worthwhile measurement. It could also be used to take data with the valve operating with and without duty cycle modulation. This type of measurement would be very helpful for showing how the flame reacts to the control temporally. Once it is known how the flame reacts to the fuel injection, a more optimized method could be devised that would increase the range of control.

Testing with a higher energy fuel is also something to consider. Use of a fuel like hydrogen that produces less of diffusion flame could increase the bandwidth of control greatly. This exploration would need to be handled with great care due to the volatility of hydrogen.

Although it would be a considerable time investment developing an actuator to perform secondary fuel actuation would be a wise venture. The actuator could be custom designed to meet the requirements for control the system. Research into alternative actuation means such as piezo-stacks and magnetostrictive would prove to be a worthwhile development. The actuator appears to be a limitation of secondary fuel actuation for combustion control.

The final and ultimate future work will be secondary fuel control on a much higher power combustors where temperatures, pressures, and flow rates are more comparable to full-scale rigs. Though the actuation system will certainly be different, some of the issues learned about the simple tube combustor are invaluable.

REFERENCES

1.) M.G. Allen, C.T. Butler, S.A. Johnson, E.Y. Lo, and F. Russo, "An Imaging Neural Network Combustion Control System for Utility boiler Applications," Combustion and Flame 94: 205-214, 1993.

2.) A.M. Annaswamy, A. F. Ghoniem, "Active control in combustion systems," IEEE Control Systems Magazine, vol. 15, pp. 49-63, 1995.

3.) A.M. Annaswamy, J.P. Hathout, M. Fleidil, A.F. Ghoniem, "A model-based active control design for thermoacoustic instability," submitted to Combustion Science and Technology, 1997.

4.) G. Billoud, M.A. Galland, C. Huynh, S. Candel, "Adaptive Active Control of Combustion Instabilities," Combustion Science and Technology Vol. 81, pp. 257-283.

5.) G.J. Bloxsidge, A.P. Dowling, N. Hooper, P.J. Langhorne, "Active Control of Reheat Buzz," AIAA Journal Vol. 26 No. 7, pp. 783-790.

6.) S.M. Candel, "Combustion Instabilities Coupled by Pressure Waves and Their Active Control," 24th International Symposium on Combustion, pp. 1277-1296.

7.) Cohen J. M., Rey N. M., Jacobson C. A., Anderson T. J., "Active Control of Combustion Instability in a Liquid-Fueled Low-NO_x Combustor" 43rd ASME/IGTI Gas Turbine Expo and Congress, ASME Paper 98-GT-267, 1998.

8.) R.H. Dorf, R.C. Bishop, "Modern Control Systems", Addison Wesley Publishing Company, Reading, 1995.

9.) Franklin, Powell "Digital Control of Dynamic Systems", Addison Wesley Publishing Company, Menlo Park, 1998.

10.) Y.T. Fung, V. Yang, A Sinha, "Active Control of Combustion Instabilities with Distributed Actuators, Combustion Science and Technology, vol. 78, pp. 217-245, 1991.

11.) Y. T. Fung, V. Yang, "Active Control of Nonlinear Pressure Oscillations in Combustion Chambers," Journal of Propulsion and Power, vol. 8, pp. 1282-1289, 1992.

12.) Anil Gulati and Ramani Mani, "Active Control of Nonlinear Pressure Oscillations in Combustion Chambers, Journal of Propulsion and Power, vol. 8, 1992.

13.) Hantschk C., Hermann J., Vortmeyer D., "Active Instability Control With Direct Direct-Drive Servo Valves in Liquid-fueled Combustion Systems," 26th International Symposium on Combustion, pp. 2835-2841, 1996.

14.) R. Heising, E. Lubarsky, M. Neumair, Y, Neumeier, B.T. Zinn, "Periodic Liquid Fuel Sprays Combustion Processes and Their Damping of Combustion Instabilities," AIAA Paper 2000-1024.

15.) J. Hermann, S. Gleis and D. Vortmeyer, "Active Instability Control of Spray Combustors by Modulation of the Liquid Fuel Flow Rate," Combustion and Science Vol. 118,pp. 1-25.

16.) J.R. Hibsman, J.M. Cohen, A. Banazuk, T.J. Anderson, H.A. Alholm, (1999) "Active Control of Combustion Instability in a Liquid-Fueled Sector Combustor," submitted to IGTI June 1999.

17.) B.S. Hong, V. Yang, A. Ray, "Robust Control of Combustion Instability with Model Uncertainty," AIAA Paper 98-0354.

18.) A.J. Hull, C.J. Radcliffe, S.C. Southward, "Global Active Noise Control of a One-Dimensional Acoustic Duct Using a Feedback Controller," Transactions of ASME, vol. 115, Sept. 1993.

19.) Jefimenko, O.D. "Electricity and Magnetism", Appleton Century Crofts, New York, 1966.

20.) C.E. Johnson, Y. Neumeier, E. Lubarsky, J.Y. Lee, M. Neumaier, B.T. Zinn, "Suppression of Combustion Instabilities in a Liquid Fuel Combustor Using a Fast Adaptive Control Algorithm," AIAA Paper 200-0476.

21.) A. Kemal, C.T. Bowman, "Real-time Adaptive Feedback Control of Combustion Instability," 26th Symposium (International) on Combustion/ The Combustion Institute, pp. 2803-2809, 1996.

22.) S. Koshigoe, T. Komatsuzaki, V. Yang, "Adaptive noise control technology applied to controlling pressure oscillations in a large scale solid rocket motor," submitted to Journal of Propulsion and Power, 1997.

23.) M. Krstic, A. Krupadanam, C. Jacobson, "Self-Tuning Control of a Nonlinear Model of Combustion Instabilities," Submitted to IEEE Transactions on Control Systems Technology, 1997.

24.) S.L. Lacy, R. Venugopal, D.S. Bernstein, "Armarkov Adaptive Control of Self-Excited Oscillations of a Ducted Flame," 37th IEEE Conference on Decision & Control, pp. 4527-4528, 1998.

25.) Langhorne, P. J., Dowling, A. P. and Hooper, N., "Practical Active Control System for Combustion Oscillations," Journal of Propulsion and Power, Vol. 6 (3), 324, 1990.

26.) J. Magill, M. Bachmann, "Combustion Dynamics and Control in Liquid-Fueled Direct Injection Systems," AIAA paper 00-1022.

27.) K.R. McManus, J.C. Magill, M.F. Miller, “Control of Unstable Combustion Oscillations in Liquid-Fueled Gas Turbines,” 1998 International Conference on Control Applications.

28.) McManus K. R., Mahill J. C., Miller M. F., “Combustion Instabilities Suppression in Liquid-Fueled Combustors,” AIAA Paper 98-0642.

29.) Merkli and H. Thomas, J. Fluid Mech. 70 (1), 161 (1975).

30.) S. Murugappan, E.J. Gutmark, S. Acharya, “Application of Extremum Seeking Controller for Suppression of Combustion Instabilities in Spray Combustion,” AIAA Paper 2000-1025.

31.) K. T. Padmanabhan, C.T. Bowman, J. D. Powell, “An Adaptive Optimal Combustion Control,” Combustion and Flame 100: 101-110 (1994).

32.) C.L. Phillips, R.D. Harbor, “Feedback Control Systems”, Prentice Hall, Upper Saddle River, 1996.

33.) Plonus, M.A. “Applied Electromagnetics”, McGraw and Hill, New York, 1978.

34.) Rayleigh, L., “The Theory of Sound”, Dover Pub., New York, 1945.

35.) G.A. Richards, M.C. Janus, E.H. Robey, “Active Control of Flame Oscillations with Equivalence Ration Modulation,” AIAA Journal of Propulsion and Power 1999.

36.) Rijki, P.L., Phil. Magazine, 17,419 (1859).

37.) Rizzoni, G. “Principles and Applications of Electrical Engineering”, Irwin, Boston, 1993.

38.) W.R. Saunders, M.A. Vaudrey, B.A. Eisenhower, U. Vandsburger, and C.A. Fannin, “Perspectives on Linear Compensator Designs for Active Control,” 37th AIAA Aerospace Sciences Meeting, Reno, NV, Jan. 11-14, 1999.

39.) K.C. Schadow, E. Gutmark, K.J. Wilson, “Active Combustion Control in a Coaxial Dump Combustor,” Combustion and Science and Technology, vol. 81, pp. 285-300, 1992.

40.) J.R. Seume, N. Vortmeyer, W. Krause et al., “Application of Active Combustion Control to a Heavy Duty Gas Turbine” ASME Paper 97-AA119.

41.) M.A Vaudrey, W.R. Saunders, B.A. Eisenhower, “A Test Based Methodology for Apriori Selection of Gain/Phase Relationships in Proportional, Phase-Shifting Control of Combustion Instabilities,” submitted to the ASME Turbo Expo, IGTI, Munich, Germany, 2000.

42.) M.A. Vaudrey, W.R. Saunders, W.T. Baumann, “Control of Combustor Instabilities Using An Artificial Neural Network,” submitted to the ASME Turbo Expo, IGTI, Munich, Germany, 2000.

43.) K.J. Wilson, E. Gutmark, K.C. Schadow, R. A. Smith (1991) “Active Control of a Dump Combustor With Fuel Modulation,” AIAA Paper 91-0368.

44.) K. Yu, K.J. Wilson, and K.C. Schadow, “Active Combustion Control in a Liquid-Fueled Dump Combustor,” AIAA Paper 97-0462.

45.) K. Yu, K.J. Wilson and K.C. Schadow, “Liquid-Fueled Instability Suppression,” 27th International Symposium on Combustion, pp 2039-2046.

46.) Zinn, B.T., Neumeier, Y., ”An Overview of Active Control of Combustion Instabilities”, AIAA 97-0461, 1997.

APPENDIX A LINEAR MODEL MATLAB CODE

```
N = 63;
mu = 4*pi*1e-7;
A = 1.327e-6;
M = 0.0006;
c = .2;
k = 0;
P = 0.25*6894.757;
Al = 7.5e-5;
Fp = P*Al;
w = 50*2*pi;
R = 3;
i0= 4;
v0 =12;
x0= sqrt(N^2*mu*A*i0^2/(M*(9.81+2*Fp/M)));


Amatrix = [ -R*x0/(mu*N^2*A)  (v0-R*i0)/(mu*N^2*A)       0;  0
   0  1; 2*N^2*mu*A*i0/(M*x0^2) -2*N^2*mu*A*i0^2/(M*x0^3)-2*k/M  -
   1  2*c/M];
Bmatrix = [x0/(mu*N^2*A);0;0];
Cmatrix = [0,1,0];
Dmatrix =0;

ts= linspace(0,.3,10000);
init = [ i0,x0 ,0];
V = .5*(sin(w*ts));
%V = .1*square(w*ts);
sys = ss(Amatrix,Bmatrix,Cmatrix,Dmatrix);

[Y,T,ys] = lsim(sys,V,ts,init);

xs = ys(:,2)+x0;
is = ys(:,1) + i0;

%plot(t,y(:,2),'b',ts,xs,'r');zoom
%plot(ts,xs)
%figure
%plot(ts,is)
```

APPENDIX B PHASE SHIFTER C-CODE

```
/* ************************************************************

CHANNEL ONE ECHO TO BE USED AS A TEMPLATE FOR OTHER
PROGRAMMING
HEAVILY COMMENTED BY FORWARD SLASH-STAR STAR-FORWARD SLASH
DON'T REMOVE ANYTHING, BUT YOU MAY NEED TO ADD THINGS LIKE
VARIABLES,
FUNCTIONS, AND EQUATIONS
Mike Vaudrey Oct. 5, 1996

************************************************************************/

#include <brtenv.h>

float Samp_Freq = 11000.0;              /* EDIT SAMPLING FREQUENCY HERE */
float u, s, in_1, out_1;                /* DECLARE ALL GLOBAL VARIABLES HERE */

#define MAX_VEC_SIZE 55

float freqin = 200.0;
int delay_samples = 5;

float tester = 1.0;
float ts = 0.0;
float actual_delay = 0.0;
float actual_phase = 0.0;       /* outputs (to cockpit) */
float inp_vec[2][MAX_VEC_SIZE + 2];
float crap;

int index = 0;
int not_current = 1;
int current_row = 0;
int ind = 0;

/* Variables for execution time profiling */
#define TMR0 0                          /* timer0 definition */
float exec_time;                        /* execution time */
unsigned long count0;                   /* timer0 time count */


/* error flag for CHKERR at last dual-port memory location */
volatile int *error = (int *) (DP_MEM_BASE + DP_MEM_SIZE - 1);


/* Input macros via DS2201 ADC channels 1 and 2 */
```

```
 #define Input_Chan1(u)                \
 start_ds2201ad(DS2201_1_BASE); \
 u = ds2201ad(DS2201_1_BASE, 1)


/* Output via DS2201 DAC channel valid channels from 21 to 28 (1-8)*/

  #define Output_Chan1(s)    \
  ds2201da(DS2201_1_BASE, 21, s);


/*---------------------------------------------------------------------*/
/* MAIN PROGRAM FUNCTION, INCLUDE INITIALIZATIONS, ETC. IF
NEEDED BUT NOT
THE EXECUTED (OR CONTROL) CODE */
/*---------------------------------------------------------------------*/



main()
{

 float DT = 1.0/Samp_Freq;     /*finds sampling period for interrupt routine*/

 init();                          /* initialize hardware system */

/*initial with for loop inp_vec */


         for(index = 0; index < MAX_VEC_SIZE+1; index ++)
         {
          inp_vec[0][index] = 0.0;
          inp_vec[1][index] = 0.0;
         }

 *error = NO_ERROR;                       /* initialize error flag */
 start_isr_t0(DT);                  /* START sampling clock timer */

/*=====================================================
=================*/



  while (*error == NO_ERROR)                  /* background process */
    service_cockpit();                      /* call COCKPIT code */
```

```
}


/*---------------------------------------------------------------------*/
/* INTERRUPT SERVICE ROUTINE.  INCLUDE CONTROL CODE HERE
BETWEEN SHORT LINES*/
/*---------------------------------------------------------------------*/

isr_t0()                    /* timer0 interrupt service routine */
{
 begin_isr_t0(*error);                  /* overload check */
 count0 = count_timer(TMR0);            /* save current timer count */

/*---------------------*/
/*CONTROL CODE GOES HERE*/

 ts = 1/Samp_Freq;
 actual_delay = delay_samples*ts;
 actual_phase = 360*freqin*actual_delay;


 Input_Chan1(in_1);                     /*reads chan1 and saves as in_1 */


 inp_vec[current_row][0] = in_1;


        for(ind = 0; ind < MAX_VEC_SIZE; ind++)
                {
                inp_vec[not_current][(ind+1)] = inp_vec[current_row][ind];
                }

        if (current_row == 0)
                {
                current_row = 1;
                not_current = 0;
                }
        else
                {
                current_row = 0;
                not_current = 1;
                }


 out_1 = inp_vec[not_current][delay_samples];


 Output_Chan1(out_1);                   /*sends out_1 out of dac channel 1 */
```

```
/*CONTROL CODE STOPS HERE*/
/*-----------------------*/


  service_trace();                          /* call TRACE code */
  exec_time = time_elapsed(TMR0, count0);  /* calculate execution time */
  end_isr_t0();                  /* end of interrupt service routine */
}
```

APPENDIX C SQUARE WAVE GENERATION CODE

```
;This is my phase shifting controller with variable duty cycle.  I will bring in the phase shift on
; A2D Channel 0 and the duty cycle on A2D channel 2.  I will output the square wave from PORTA bit 3.
; The input will be the interrupt from the trigger circuit on RB0.  The prescaler will be set to 32 to
; maximize resolution for the typical operating frequency of 200 Hz.  I will use a series of subroutines
; to do the a2d conversion and the pwm.  I will use a divide macro to do any division that may be
; required
;
;Author:  John Richards
;
;Subject:  Phase shifter with variable duty cycle

        LIST P=PIC16F84
        __CONFIG _HS_OSC&_WDT_OFF&_PWRTE_ON&_CP_OFF

        include <c:\progra~1\mplab\p16f84.inc>
;       include <d:\mplab\p16f84.inc>

        CBLOCK      0x0C
                LOOPCOUNT
                AARGB0
                REMB0
                BARGB0
                MUX
                RESULT
                COUNT
                PWL
                PWH
                time
                PHASE
                DUTY
                test
                OLDPHASE
                DEL
                DEL2
                PERFIX
                CYCLES
                EXTRA
                NEWTIME
                DELOUT
                DELIN
```

```
                pwmgen1
                pwmgen2
                timeuse
                temp
                temp2
        ENDC

CH0     EQU   0X03          ;SETS UP A2D FOR CHANNEL 0
CH2     EQU   0x13          ;SETS UP A2D FOR CHANNEL 2
CLK     EQU   0X01
DIDO    EQU   0X02
CS      EQU   0X00
PWM     EQU   0X03          ;BIT ON PORT A FOR OUTPUT SQUARE WAVE
PRE     EQU   0X44          ;SETS THE PRESCALER TO BE 1:32 TO OPTIMIZE
FOR 200 HZ
INTER       EQU   0X90          ;SETS UP THE INTCON REGISTER FOR THE
INTERUPT

        #define     bank0  bcf    STATUS, RP0
        #define     bank1  bsf    STATUS, RP0


;-----------------------------------------------------------
; Clock up Macro

CLKUP       MACRO
        bsf     PORTA,CLK
        nop
        ENDM
;-----------------------------------------------------------
;-----------------------------------------------------------
; Clock down Macro

CLKDN       MACRO
        bcf     PORTA,CLK
        nop
        ENDM
;-----------------------------------------------------------
;***********************************************************
;----------------MAIN PROGRAM-------------------------------
        org     0x00
        goto    Start

        org     0004h
        goto    int_service

        org     0005h
```

```
Start
        clrf    OLDPHASE
        clrf    test
        clrf    TMR0
        clrf    INTCON
        clrf    PORTA
        clrf    PORTB
        bank1
        clrf    TRISA           ;porta as outputs
        movlw 0x01              ;Sets up RB0 as an input and all the rest
        movwf TRISB             ;outputs.
        movlw PRE
        movwf OPTION_REG        ;SETS PRESCALE TO 1:2 FOR TESTING
        bank0
        movlw INTER
        movwf INTCON            ;SETS up external interupts
        bcf     OPTION_REG,5    ;start TMR0
        movlw 0x50
        movwf DUTY
        movlw 0x00
        movwf PHASE
        movlw 0xA0
        movlw time

;%%%%%%%%%%%%%%%%%%%%%%%%%%%%%%%%%%%%%%%%%%%%%%%%%%%
%%%%%%%%%%%%%%%%%%%%%%%%%%%%%%%%%%%%%%%%
;Subroutine: Main Loop
; This does the a2d of the duty cycle and square wave generation.

Main

        goto    Main




;//////////////////////////////////////////////////////////////////////////
//////

int_service

        movlw 0x00
        movwf time
        movf    TMR0,W
        movwf time
        movlw 0x02
```

```
        subwf  time,F
        bank1
        bcf    INTCON,1      ;clears the interupt
        bcf    OPTION_REG,5
        bank0
        clrf   TMR0          ;clears the TMR0 and Prescale and stops
        bank1                ;TMR0 counter
        movlw PRE            ;sets up the TMR0 and starts the TMR0 counter
        movwf OPTION_REG
        bank0
        movf   DUTY,w
        movwf temp
        movlw 0x02
        movwf temp2
        bsf    PORTA,PWM
ltest1
        movf   DUTY,w
        movwf temp
ltest   decfsz temp,f
        goto   ltest
        decfsz temp2,f
        goto   ltest1
        movf   DUTY
        movwf temp
ltest2  decfsz temp,f
        goto   ltest2

        bcf    PORTA,PWM
;%%%%%%%%%%%%%%%%%%%%%%%%%%%%%%%%%%%%%%%%%%%%%%%%
%%%%%%%%%%%%%%%%%%%%%%%%%%%%%%%%%%%%%
; A2D conversion (DUTY)
        movlw CH2            ;does the A2D conversion for channel 2
        movwf MUX            ;and stores the result in DUTY
        call   ATOD
        movf   RESULT,W
        movwf DUTY
;%%%%%%%%%%%%%%%%%%%%%%%%%%%%%%%%%%%%%%%%%%%%%%%%
%%%%%%%%%%%%%%%%%%%%%%%%%%%%%%%%%%%%%

        retfie
;///////////////////////////////////////////////////////////////////////
/////
;--------------------------------------------------------------------------
;%%%%%%%%%%%%%%%%%%%%%%%%%%%%%%%%%%%%%%%%%%%%%%%%
%%%%%%%%%%%%%%%%%%%%%%%%%%%%%%%%%%%%%


;--------------------------------------------------------------------------
```

```
;Subroutine: ATOD
;Purpose: This subroutine commands the ADC0838 to perform a conversion on the
;          channel specified in the file MUX.  The result of the conversion
;          is returned in the file RESULT.
;
ATOD
        movlw 0x05
        movwf COUNT
        bcf     PORTA,CS    ;enable ADC0838
SETUP   btfsc   MUX,0       ;is this bit a zero?
        bsf     PORTA,DIDO
        CLKUP
        CLKDN
        bcf     PORTA,DIDO
        rrf     MUX,F               ;position the next bit to send
        decfsz  COUNT,F             ;have all bits been sent?
        goto    SETUP
        bank1
        movlw 0x04
        movwf TRISA         ;setup to input DIDO
        bank0
        CLKUP
        CLKDN                       ;allow MUX to settle
        movlw 0x08
        movwf COUNT
RESLT
        bcf     STATUS,C
        CLKUP
        btfsc   PORTA,DIDO          ;is this bit a zero?
        bsf     STATUS,C
        rlf     RESULT,F    ;store the bit
        CLKDN
        decfsz  COUNT,F
        goto    RESLT
        bsf     PORTA,CS    ;disable ADC0838
        bank1
        clrf    TRISA       ;set DIDO as output
        bank0
        return
;-------------------------------------------------------------------------

        END
```

VITA

John Richards was born in Altoona, Pennsylvania on March 31, 1975. After many moves he ended up in Stephens City, Virginia where he graduated with honors from James Wood High School. After graduation he enrolled at Lord Fairfax Community College. While there he received numerous awards for his dedication to being a peer tutor. After three semesters John left Lord Fairfax to study at Virginia Tech. While at Tech he was once again awarded for his accomplishments as a peer tutor. Two semesters after his enrollment he started the coop program with Entergy Operations. Two coop semesters and four class semesters later, John graduated Cum Laude in 1998. Immediately after, he married, and entered the Graduate program in Mechanical Engineering also at Virginia Tech. Twenty-two months later he successfully defended his thesis. His future plans include moving into his new home and beginning the life he and his wife had been waiting for.